N° d'ordre : 42351

Thèse

Development and optimization of the tufting process for textile composite reinforcement

Présentée par :

Lingshan LIU

pour obtenir le grade de Docteur de l'Université de Lille 1

Discipline : Mécanique

Soutenue le 13/06/2017 devant la commission d'examen

Jury :

Mme Nadia BAHLOULI	Professeur Université de Strasbourg	Présidente du jury Examinatrice
M Artan SINOIMERI	Professeur Université Haute-Alsace	Rapporteur
M Zoheir ABOURA	Professeur Université Technologique de Compiègne	Rapporteur
M Damien SOULAT	Professeur des Universités, ENSAIT, Roubaix	Directeur
M Xavier LEGRAND	Maître de conférences, HDR, ENSAIT, Roubaix	Co-directeur
M Peng WANG	Maître de conférences, ENSAIT, Roubaix	Encadrant

ACKNOWLEDGEMENTS

Firstly, I would like to express my sincere gratitude to my project directors: Prof. Damien SOULAT, Dr. Xavier LEGRAND and Dr. Peng WANG, for the continuous support of my Ph.D study and related research, for their patience, motivation, and immense knowledge. Their consistent concern and valuable guidance has helped me in all the time of research and writing of this thesis. All of my Ph.D supervisors have remained kind throughout and favoured me a lot.

I am very much thankful to my predecessors of the same research group: Jean-Vincent RISICATO and Ahmed Rashed LABANIEH for their assistance during my research work.

Thanks to my research contemporary friends Boris DUCHAMP, Fatma OMRANI, Tao ZHANG and Chang LIU for technical discussions and knowledge-sharing during my time spent for Ph.D thesis.

Especially heartfelt thanks to my best friend Fatma for her encouragement and company during the last four years. From the first day of Ph.D life, we have seen and helped each other through both good times and bad. I will always remember the great conversations we had over lunch, and I know that we will break bread together many more times.

I am also indebted to my fiancé Ye LV, for his enduring love, for believing in me long after I'd lost belief in myself, and for sharing my wish to reach the goal of completing this task, but caring enough to love me even if I never achieved it.

Last but not the least, I would like to thank my parents Xiangyu LIU and Qiuhong HUANG, for giving birth to me at the first place and supporting me spiritually throughout my life.

CONTENTS

LIST OF TABLES

LIST OF FIGURES

GENERAL INTRODUCTION

Problem statement

Laminated composites are wildly used in many industrial fields such as transport, construction, energy and defense. Comparing with metal materials, laminated composite presents better mechanical performances such as high specific strength and stiffness, high-specific energy absorption, and excellent fatigue performance. Laminated structures are constituted by laying up different laminas (unidirectional ply or 2D woven ply) in different orientations. However, the laminations of two-dimensional layered fibre structure show limitations including high cost and some inferior mechanical properties such as impact resistance and poor delamination resistance [1, 2]. Therefore, a large number of works are conducted on the development of 3D preforms with reinforcements of high in plane densities, and including also the insertion of binding fibres to connect layers thereby combining excellent mechanical properties of layers to improve the resistance to delamination and impact resistance [3, 4]. Different approaches of manufacturing 3D preforms are brought out and classified according to through-the-thickness reinforcement (TTR) methods [5, 6]. Thick or multilayered weaving and other specific technologies such as stitching, z-pinning and tufting are applied on insertion of through thickness fibrous structure in order to obtain 3D preforms.

Tufting emerges as a popular method of localized Through-Thickness Reinforcement (TTR) for dry preforms. The tufting process involves inserting a single threaded needle through a preform, where friction within the preform is responsible for holding the thread in place as the needle is retracted [7]. Tufting can be used to reinforce different types of textiles such as woven fabric, braided fabric or non-crimped fabric (NCF) layers. It requires only one side access of thread and does not require the use of second thread which makes it simpler and cost economic. Tufting thread is held by fabric itself with low tension which results in a reduction of the stitching effect on the in-plane properties and the possibility of manufacturing complex and large composite structures. This technology is still under development and few works have been realized to characterize the geometry and the mechanical performance of produced preform. Recently Hartley [8] et al. show that, with an experimental study that increasing the number of tufts (less than 3 tufts) within a sample did significantly increase the crushing performance by as much as 25 %, when compared to the untufted coupons. Colin de Verdiere et al. [9] investigate the effect of tufting on the in-plane and out-of-plane mechanical response of NCF. They show that tufting increases considerably delamination resistance in mode I but to a lesser extent in mode II. However, in these studies the influence of the specific parameters of the binder reinforcement on the mechanical performance is less demonstrated. It is important to investigate and control tufting parameters for optimizing the process of tufting and mechanical performances of tufted composite.

In order to produce 3D composite parts from 3D preforms, the first step is to understand the deformability of preform on more and more complex shapes (given by punch and die). Some experimental works on the 3D woven interlock [10, 11] and numerical works [12, 13] on the development of specific behavior laws for the preforming simulation are brought out. The deformability of NCF (Non Crimp Fabrics), the fabric reinforced through thickness by stitching, during the preforming is well presented [14-17]. On the contrary, in these studies the influence of the specific parameters of the binder reinforcement (density of stitching, orientation relatively to the punch, stitching yarns direction, etc...) on measurement criteria during the preforming is not demonstrated. Moreover, the influence of through-thickness fibres on the preforming defects is not described. The literature on preforming of dry 3D tufting preforms is null. Research works are needed to improve the understanding of formability of the tufted 3D fabric during manufacturing.

Thesis overview

This study is dedicated to the development of tufting technology and the analysis of the influence of tufting parameters on preforming behaviours and mechanical properties of tufted preform and composite.

The chapter 1 is a review of the fibre reinforced composite. The composition of composite materials, the process of composite manufacturing, the basic concept of the used technology, the essential advantages and disadvantages from structural and mechanical point of view are treated.

The chapter 2 is dedicated to tufting technology. The fundamental principles of this technology are defined. Self-designed automated tufting equipment configuration is detailed. Controlling of numerous associated parameters is described and the method of application of tufting equipment is listed. Two tufting threads are characterized which is to be used in following chapters.

In the chapter 3, the influence of tuft length on the characterisations of tufted composites is completely analysed. 3D reinforcement architecture is prepared by tufting process with varied tufting length and then resin transfer moulding technology is involved to manufacture the composite samples. Microscopic analysis on the cross section of 3D specimen and tensile tests are carried out to determine the influence of the tuft length on the geometrical and mechanical performance of tufted samples.

The chapter 4 is dedicated to the influence of tufting yarns during the forming of tufted 3D textile reinforcements. The preforming behaviours of tufted 3D reinforcement in the hemispherical stamping process are presented. The influence of tufting parameters including tufting yarns, tufting density, the orientation of tufting yarns on the material draw-in, interplay sliding, winkling phenomenon and misalignment defect during forming are analysed.

The last chapter is devoted to the conclusions and perspectives of this thesis.

Reference of general introduction

[1] Faggiani A, Falzon BG. Prediciting low-velocity impact damage on a stiffened composite panel. Composites Part A 2010;41:737–49.

[2] Falzon BG, Hawkins SC, Huynh CP, Radjef R, Brown C. An investigation of Mode I and Mode II fracture toughness enhancement using aligned carbon nanotubes forests at the crack interface. Composite Structures 2013;106: 65-73.

[3] Green SD, Long AC, EI Said BSF, Hallett SR. Numerical modelling of 3D woven preform deformations. Composite Structures 2014;108: 747–56.

[4] Mahadik Y, Robson Brown KA, Hallett SR. Characterisation of 3D woven composite internal architecture and effect of compaction. Composites A 2010;41:872–80.

[5] Mouritz AP, Cox BN. A mechanistic interpretation of the comparative in-plane mechanical properties of 3D woven, stitched and pinned composites. Composites Part A 2010;41:709–28.

[6] Kamiya R, Cheeseman BA, Popper P, Chou TW. Some recent advances in the fabrication and design of three-dimensional textile preforms: a review. Compos Sci Technol 2000;60:33-47.

[7] Osmiani C, Mohamed G, Treiber JWG, Allegri G, Partridge IK. Exploring the influence of micro-structure on the mechanical properties and crack bridging mechanisms of fibrous tufts. Composites Part A 2016;91:409–19.

[8] Hartley JW, Kratz J, Ward C, Partridge IK, Effect of tufting density and loop length on the crushing behaviour of tufted sandwich specimens, Composites Part B 2017;112:49-56.

[9] Colin de Verdiere M, Pickette AK, Skordos AA, Witzel V. Evaluation of the mechanical and damage behaviour of tufted non crimped fabric composites using full field measurements. Compos Sci Technol 2009;69:131–38.

[10] Dufour C, Wang P, Boussu F, Soulat D. Experimental Investigation About Stamping Behaviour of 3D Warp Interlock Composite Preforms. Applied Composite Materials 2014;21(5):725-38.

[11] Zhang YF, Sun F, Wang YJ, Chen L, Pan N. Study on intra/inter-ply shear deformation of three dimensional woven performs for composite materials. Mater. Des. 2013;49:151-9.

[12] De Luycker E, Morestin F, Boisse P, Marsal D. Simulation of 3D interlock composite preforming. Compos Struct 2009;88:615–23.

[13] Charmetant A, Orliac JG, Vidal-Sallé E, Boisse P. Hyperelastic model for large deformation analyses of 3D interlock composite preforms. Composites Science and Technology 2012;72:1352-60.

[14] Duhovic M, Mitschang P, Bhattacharyya D. Modelling approach for the prediction of stitch influence during woven fabric draping. Composites Part A 2011;42:968-78.

[15] Pazmino J, Carvelli V, Lomov SV. Formability of a non-crimp 3d orthogonal weave e-glass composite reinforcement. Composites Part A 2014;61:76-83.

[16] Carvelli V, Pazmino J, Lomov SV, Verpoest I. Deformability of a non-crimp 3D orthogonal weave E-glass composite reinforcement. Composites Science and Technology 2012;73:9-18.

[17] Margossian A, Bel S, Balvers JM, Leutz D, Freitas R, Hinterhoelzl R. Finite element forming simulation of locally stitched non-crimp fabrics. Composites Part A 2014;61:152-62.

1 STATE OF THE ART

1.1 Introduction

Advanced fibre-reinforced composite materials are widely used in various industries, from sporting goods to aerospace vehicles for their lightweight, high strength and superior structural durability. In this chapter, current and historical literature on the introduction of textile composites is reviewed with the aims of obtaining a broad view of the field.

Firstly, the definition of composite materials and its applications are introduced. Comparing to other materials, composite materials present a number of advantages and also some limitations which are listed in this part. The components of composites: matrix and reinforcement are introduced in detail. The process of manufacturing composite materials including the manufacturing of prepreg composite materials and also the Liquid Composite Molding are described. And textile preforms are briefly presented.

In the second part, architectures of the 2D/3D fibre reinforced composites produced by different textile technologies, in addition to their advantages and disadvantages, are briefly presented. Then, the necessity to elaborate tufting reinforcements, which are the focus of this thesis, is presented.

1.1.1 The composite materials

Since the end of the 19th century, textile composite materials have been used with outstanding success in industrial manufacture. Nowadays, they are increasingly used in many sectors such as aeronautics, space, sporting goods, marine, automotive, ground transportation and off-shore thanks to its light weight, high specific stiffness, high specific strength, excellent corrosion resistance, fatigue resistance and impact resistance compared to common metallic alloys [1,2].

Figure 1-1 Applications of composite materials [3]

The composite material is a material made from two or more constituent materials with significantly different physical or chemical properties that, when combined, produce a material with characteristic different from the individual components. The individual components remain separate and distinct within the finished structure [4-6].

The reinforced composite material is composed of reinforcing phase and matrix phase. The reinforcing phase which has the main function of resisting mechanical stress is embedded in continuous matrix phase. The matrix fixes the reinforcement in position to guarantee the geometrical characteristics of the product. It transfers and distributes the loads between the reinforcing components by the shear adhesion forces and preserves the reinforcement from the external environment conditions [7].

The most used fibre reinforcement is carbon, glass, aramid or any combination of these fibres. The orientation and distribution of reinforcement within the composite material depend on the stiffness and strength properties imposed on the composite structure.

The two kinds of polymer matrix materials are thermoset polymer and thermoplastic polymer. It helps to carry out and maintain the liaison between reinforcements and to transfer the stresses to the reinforcements. It can also protect the reinforcements from aggressive agents and to keep the shape of the composite product.

Besides these two main components, some additives such as organic origin (mold release agent, stabilizers) or mineral (fillers, pigments) can be added in order to modify some of its characteristics. For example, the mechanical behavior of the resin can be improved by adding fillers which may be in the form of microbeads, metal powders or mineral materials (quartz, silica, chalk, etc.). The behavior of the resin can also be modified by adding pigments in order to color the resin or by adding anti-UV agents in order to delay its aging. A catalyst can be added to the resin to start the curing process of the resin and an accelerator can be used to improve the cure rate [8].

Within composite materials, the presence of undesirable elements such as holes or porosities affects the quality of composite parts. In order to improve the mechanical performance of composite products, it is important to reduce the number and the size of these porosities during the manufacturing process. Furthermore, the composite materials are usually highly anisotropic, which is to say that their mechanical properties are different according to the direction of stress. Therefore, during the manufacturing of the composites, the orientation of reinforcement should be taken into account [9].

Composite materials present a number of advantages. Comparing with most woods and metals, composites are lightweight with densities between 1 and 3.5g/cm^3. This property provides a better fuel efficiency so that composite materials play an important role in the aeronautics, space and transport industries. In these industries, a high strength-to-weight ratio is usually needed. Some metal materials such as steel are strong, but heavy. While composites can be designed to be both strong and light.

Table 1-1 shows the mechanical properties of certain unidirectional composites with a fibre content ratio of 60% and classical metal alloys. In this table, differences in mechanical characteristics relative to mass or density between composites and metals are shown. The tensile strength per unit mass of the unidirectional composites in the direction of the fibres is three to five times greater than those of metals. And the modulus per unit mass of unidirectional composite material in the direction of the fibres varies from 2650 to 11800 km which is one to five times of those of metal alloys [10].

Despite the high strength-to-weight ratio, composites structures provide a lot of other advantages such as corrosion resistance, high-impact strength, design flexibility, part consolidation, and durability. These properties make composites widely applied in the fabrication of bulletproof vests, shield airplanes, cable protectors, etc [12].

Table 1-1 Comparison of characteristics between composite materials and metals [11]

Characteristics	**metals**		**Composites with organic matrices***		
	Steel 35NCD16	Aluminum alloy AU4SG	High-resistance carbon Epoxy resin	High-modulus carbon Epoxy resin	R-glass epoxy resin
Tensile characteristics: Tensile strength TS (MPa) Young's modulus E (GPa)	1850 200	500 72	1000-1300 130	1000 200	1800-2000 53
Density ρ (g/cm^3)	7.9	2.8	1.5	1.7	2
Tensile strength per unit mass TS/ ρg (km) Young's modulus per unit mass E/ ρg (km)	24 2500	18 2600	65-85 8700	60 11800	90-100 2650
Coefficient of linear expansion: Longitudinal ($10^{-6}K^{-1}$) Transversal($10^{-6}K^{-1}$)	12 12	23 23	-0.2 35	-0.8 35	6 31

* Unidirectional composites with a fibre content ratio of 60%

Composite materials present also certain limitations. Composites are usually heterogeneous, that reinforcement and matrix always present very different functional properties. The presence of resin rich area and dry area can lead to a large degradation of mechanical properties in the final product. Dry area can increase moisture absorption and decrease chemical resistance. And a large difference of coefficient of thermal expansion is created between these two areas. It is important to handle the problem of homogeneity. There are some other limitations such as the high cost of fabrication, difficulty of recycling, problems of stabilization, bonding between the composite part and other composite part or metal part. More research works are needed to overcome these challenges [13,14].

1.1.2 Composition of composite materials

As previously explained, composites are made up of individual constituent materials: matrix and reinforcement. The matrix is used to hold the reinforcements in an orderly pattern and helps to transfer load which is also called resin system. The matrices can be divided into three categories: thermosetting resins, thermoplastic resins and metallic matrices [15]. Among these matrices, thermosetting resins and thermoplastic resins are more commonly used in textile composite materials. The molecular structures of these two resins are different. The bonds between macromolecular chains are linear in thermoplastics, and three-dimensional in thermoset resins [16].

Thermosetting resins are widely used in the industry for Liquid Composite Molding (LCM) processes. In a thermoset resin, the raw uncured resin molecules are crossed linked through a catalytic chemical reaction. Through this chemical reaction, most often exothermic, the resin creates extremely strong bonds to one another which cannot be broken by physical action, such as heat and pressure. The thermosetting resin irreversibly changes state from a liquid to a solid [15].

The choice of a resin system depends on their characteristics, including adhesive properties, mechanical properties, micro-cracking resistance, fatigue resistance and degradation from water ingress etc. Considering these characteristics, the most commonly used resin systems are polyester resins, vinyl ester resins, epoxy resins. Polyester resins are generally used with glass fibres, while epoxy resins are often used with carbon fibres in the aerospace industry. Vinyl esters are widely used for many similar applications with polyesters, but have an improved durability and impact resistance in composites. However, vinyl esters are more expensive. There are other resins, including phenolic resins and polyimide resins. Phenolic resin is usually used to produce fire resistant composites. There is little use of polyimide resins because their high price. Table 1-2 shows comparisons of the characteristics of thermosetting resins used in industry.

Table 1-2 Main characteristics of most used thermosetting resins [15,17]

Type of resins	**Polyesters**	**Vinyl esters**	**Epoxy**	**Phenolic**	**polyimide**
Mechanical characteristics	Average	Good	Very good	Poor	Excellent
Impact resistance	Very good	Very good	Good	Bad	Very good
Fatigue resistance	Poor	Good	Average	Poor	Good
Adhesive power	Average	Very good	Very good	Average	Very good
Maximum operating temperature	140 ℃	190 ℃	190 ℃	130 ℃	260 ℃
Fire resistance	Very bad	Very good	Average	Good	Very good
Withdrawal	Large	Large	Little	Very little	Very little
Duration of polymerization	Short	Short	Long	Short	Average
Implementation	Very easy	Very easy	Easy	Difficult	Difficult
Relative price	2	4	5	1	16

Thermosetting resins are popular because uncured, at room temperature, they are in a liquid state. This allows for convenient impregnation of reinforcing fibres such as fibreglass, carbon fibre or Kevlar. Laminators can easily remove all air during manufacturing, and it also allows the ability to rapidly manufacture products using a vacuum or positive pressure pump. Beyond ease of manufacturing, thermosetting resins can exhibit excellent properties at a low raw material cost.

Once a thermoset resin is catalyzed, it cannot be reversed or reformed. That means once a thermoset composite is formed, it cannot be remolded or reshaped. Because of this, the recycling of thermoset composites is extremely difficult. The thermoset resin itself is not recyclable, however, there are a few new companies who have successfully removed the resin through pyrolization and are able to reclaim the reinforcing fibre.

Thermoplastic resins are less used compared with thermoset resins. In thermoplastic resins, the macromolecular chains are linked together by weak bonds. These bonds are easily to be broken by physical action. The most used thermoplastic resins are polystyrene resins, polyamide resins, Teflon, PVC, etc.

Thermoplastic composites have some advantages. Many thermoplastic resins have an increased impact resistance compare to thermoset composites. Another advantage of thermoplastic composites is the ability of reforming and reshaping. It is easy to use thermoplastic resins because there is no need for crosslinking. And the storage time is unlimited.

However, thermoplastic resins present some disadvantages. A major limitation is the need of special tooling, technique, and equipment which are very expensive. This type of resin has a poor resistance to chemical aggressions. The maximum operating temperature is limited at about 100 ℃ [18].

Reinforcement plays a role to fundamentally increase the mechanical properties. All of the different fibres used in composites have different properties and so affect the properties of the composite in different ways. The four main factors that govern the fibre's contribution are the basic mechanical properties of the fibre itself, the surface interaction of fibre and resin (the interface), the amount of fibre in the composite (fibre volume fraction) and the orientation of the fibres in the composite. The most widely used fibre reinforcements are carbon fibre, glass fibre, aramid fibre, etc.

Carbon fibres are the oldest of the industrial fibres which are obtained by pyrolysis of polyacrylonitrile yarns (PAN). Depending on the manufacturing conditions, high performance carbon fibres can be classed in three categories, high resistance (HR), intermediate module (IM) and high modulus (HM) [19].

The carbon fibres are highly anisotropic with high values of stiffness and strength in the longitudinal direction. But their transverse mechanical properties are much lower than the longitudinal properties. They are conductive fibres with a low density. They are widely used in numerous applications in aeronautics, space and transport because of their perfect mechanical properties and very low coefficient of expansion (negative for some types of carbon fibre, such as carbon T1000). However, carbon fibres have a low impact resistance and the price of this type of fibre remains relatively high.

Comparing with carbon fibres, glass fibres have lower mechanical properties but an excellent ratio of mechanical performances and the price. They can be divided into different types of glass according to their chemical compositions. Glass E is commonly used which has good electrical properties. Glass D has high dielectric properties. Glass C has a good chemical resistance And glass R or S have high mechanical strength. Glass fibre reinforced composite materials are usually used in building and boating.

Aramid fibres, in which the best known is Kevlar which is produced by the company DuPont de Nemours, are aromatic polyamides. They have a very low density, very good tensile characteristics and good impact strength. On the other hand, they exhibit poor compressive strength, high moisture recovery and high sensitivity to ultraviolet rays. Table 1-3 shows the comparison of typical properties of some reinforcements.

Table 1-3 Typical properties of some reinforcement [17, 20]

Material type	**Tensile strength (MPa)**	**Tensile modulus (GPa)**	**Typical density (g/cm^3)**	**Specific modulus**
Carbon HS	3500	160-270	1.8	90-150
Carbon IM	5300	270-325	1.8	150-180
Carbon HM	3500	325-440	1.8	180-240
Carbon UHM	2000	440+	2.0	200+
Aramid LM	3600	60	1.45	40
Aramid HM	3100	120	1.45	80
Aramid UHM	3400	180	1.47	120
Glass - E glass	2400	69	2.5	27
Glass - S2 glass	3450	86	2.5	34
Glass - quartz	3700	69	2.2	31

1.1.3 The process of composite manufacturing

Since composites are used in many industries, the manufacturing processes of composite materials become also important. The matrix material can be introduced to the reinforcement before or after the reinforcement material is placed into the mold cavity or onto the mold surface. The matrix material experiences a melding event, after which the part shape is essentially set. Depending upon the nature of the matrix material, this melding event can occur in various ways, such as chemical polymerization or solidification from the melted state. In general, the reinforcing and matrix materials are combined, compacted and processed to undergo a melding event. After the melding event, the part shape is essentially set. There are different types of moulding processes which can be utilized to form a composite material.

The Liquid Composite Molding (LCM) processes are increasingly used in the manufacture of advanced composites in several fields which include more than a dozen different types of manufacturing processes [22]. In LCM processes, the resin is injected into the reinforcement and fills the stack of the preform, and then converted from liquid to solid state by the thermally activated crosslinking reaction. There are two major processes in LCM family, injection process and infusion process.

Resin Transfer Moulding (RTM) is a vacuum-assisted process where resin is injected into fibrous preforms which are held between two solid and closed molds. The stack of the reinforcement is placed in the mold before its closing and clamping. Low viscosity resin is then pumped into the mold to displace the air, until the mold is filled. The injection points are defined according to the size and complexity of the composite part. As soon as the preforms are filled and the resin is discharged through the vent, the temperature cycle is imposed. Finally after cooking, the final part can be ejected. Figure 1-2 describes the RTM manufacturing process. The final parts present an increased laminate compression, a high glass-to-resin ratio, and outstanding strength-to-weight characteristics [23].

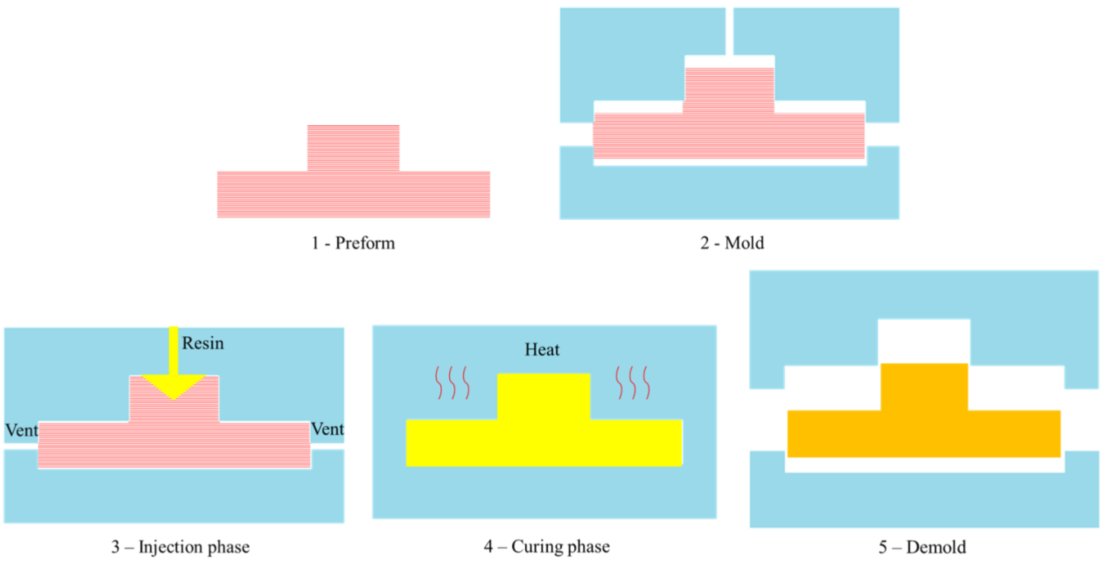

Figure 1-2 Resin Transfer Moulding injection process

Vaccum Infusion Process (VIP) is a cost effective process which can be used under flexible conditions, for example, in open and low-cost nylon or silicone vacuum bag molds. It utilize only atmospheric pressure to push the resin into the mold cavity. Resin Film Infusion (RFI) and Liquid Resin Infusion (LRI) are new processes to manufacture complex or large dimension composite parts.

The principle of Resin Film Infusion process is shown in Figure 1-3 [8, 24-28]. A layer of solid resin is placed below the fabric stack. To ensure the quality of upper surface of the flat composite part, an aluminum plate is placed on the fibre/resin stack. A mesh is placed on the fabric stack to absorb excess resin. Several non-stick plastic films are utilized to isolate the composite from the vaccum bag. Due to the temperature cycle created by autoclave or heating table, the resin become less viscous that allows the resin infuse through the thickness of fabric stack. After the resin fill the system, a heat-curing phase will be achieved under the cycle of temperature and the pressure.

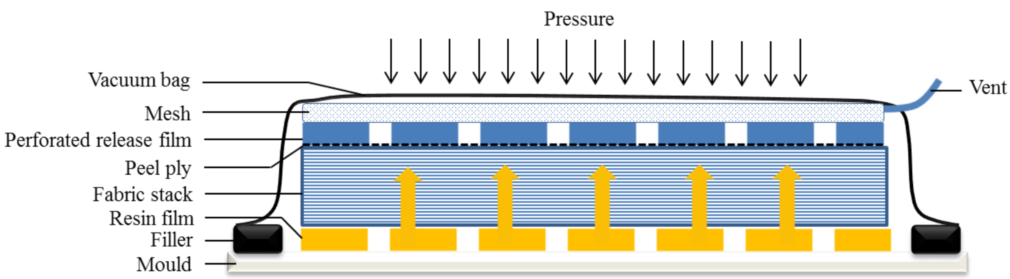

Figure 1-3 Principle of RFI process.

Liquid Resin Infusion was developed more recently. A highly permeable draining fabric is used in this process which helps to produce a layer of resin above the preform, as shown in Figure 1-4. The entire infusion system is enclosed in a vaccum bag. A perforated release film can be used to improve the surface quality of the final part. A differential pressure is created by a vacuum at the vent of the system, it leads to the impregnation of the compressible perform in the transverse direction. Then a temperature cycle and pressure are added to the system during curing process. Once the cross linking has been completed, the composite part can by removed from the mold after cooling.

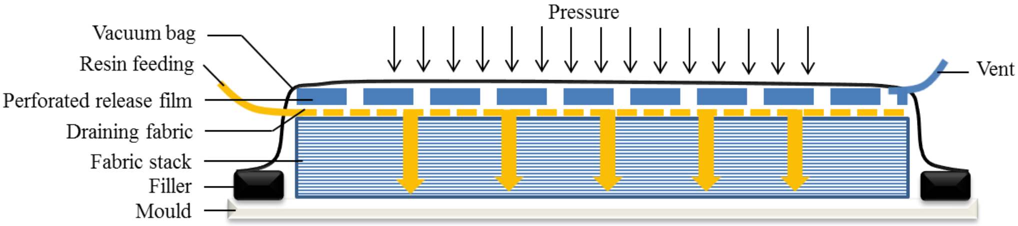

Figure 1-4 Principle of LRI process.

Vacuum infusion process presents a lot of advantages. It provides a possibility to manufacture complex and thick parts with high mechanical properties. The standard fibre volume fraction of the composites produced by infusion process is 55%, sometimes can rise up to 60% under certain conditions. Moreover, due to the needless of mold on the upper part and the reuse of the mold at the lower part, composite parts can be produced with a lower cost.

However, during the infusion process, a vacuum bag is used to replace the rigid mold which will lead to an uncontrolled fibre volume fraction. Moreover, it is difficult to measure the transverse permeability of the preform which plays an important role in the infusion process.

Prepreg composite material is another common material in the composite industry due to their ease of use, consistent properties, and high quality surface finish [18]. In prepreg materials, a reinforcement fibre is pre-impregnated with a thermoplastic or thermoset resin matrix in a certain ratio with a desired geometry. Prepregs are cured under high temperatures and pressures. Generally, the resin matrix in prepregs is partially cured for ease of handling and is stored in a cool place to prevent complete polymerization. Then the prepreg will need to be heated in an autoclave or oven during manufacture of composite materials to achieve full polymerization. The reinforcement in a prepreg can be unidirectional carbon, glass of aramid fibres or a fabric. Prepregs are produced using two main processes: hot melt process and solvent dip process. Both fabric and unidirectional prepregs can be produced using the hot melt process. A thin film of the heated resin is coating on a paper substrate. The reinforcement material and the resin are allowed to interact in the prepreg machine. The resin is impregnated into the fibre under the pressure and heat, resulting in the final prepreg, which is ultimately wound on a core. Solvent dip process can only be used to produce fabric prepregs. The resin is dissolved in a solvent bath and fabric reinforcement is dipped in the resin solution. By using a drying oven, the solvent is then evaporated off the prepreg [21].

The pre-impregnated processes are widely used in the civil and military fields, including the aeronautics sector, sports and leisure activities. High-level mechanical performance can be achieved by pre-impregnated technology. It is easy to control the properties of final parts, in particular the fibre volume fraction, but the cost of the storage and raw materials are very high.

1.1.4 Textile preforms

Composites consisting of fillers in the form of fibre or powder of relatively high strength and modulus embedded in or bonded to a matrix with distinct interface between them [29]. In prepreg materials, fibres and resin are mixed together at the beginning. While for the LCM processes, reinforcing materials including mats, woven fabrics, braids, knitted fabrics and hybrid fabrics are needed. Figure 1-5 shows the fibres used to reinforce composites which are supplied in different forms: unidirectional (fabric UD), bidirectional (woven, braided), multiaxial (non-crimp fabrics, non-crimp new concept).

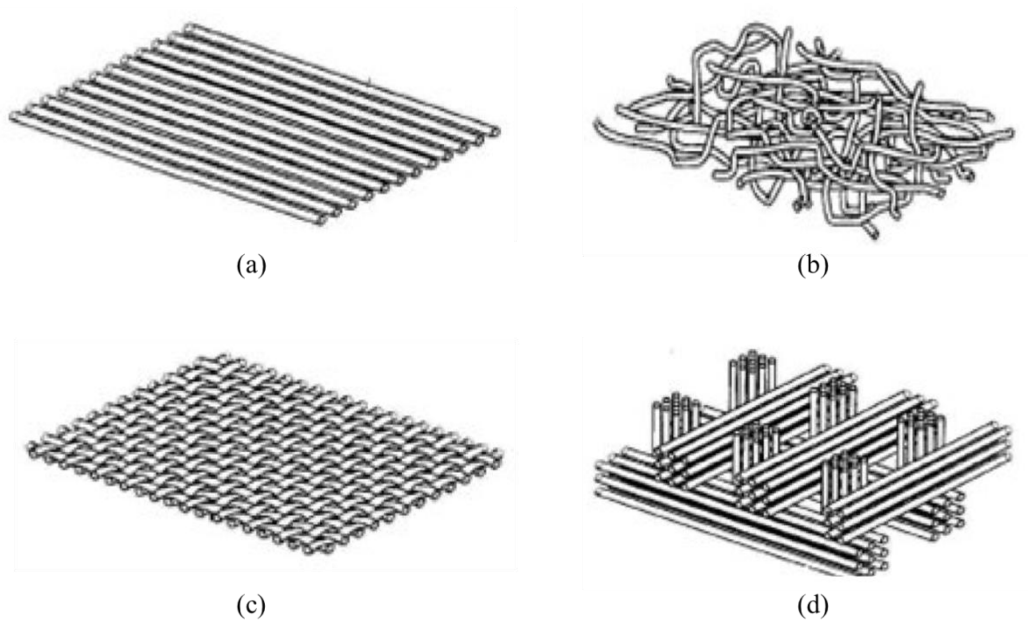

Figure 1-5 Different forms of reinforcement: (a) UD sheet, (b) mat, (c) woven fabric, (d) three-dimensional orthogonal woven fabric [8]

Textile preforming operations play a key role in most of the composite manufacturing processes. In textile process, there is direct control over fibre placements and ease of handling of fibres. Textile preform technologies provide homogenous distribution of matrix and reinforcing fibre. Thus, textile preforms are considered to be the structural backbone of composite structures. High performance multifilament fibres, such as glass, aramid and carbon fibres, which provide high tensile strength, modulus, and resistance to chemicals heat to various types of preforms, can be bound by necessary textile technologies. With textile preforming techniques, 2D/3D reinforced composites have achieved outstanding performances.

1.2 Laminate fibre reinforced composites

In reinforced composite material, reinforcement plays a role to fundamentally increase the mechanical properties. As previously mentioned, the typical used fibre material is carbon, glass, aramid, etc. Several thousand fibres are placed side by side with known directions and positions form textile reinforcement. Regarding the fabrication technology, the conventional textile technologies are used to design and manufacture fibre-reinforcements such as weaving, knitting, braiding and stitching.

In terms of the alignment plans of the constitutive fibres, the fibre-reinforcement can be classified into three groups: 1D fibre reinforcement in which the fibre are parallel and aligned in one direction; 2D fibre reinforcement in which the fibre are aligned on one plane of the structure (XY plane); and 3D fibre-reinforcement in which a set of fibres are aligned along the orthogonal axis (Z axis) corresponding to through thickness axis of the structure [31].

The laminated fibre reinforced composites are 2D structures which have been used for over 65 years in maritime craft, aircraft, automobiles and civil infrastructures. It becomes the majority of highly structural sectors because of the high stiffness and strength at low-density, high-specific energy absorption behavior and excellent fatigue performance [32].

As a two-dimensional layered fibre structure, the laminated fibre reinforcement is made by stacking various laminas one upon the other in specific order and relative orientation which is illustrated in Figure 1-6. Each ply can be a unidirectional layer of paralleled long continuous fibres aligned on one plane, or a layer of conventional 2D woven fabrics, as shown in Figure 1-7. The orientation of the lamina refers to the orientation of the longitudinal axis of the fibres in the case of unidirectional lamina. While in the case of 2D woven fabric, it refers to the orientation of the longitudinal axis of the warp yarns. The orientation of stacked laminas could vary between -90 ° and +90 °.

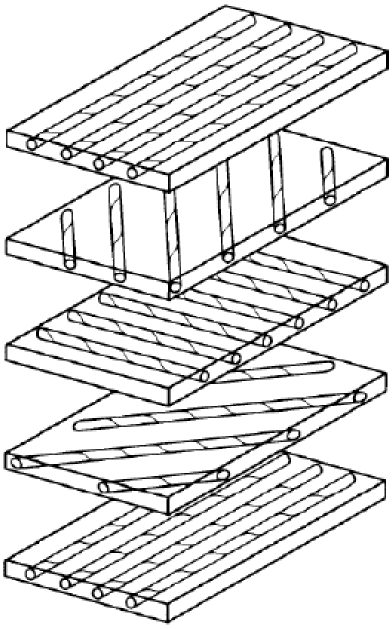

Figure 1-6 Laminate made by stacking laminas in different orientation. [33]

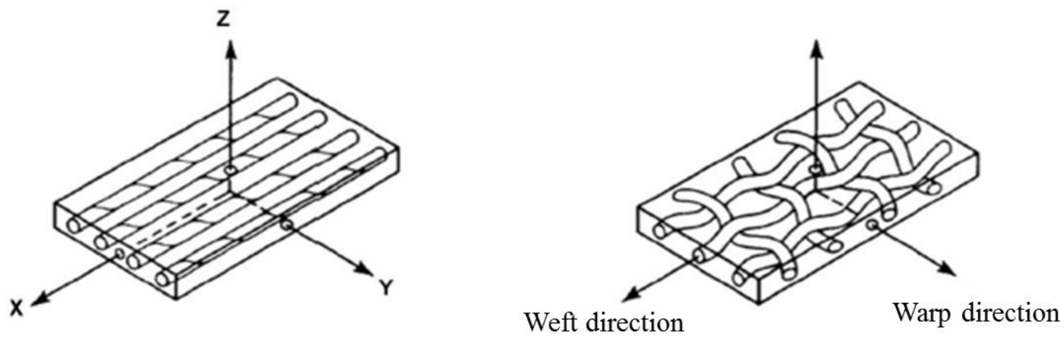

(a) (b)

Figure 1-7 Lamina fibre reinforced composite: (a) lamina with unidirectional fibre; (b) lamina with 2D woven fabric. [33]

Before lay-up process, unidirectional lamina made by filaments is usually saturated with resinous material which is called prepregs. The resinous materials are used as matrix which helps to maintain the aligned filaments in parallel and allows the easily handling in the next process.

The lay-up process consists of laying dry fabric layers or prepreg plies, onto a tool in specific orientation to form a laminate stack. For prepregs, filaments are already saturated with matrix material. While for dry piles, resin is applied after layup is complete. The principle lay-up processes include winding, laying and molding [33, 34].

Curing process consists of solidification of the matrix material to get the final rigid desired shape. Several curing methods are available. Cure can be accelerated by applying heat, typically with an oven, and pressure, by means of a vacuum.

The laminate composites provide a number of advantages. Comparing to metallic materials, the laminate composite presents high in-plane specific strength and high in-plane specific stiffness. In Figure 1-8, the comparison of specific strength and specific modulus between metallic materials (steel and aluminum) and laminate composite (graphite fibre, unidirectional graphite/epoxy lamina and cross-ply graphite/epoxy laminate) is illustrated [35]. The initial cost of the laminate composite material (raw material, design, fabrication and assembly) as well the operating cost is lower than in comparison with metallic materials [33]. The laminate composites have a light weight but high specific strength and specific stiffness which are used for transport applications to save the fuel cost.

But the use of laminate composites in many structural applications has been limited by their several drawbacks. As a directional material, its mechanical properties are not identical in all direction and they depend on the fibres directions which is the principal drawback. Their application in some critical structures in aircraft and auto mobiles has been restricted due to the absence of the through-thickness fibre reinforcement which reduces delamination resistance, damage tolerance, impact resistance and post impact properties [32, 36-38]. As presented in Figure 1-9, the strength and stiffness properties, in the through-thickness direction of the laminate, are often less about 10% of the in-plane properties [34]. Poor post impact mechanical properties of the laminates by showing the degradation of the in-plane tensile and compressive strength after impact are illustrated in Figure 1-10 [34]. Another drawback of the laminate composites is the increasing cost of forming a complex part shape because of the process of assembling and the high labor requirement [33]. In some industries, particularly the aircraft industry, the production cost is increased when fabricating laminates from prepreg tape, because expensive refrigeration facilities are needed to prolong the shelf lives of the prepreg before the resin begins to cure. This is a major problem in the aircraft industry, where structures such as wings need to be made from a large number of smaller composite parts such as skin panels, stiffeners and stringers, rather than being fabricated as a single integral structure [32]. Furthermore, the laminate composites present high thermal and moisture expansion coefficient and low operating temperature when use polymer matrix [35].

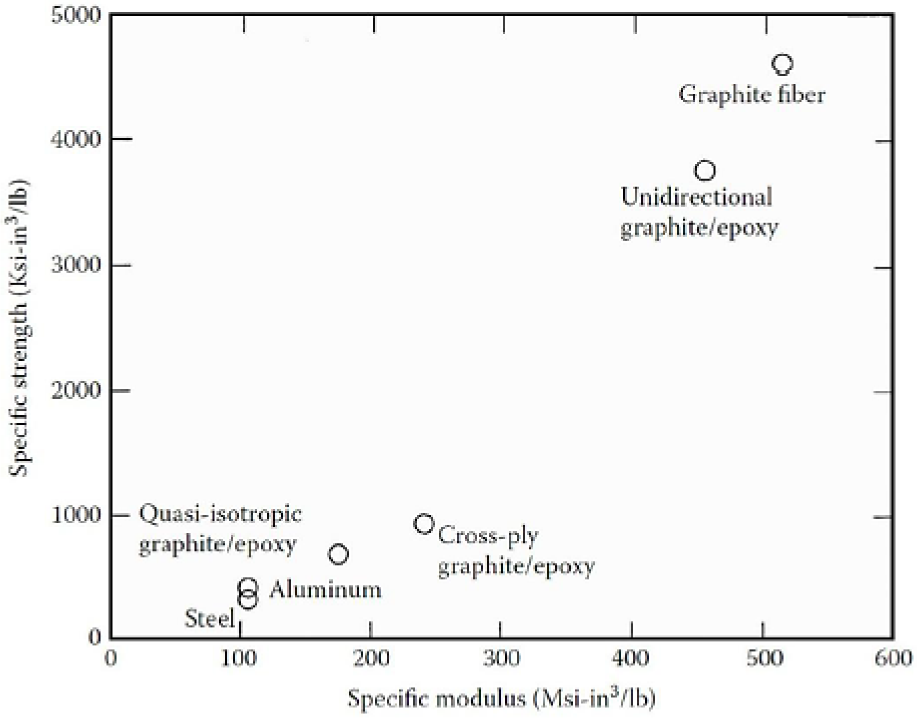

Figure 1-8 Specific strength in function of specific modulus of fibre, lamina, laminate and metals. [35]

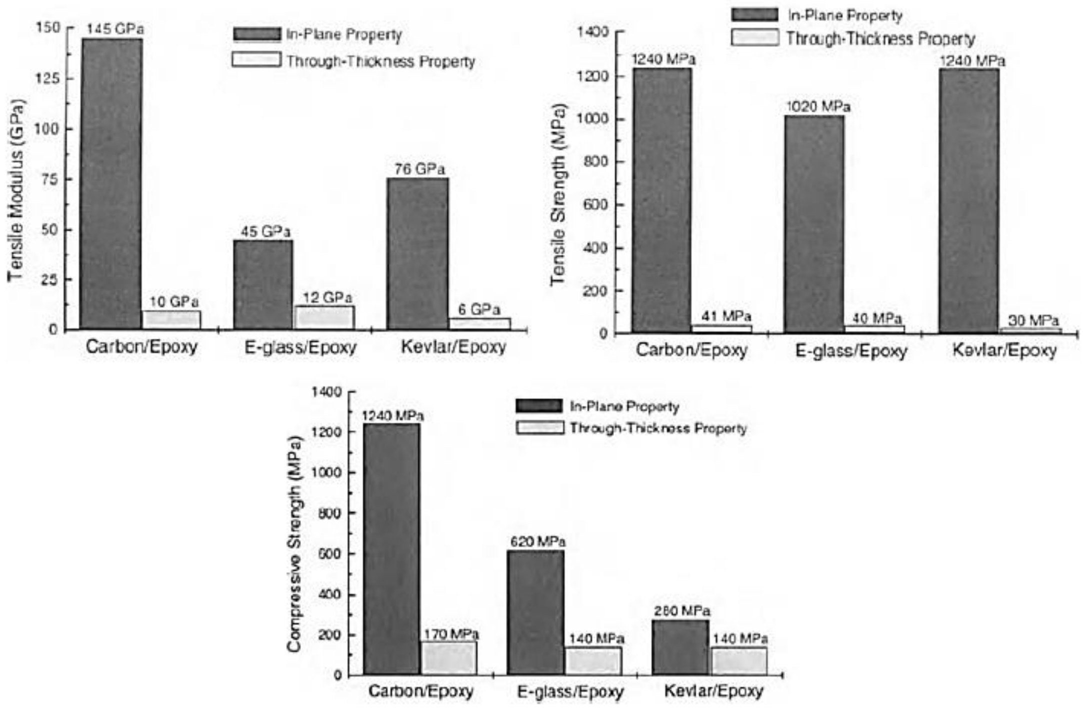

Figure 1-9 Comparison of the in-plane tensile modulus, tensile strength and compressive strength to that in the through thickness properties for laminate composite materials. [35]

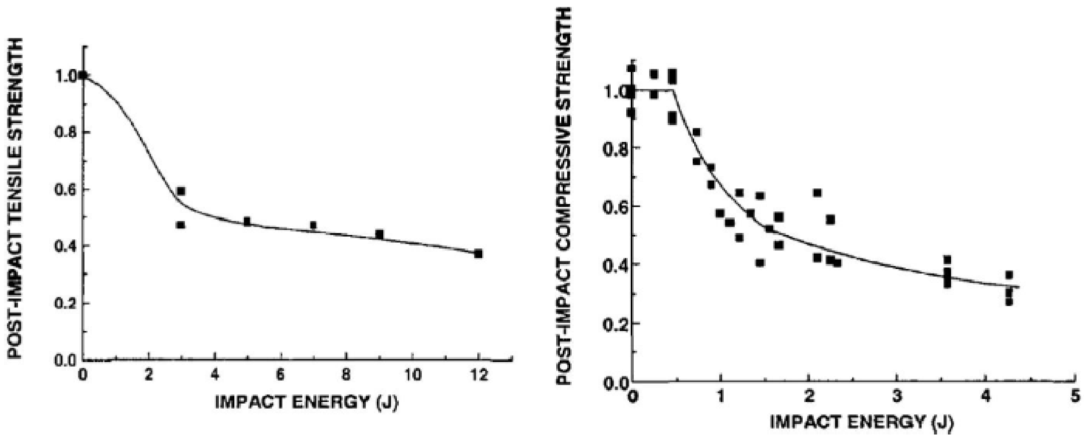

Figure 1-10 Degradation of the in-plane tensile and compressive strength after impact normalized to the strength before impact in function of the impact energy. [35]

1.3 The 3D reinforcements

In an attempt to overcome the problems appeared in laminate composites, the second generations of materials, 3D textile reinforced composite materials are obtained by applying highly productive textile technologies in the manufacture of fibre preforms [32].

The aim of 3D reinforcement is to introduce reinforcements on the third direction by using through-thickness fibres to improve their damage tolerance and the impact resistance. The simplest method is to insert fibrous structure through the thickness between the different plies of the composite laminate, this link being a stiff carbon fibre rod in the case of Z-pinning [40-43], or a thread (glass, carbon or aramid) in the case of stitching or tufting [43-45]. These fabrics are sometimes referred to as 2.5D fabrics, as the amount of fibres in the thickness direction is less than the fibres in the planar direction of the fabric [2]. Because of the existence of reinforcements in the thickness direction, the damage tolerance and the impact resistance are increased since the trend to delamination is drastically diminished [39]. The fully integrated system where fibres are oriented in various in-plane and out-of plane directions is called 3D structures. The additional reinforcement in the through-thickness direction makes the composite virtually delamination-free. Fully integrated 3D textile structures such as 3D woven, knits, braids and non-wovens can assume complex structural shapes [2]. Composite structures made with 3D textile fabrics are potentially less expensive to manufacture and provide better through-thickness mechanical properties compared to composites made with the traditional 2D fabrics [32]. The through-thickness fibres inserted by using a variety of textile processes, including 3D weaving, knitting, braiding, stitching or by specialist techniques such as z-pinning and tufting are introduced in this part.

1.3.1 Woven fibre reinforced composites

3D woven fabric or multilayered fabric is composed of several in-plane woven layers linked together by yarns passing in the through thickness direction of the fabric called binder yarns or weaver yarns. According to different weave patterns for binder yarns, 3D woven fabrics can be classified into three categories: layer-to-layer angle interlock, through-the-thickness angle interlock and orthogonal, as shown in Figure 1-11. In layer-to-layer angle interlock, the binder yarn passes from a layer to adjacent one, then it returns to the first layer thus it links just two adjacent layers. In through-the-thickness angle interlock, binder yarns pass through whole the thickness of the fabric across more than two columns of weft yarns. In orthogonal, binder yarn passes through whole the thickness of the fabric for each column of weft yarns. There is no interlacing between warp and weft yarns and they are straight and perpendicular to each other. Z-yarns combine the warp and the weft layers by interlacing along the y-direction over the weft yarn. Interlacing occurs on the top and the bottom surface of the fabric [46-49].

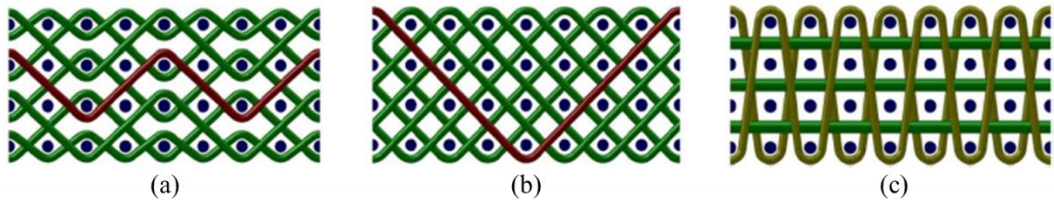

Figure 1-11 Typical 3D woven architectures: (a) layer-to-layer angle interlock; (b) through-thickness angle interlock; (c) orthogonal. [31]

The multilayered woven preform could be produced on a 3D weaving loom. Warp yarns are contained on a creel and fed into the weaving loom through a lifting mechanism, which selects and lifts the required yarns and creates a shed into which the weft yarns are inserted at right angles to the warp. The binder yarns can by aligned in the warp direction or inserted in the weft direction and their path through-the-thickness of the preform is controlled by the lifting sequence. [32]

3D weaving composites have many advantages comparing with 2D laminates. It can produce complex near-net-shape preforms, which can greatly reduce de cost of a component by reducing material wastage, the need for machining and joining, and the amount of material handled during lay-up. The binder yarn provides 3D woven composites with a high ballistic impact damage resistance, low-velocity impact damage tolerance, greatly increased tensile strain-to-failure values and higher interlaminar fracture toughness properties [32]. Guénon et al. [50] showed that even for low binder yarns content about 1% in 3D carbon/epoxy composite the delamination toughness for mode I is about 14% higher than for 2D carbon/epoxy prepreg laminates. Cox et al. [51] studied the failure mechanisms of 3D woven carbon reinforced polymer composites on tension, compression and bending. They observed that the 3D woven composites exhibit high strain to failure in tension as well in compression. Lomov et al. [52] compared between non-crimp 3D orthogonal woven composites and four-ply laminates of plain weave. He mentioned that 3D woven composites have a higher strength and failure strain.

1.3.2 Knitted composites

Knitting processes can be divided into two basic types: warp knitting and weft knitting (Figure 1-12). In weft knitting process, a single yarn is fed into the transversal direction of the knitting machine which forms a row of knit loop. In warp knitting process, multiple yarns are fed into the longitudinal direction of the machine and each yarn forms line of knit loops in the fabric direction.

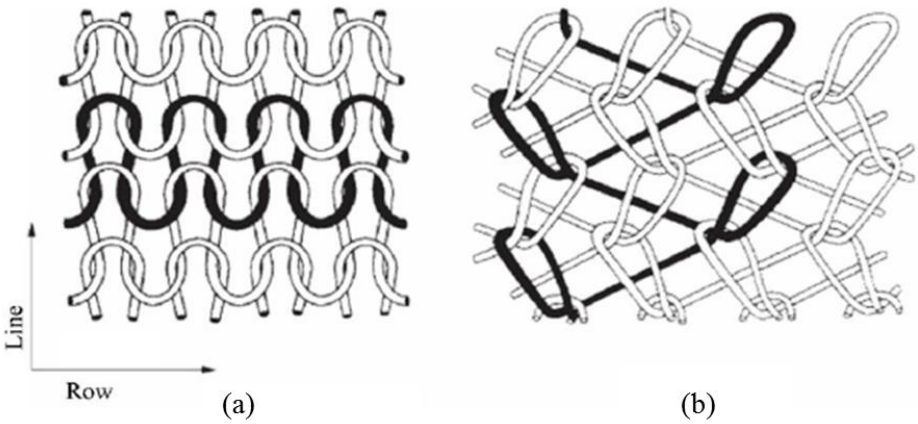

Figure 1-12 (a) Shematic of weft knitted fabric; (b) shematic of warp knitted fabric

3D knitted composites can be divided into three types which are broadly categorized as sandwich, non-crimp and near-net-shape composites. With the existence of loop form, knitting composites have better formability and can produce more complex near-net-shape preforms. They can be produced on existing automatic machines with little modification. However many 3D knitting machines are under developed and cannot make thick preforms. Knitted composite exhibits fracture toughness greater than conventional 2D woven, unidirectional or random mat composite [32].And some types of 3D knitted composites have lower specific density, higher impact damage tolerance and energy absorption properties [53]. 3D knitted composites generally have lower stiffness and strength properties. From the experimental study weft knitted composites present a similar in-plane performance with the random mat composite, which is much lower than that of conventional 2D woven composite [54, 55]. Weft knitting of non-crimp fabrics causes breakages and distortions to the in-plane fibres [32].

1.3.3 Braided composites

Braiding was the first textile process used to manufacture a 3D fibre preform for a composite [32].

Figure 1-13 illustrates a conventional braiding machine. Braiding yarns are held on carriers which are placed on a circular platform. The warp carriers move in a counter-clockwise direction, and the weft carriers move in a clockwise direction to form a 2D braid construction. A mandrel is placed in the center of the braiding platform to allow the braid to be constructed on its entire surface. In the case of 3D braiding, the carrier platform contains several rows of carriers. The carriers travel from row to row, creating an interlocking of the two-by-two layers (Figure 1-14) [56].

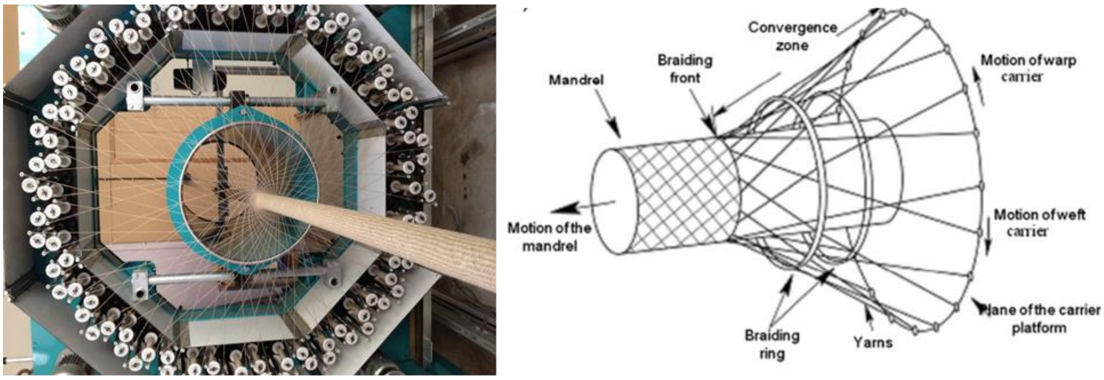

(a) (b)

Figure 1-13 (a) Overall view of a braiding machine (GEMTEX). (b) Description of the main elements of a braiding process [56].

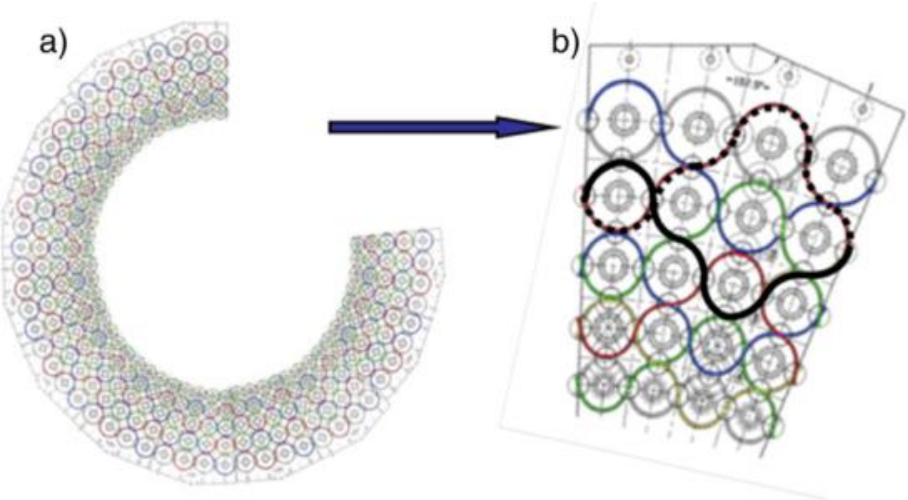

Figure 1-14 (a) Outline of the carriers on a 3D braiding machine; (b) detailed view of the motion of a horn-gear during a 3D braiding operation [56].

Braided preforms have good conformability, drapability, torsional stability and structural integrity. It is possible to produce complex near-net-shape preforms, which makes the manufacturing cost considerably lower because it reduces the amount of fabric handling and material scrap as is the need for extensive machining and joining [57]. The mechanical properties of the braided composite depend strongly on the amount of axial yarns, the angle of braided yarns and their braiding pattern. The 3D braid showed a less tensile strength in both directions and less transverse tensile modules, whereas the longitudinal compressive properties and tensile modulus were better than laminate [43]. 3D braiding composites also have higher delamination resistance, better impact damage tolerance and lower notch sensitivity than 2D laminates because of the through-thickness reinforcement [32].

3D braided composites have some limitations. One major limitation is that the preform size is relatively small because it depends on the braiding machine size, and most industrial machines are only capable of producing narrow preforms. Another limitation is the long set-up time of braiding machines. Some mechanical properties like stiffness and strength of 3D braided composites are generally lower than 2D laminates with an equivalent weight fraction of in-plane fibres [32].

1.3.4 Stitched composites

Stitched composites are 3D fibre reinforced composites produced by sewing high tensile strength yarn through an uncured prepreg laminate or dry fabric plies using an industrial sewing machine as illustrated in Figure 1-15 [43]. Glass, carbon, polyester thread and Aramid are typical reinforcing yarns. Different configuration of stitch could be sewed such as lock stitch, modified lock stitch and chain stitch. Through-thickness yarns have been stitched into composites with densities ranging from 0.4 to 25 stitches/cm^2, by using a variety of sewing machines which can usually be classified as single-needle or multi-needle machines [32, 43].

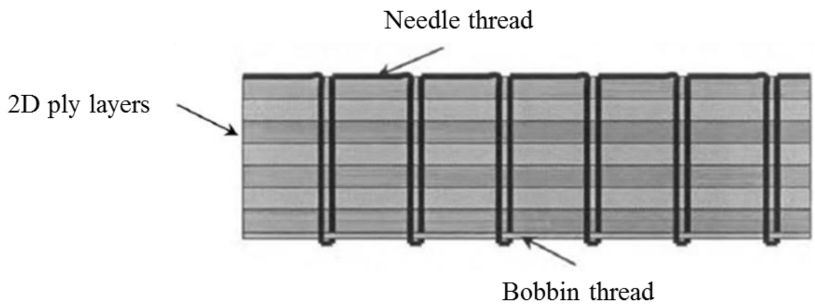

Figure 1-15 Stitched composite: stacked 2D laminas sewed with modified lock stitch. [43]

Stitching process is inexpensive and simple to manufacture. Stitching has considerable potential for joining composites and for improving the damage tolerance of structures such as aircraft wing panels. In contrast to the integral three-dimensional (3D) fibre structures typical of woven, knitted, and braided composites, the stitching process is characterized by the insertion of a through-the-thickness yarn into traditional two-dimensional (2D) preforms as a secondary processing step following lay-up [58]. Many mechanical properties are improved like impact damage tolerance, delamination resistance to ballistic impact and blast loading, interlaminar fracture toughness, interlaminar fatigue resistance, through-thickness tensile modulus and strength. Stitching increases the delamination resistance by reducing the crack opening displacement in mode I loading and resisting crack sliding displacement in mode II [59-61]. Bridging force offered by stitches significantly increases the ultimate strength of the material through high energy absorption in the process of fibre fracture and frictional pull-out [62]. Stitching arrests and improves crack closure by shielding the crack tip from the full effect of the crack opening stress [63, 64].

Over the past few years there have been a number of developments in stitching. A large, high-speed and multi-needle advanced stitching machine was designed and built under the ACT program by NASA to stitch large, thick, complex wing structures [65]. One-sided stitching (OSS®) technique is developed by inserting the thread under an angle of 45 ° and 90 ° [66-68]. Potluri et al. [69, 70] developed a single-needle stitching process for rigid and close-cellular foam core sandwich composites. However most industrial-grade sewing machines can only handle preforms less than 1m wide and 5mm thick which is too small for many aircraft structures. And industrial sewing machines can’t stitch preforms with complex structures because of the limited access for the needle head. Stitching usually degrades the in-plane mechanical properties because of the in-plane fibres being broken and distorted [32].

1.3.5 Z pinned composites

Z-pinning process can be defined as a kind of one-side stitching process. Thin pins are inserted into laminates through the thickness using manual of automated pinning process. Figure 1-16 presents the principal of z-pinned process. Pins are made of high stiffness and high strength material, such as fibrous carbon composites or titanium alloys [71].

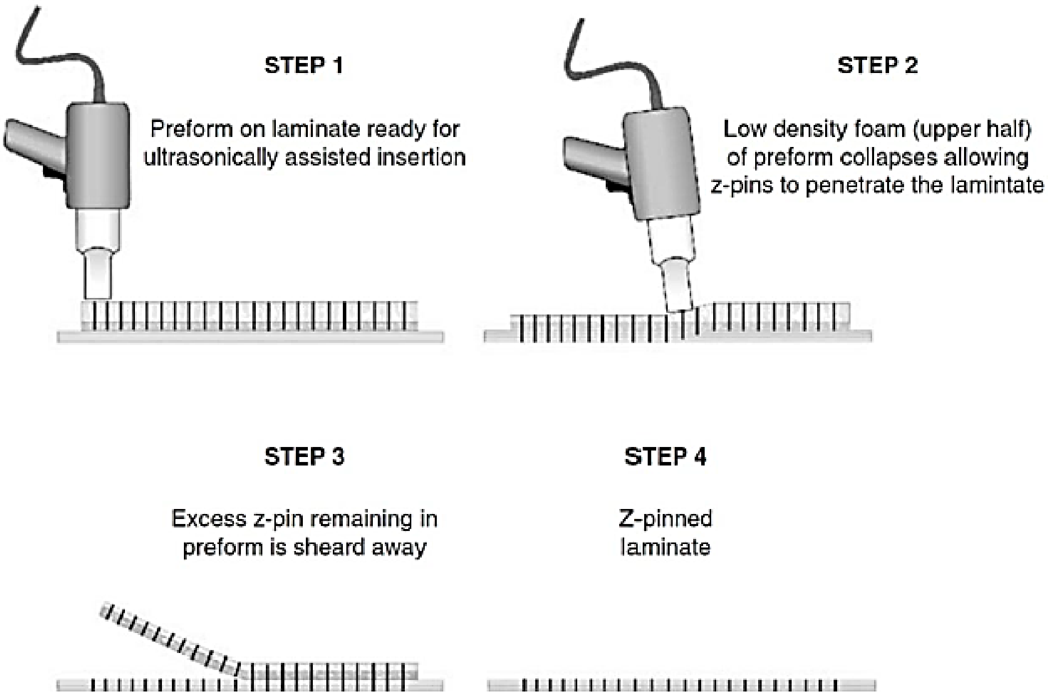

Figure 1-16 Schematic of the Z-pinning process of laminate composite [72].

The pins increases the delamination toughness, damage tolerance and the through thickness properties of the laminate [71, 73-78]. However, insertion of the pins in the through-thickness of the laminate causes microstructure damages: in-plane waviness, out-of-plane crimping and breakage of fibres, resin-rich regions and swelling of the laminate (to accommodate the pins). These microstructure damages lead to a reduction of the in-plane strength, stiffness and fatigue life of composite in comparison with equivalent laminate. Moreover, this reduction increases with the volume content increase and diameter of pins increase [79].

1.3.6 Tufted composites

Tufting process or Aerotiss® 03S is a typical one-side stitching technology [80]. It uses a single needle to introduce a thread from one side into the structure through the thickness without tension [81]. Tufting is considered a more economical and flexible method compared to 3D weaving or 3D braiding to include z-fibres in laminated composites. The most used tufting threads are Kevlar, glass fibres, carbon fibres and PET. Figure 1-17 shows the schematic of tufting process.

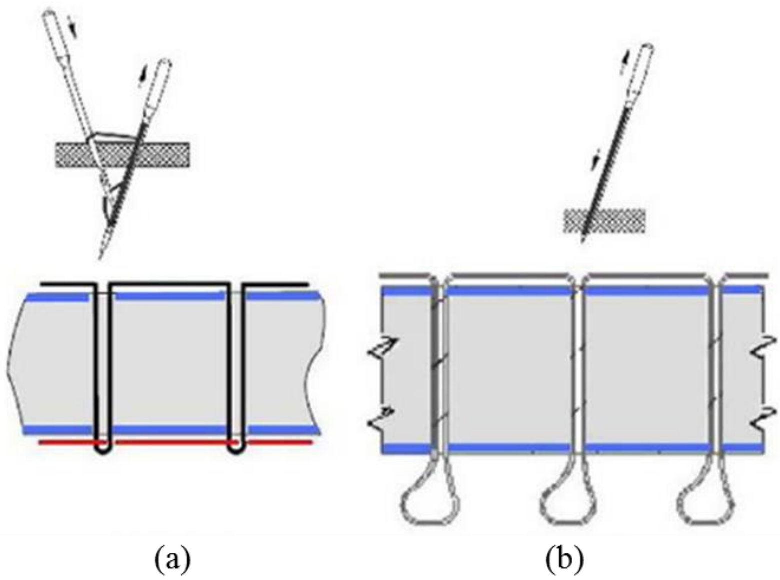

Figure 1-17 Schematics of (a) stitching and (b) tufting process applied to sandwich panels [80].

Comparing with the traditional stitching technology where two threads are bind by forming a knot in the preform which weakens the performance of reinforcement, tufting technology applies a tension-free tuft which can reduce the sewing effect to interlaminar performance and avoid weakened zone around the tuft [82-84]. Comparatively to the untufted panels, tufting increases significantly the stiffness and ultimate stress under bending, core shear and flatwise compression. Giuseppe Dell Anno et al [85, 86] have observed an increase of compression after impact strength by 25% and 27% of tufted composites due to the presence of carbon and glass tufting threads. They also found that there was a reduction in tensile strength by 10% and 5% in stiffness over the untufted specimens. Mathieu de Verdier et al [87] have experimented the effectiveness of the tufting in enhancing the through the thickness properties of non-crimp fabric and studied the response of tufted/untufted carbon –epoxy non crimp fabric composites. The authors concluded that 13.3% reduction in tensile strength, 12.6% reduction in tensile modulus, 10.52% reduction in compressive strength and 11.2% reduction in compressive modulus. They also found that there was a 15% improvement in shear, cyclic tensile and compressive strengths. The double cantilever beam results showed that the delamination resistance had increased significantly with tufting.

1.4 Conclusion of chapter 1

Advanced 3D textile composites materials have been wildly used with outstanding success in several industrial manufactures for their light weight, high specific stiffness, excellent corrosion resistance, fatigue resistance and impact resistance. Composites are made up of two constituent materials: matrix and reinforcement. Matrix is used to hold the reinforcements in an orderly pattern and helps to transfer load which includes thermosetting resins, thermoplastic resins and metallic matrices. Reinforcement plays a role to fundamentally increase the mechanical properties which can be carbon fibre, glass fibre, aramid fibre, etc. The main manufacturing processes of composite materials are also introduced in detail including the pre-impregnated processes and the liquid composite molding processes.

Conventional textile technologies are used to design and manufacture fibre-reinforcements. According to the alignment plans of the constitutive fibres, the fibre-reinforcement can be classified into three groups: 1D, 2D and 3D fibre-reinforcement. The laminated fibre reinforced composites are 2D structures which have been used for many decades. As a directional material, the lack of the through-thickness fibre reinforcement results in a low delamination resistance, poor through the thickness properties and poor toughness. 3D textile reinforced composite materials are developed to overcome these problems. Through-thickness fibres are introduces between the different plies of the composite laminates by different textile technologies such as 3D weaving, stitching, knitting, braiding, or by specialist techniques such as z-pinning and tufting. The manufacturing of perform using a particular process depends on the end application.

In contrast to the integral 3D fibre structures, the stitching process is characterized by the insertion of a through-the-thickness yarn into traditional 2D preforms as a secondary processing step following lay-up. Comparing with other manufacturing processes, stitching is simple to manufacture. While the formation of knots and the resulting tensioning of the thread can considerably weaken the mechanical properties due to undulation and constrictions. And the accessing of the needle from the underside to form the stitch is another drawback which increases the manufacturing complexity. As a result, tufting technology, a one-side stitching process has been explored.

The tufting process involves the insertion of a thread needle into a dry fabric or binder preform from one side and its removal from the fabric along the same trajectory. Tufting thread is held by fabric itself with low tension which results in a reduction of the stitching effect on the in-plane properties and the possibility of manufacturing complex and large composite structures. This technology is still under development and few works have been realized to characterize the geometry and the mechanical performance of produced preform. In next chapters, research works are carried out on the development of self-designed tufting equipment, influence of tufting parameters on characterizations and formability of tufted 3D composite reinforcements.

Reference of chapter 1

[1] Kaw AK. Mechanics of composite material. Taylor & Francis Group, United States of America, 2006.

[2] Miravete A. 3-D Textile Reinforcements in Composite Materials. Cambridge: Wookhead Publishing, 1999.

[3] Marwat MA. Composite materials, Presentation of University of engineering and technology. Peshawar materials engineering department. Available from:http://www.slideshare.net/MohsinAli70/composite-presentation-32469042

[4] Gay D. Matériaux composites. 4ème éd. Paris: Hermès, 672 p. (Matériaux) ISBN 2-86601-586-X, 1997.

[5] Ogin S. L. Textile-reinforced composite materials, chapter of Handbook of technical textile edited by Horrocks A. R. Anand S. C. Woodhead publishing Limited, England, 2000.

[6] Lucas P, Zanella G. Mise en oeuvre des composites TP. Compounds à fibres courtes et longues. Techniques de l'ingénieur, AM 5235, 8p., 2007.

[7] Peters S.T. Handbook of composites, second edition. Chapman & Hall, UK, 1982.

[8] Wang P. Etude numérique et expérimentale de procédé d'élaboration des matériaux composites par infusion de résine. Thèse de doctorat, Ecole Nationale Supérieure des Mines de Saint-Etienne, 2010.

[9] Negrier A, Rigal J.C. Présentation des matériaux composites. Techniques de l'ingénieur, A 7790.

[10] Chatain M. Matériaux composites : présentation générale. Techniques de l'ingénieur, AM 5000.

[11] Negrier A, Rigal JC. Présentation des matériaux composites. Techniques de l'ingénieur, A 7790.

[12] Premix. Why composites. Available from: http://www.premix.com/why-composites/adv-composites.php.

[13] Jedidi J. Etude du comportement en cyclage hygrothermique d'un matériau composite épais. Thèse de doctorat, Ecole Nationale Supérieure des Mines de Saint-Etienne, 2004

[14] Liotier PJ. Durabilité de nappes renforcées par nappes unidirectionnelles cousues. Thèse de doctorat, Ecole Nationale Supérieure des Mines de Saint-Etienne, 2008.

[15] Barrau JJ, Guedra D. Structures en matériaux composites. Techniques de l'ingénieur, BM 5080.

[16] Dursapt M. Mise en forme des matériaux composites. Cours de l'Ecole Nationale d'Ingénieurs de Saint-Etienne.

[17] Comparison of three resines. Shanchuan composites. Available from: http://www.qdscsz.com/Article/hyszyxjszy_1.html

[18] What are prepregs. About money. Available from: http://composite.about.com/od/eqptprepreggers/a/What-Are-Prepregs.htm

[19] Barala N, Guezenoca H, Daviesb P, Baleya C. High modulus carbon fibre composites: Correlation between transverse tensile and mode I interlaminar fracture properties. Materials Letters, 2008; 62(6-7): 1096-1099.

[20] Paracha WY. Textile composites. Course of Textile Institute of Pakistan. Available from: http://www.slideshare.net/wakasyounus/textile-composites

[21] Thomas GP. Composite prepregs- Manufacturing, benefits and applications. Available from: http://www.azom.com/article.aspx?ArticleID=8353

[22] Celle P. Couplages fluide/milieu poreux en grandes déformations pour la modélisation des procédés d'élaboration par infusion. Thèse de doctorat, Ecole Nationale Supérieure des Mines de Saint-Etienne, 2006.

[23] Resin transfer molding process. Molded fibre glass companies. Available from: http://www.moldedfibreglass.com/processes/processes/closed-molding-processes/resin-transfer-molding

[24] Qi B, Raju J, Kruckenberg T, Stanning R. A Resin Film Infusion process for manufacture of advanced composite structures. Composite Structures, 1999; 47 (1-4): 471-476.

[25] Antonucci V, Giordano M, Inserra S, Nicolais L. A case study of resin film infusion technology: the manufacturing of a composite stringer. In: the 10th European Conference on Composite Materials (ECCM-10), 3-7 June, Brugge, Belgium, 2002.

[26] Thibaudeau M, Shenoi RA. Understanding flow behaviour in the resin infusion process. In: 10th European Conference on Composite Materials (ECCM-10), 3-7 June, Brugge, Belgium, 2002.

[27] Antonucci V, Giordano M, Nicolais L, Calabro A, Cusano A, Cutolo A, Inserra S. Resin Flow monitoring in resin film infusion process. Journal of Materials Processing Technology, 2003; 143-144: 687-692.

[28] Wang P, Molimard J, Drapier S, Vautrin A, Henrat P. Monitoring the Liquid Resin Infusion (LRI) manufacturing process under industrial environment using distributed sensors. 17th International conference on composites materials (ICCM-17), July, Edinburgh, Uk, 2009.

[29] Ogale V, Alagirusamy R. Textile preforms for advanced composite. Indian journal of fibre & textile research, 2004; 29: 366-375.

[30] Willians C, Summerscales J, Grove S. Resin infusion under flexible tooling (RIFT): a review. Composites Part A: Applied Science and Manufacturing, 1996; 27 (7): 517-524.

[31] Labanieh AR. Development of 3D multiaxis woven preforms for composite structures technology, modelling and optimization. Doctoral thesis, Université de Lille 1, 2016.

[32] Mouritz AP. Review of applications for advanced three-dimensional fibre textile composites. Composite: Part A, 1999; 30: 1445-61.

[33] Robert MJ. Mechanics of composite materials, 2nd ed., Taylor & Francis Group, United States of America, 1991.

[34] Tong L, Mouritz AP. and Bannister M.K. 3D fibre reinforced composites. Elsevier Science Ltd. UK, 2002.

[35] Kaw A.K. Mechanics of composite material. Taylor & Francis Group, United States of America, 2006.

[36] Anahara M, Yasui Y, Omori H. Three-dimensional textile and method of producing the three dimensional textile. European patent, 1991: 0-426-878-A1.

[37] Chou TW. Microstructural design of fibre composites. Cambridge: Cambridge University Press,1992: 382–390.

[38] Sih GC and Skudra A. Failure mechanics of composites. New York: Elsevier Science Publishers BV, 1986.

[39] Miravete A. 3-D Textile Reinforcements in Composite Materials. Cambridge: Wookhead Publishing, 1999.

[40] Partridge IK, Cartié DDR, Bonnington T. Manufacture and performance of Z-pinned composites. In: Advani S, Shonaike G, editors. Advanced polymeric materials: structure-property relationships. CRC Press, 2003; ISBN 1-58716-047-1.

[41] Partridge IK, Cartié DDR. Delamination resistant laminates by Z-Fibre® pinning. Part I Manufacture and fracture performance. Composites A, 2005; 35: 55–64.

[42] Rugg KL, Cox BN, Massabò R. Mixed mode delamination of polymer composite laminates reinforced through the thickness by z-fibres. Composites A, 2002;33:177–90.

[43] Tong L, Mouritz AP, Banninster MK. 3D fibre reinforced polymer composites. Elsevier, 2002.

[44] Wittig J. Recent development in robotic stitching technology for textile structural composites. J Text Apparel Technol Manage, 2001; 2: 1–8.

[45] Sickinger C, Herrmann A. Structural stitching as a method to design high-performance composites in future. Available from: http://www.dlr.de/fa/publikationen/2001/11_sickinger.pdf.

[46] Lomov S, Verpoest I and Robitalle F. Manufacturing and internal geometry of textiles, Woodhead publishing limited. Design and Manufacture of Textile composites, 2005: 1-61.

[47] Leong KH, Lee B, Herszberg I, Bannister MK. The effect of binder path on the tensile properties and failure of multilayer woven CFRP composites, 2000; 60: 149–56.

[48] Khokar N. 3D-weaving: Theory and Practice. Journal of the Textile Institute, 2001; 92(2): 193-207.

[49] Khokar N. Noobing: A Nonwoven 3D Fabric-forming process explained. Journal of the Textile Institute, 2002; 93(1): 52-74.

[50] Guenon VA, Chou TW, Gillespie JW. Toughness properties of a three-dimensional carbon-epoxy composite. Journal of Material Science, 1989: 24: 4168-4175.

[51] Cox BN, Dadkhah MS, Morris WL, Flintoff JG. Failure mechanisms of 3D woven composites in tension, compression, and bending, Acta Materialla Material, 1994; 42(12): 3967-3984.

[52] Lomov SV, Ivanov DS, Perie G, Verpoest I. Modelling 3D fabrics and 3D reinforced composites: challenges and solutions. 1st World conference on 3D Fabrics, Manchester, 2008.

[53] Pandita SD, Falconet D, Verpoest I. Impact properties of weft knitted fabric reinforced composites. Composite Science Technology, 2002; 62: 1113–1123.

[54] Ramakrishna S. Characterization and modeling of the tensile properties of plain weft-knit fabric-reinforced composites. Composites Science and Technology, 1997; 57: 1-22.

[55] Huang ZM, Zhang Y, Ramakrishna S. Modeling of the progressive failure behavior of multilayer knitted fabric-reinforced composite laminates. Composite Science Technology, 2001; 61(14): 2033–2046.

[56] Guyader G. Analysis of 2D and 3D circular braiding processes: Modeling the interaction between the process parameters and the pre-form architecture. Mechanism and Machine Theory, 2013; 69: 90-104.

[57] Tolosana N. Development of a geometrical model for a 3D braiding unit cell based on braiding machine emulation. Finite element modeling of textiles and textile composites, 26-28 September 2007.

[58] Zhang X. Mechanical behavior of stitched 3D composite. 15h European conference on composite materials, Venice, Italy, 24-28 June 2012

[59] Sun X, Tong L, Wood MDK, Mai YW. Effect of stitch distribution on mode I delamination toughness of laminated DCB specimens. Compos Sci Technol, 2004; 64: 967-981.

[60] Tan KT, Watanabe N, Iwahori Y, Hoshi H, Sano M. Interlaminar fracture toughness of vectran-stitched composites-experimental and computational analysis. J Compos Mater, 2010; 44: 3203-3229.

[61] Massabo R, Cox BN. Concepts for bridged mode II delamination cracks. J Mech Phys Solid, 1999; 47: 1265-1300.

[62] Tan KT, Watanabe N, Iwahori Y. Experimental investigation of bridging law for single stitch fibre using interlaminar tension test. Compos Struct, 2010; 92: 1399-1409.

[63] Cox BN. Constitutive model for a fibre tow bridging a delamination crack. Mech Compos Mater Struct, 1999; 6: 117-138.

[64] Cox BN, Massabo R, Kedward KT. Suppression of delaminations in curved structures by stitching. Composites Part A, 1996; 27A: 1133–1138.

[65] The advanced stitching machine. NASA, Langley Research Centre. August 1997. Available from: http://oea.larc.nasa.gov/PAIS/ASM.html.

[66] Mitschang P, Ogale A. Tailoring of textile preforms for fibre-reinforced polymer composites. Journal of Industrial Textiles, 2004; 34(2): 77-96.

[67] Wittig J. Robotic Three-Dimensional Stitching Technology, Proc. Int. SAMPE Conference: A material and Processes Odyssey, Long Beach, California, USA, 6-10 May 2001.

[68] Wittig J. Recent development in the robotic stitching technology for textile structural composites. Journal of Textile and Apparel, Technology and Management, 2001; 2(1).

[69] Potluri P, Kusak E, Cumellas AJ. Structural performance of orthogonal and bias stitched sandwich structures with rigid close-cellular foams. American Institute of Aeronautics and Astronautics, 2003.

[70] Potluri P, Kusak E, Reddy T Y. Novel stitch-bonded sandwich composite structures. Composite Structures, 2003; 59: 251-259.

[71] Mouritz AP. Compression properties of z-pinned composite laminates. Composite Science Technology, 2007; 67(15-16): 3110–3120.

[72] Chang P, Mouritz AP, Cox BN. Elevated Temperature Properties of Pinned Composite Lap Joints. Journal of Composite Material, 2008 ; 42(8): 741–769.

[73] Pegorin F, Pingkarawat K, Daynes S, Mouritz AP. Influence of z-pin length on the delamination fracture toughness and fatigue resistance of pinned composites. Composites Part B, 2015; 78: 298-307.

[74] Cartié DDR, Troulis M, Partridge IK. Delamination of Z-pinned carbon fibre reinforced laminates. Composite Science and Technology, 2006 ; 66(6): 855–861.

[75] Nanayakkara A, Feih S, Mouritz AP. Experimental impact damage study of a z-pinned foam core sandwich composite. Journal Sandwich Structure Material, 2012; 14(4): 469–486.

[76] Koh TM, Isa MD, Chang P and Mouritz AP. Improving the structural properties and damage tolerance of bonded composite joints using z-pins. Journal of Composite Materials, 2012; 46: 3255-3265.

[77] Chang P, Mouritz AP, Cox BN. Properties and failure mechanisms of z-pinned laminates in monotonic and cyclic tension. Composites A, 2006; 37: 1501–1513.

[78] Chang P, Mouritz AP, Cox BN. Flexural properties of z-pinned laminates. Composites A, 2007: 38: 224–251.

[79] Henao A, Carrera M, Miravete A. Mechanical performance of through-thickness tufted sandwich structures. Composite Structures, 2010; 92: 2052-2059.

[80] Bertrand J, Desmars B. Aerotiss® 03S stitching for heavy loaded structures. JEC-Composites, 2005; 18: 34-36.

[81] Liu L, Zhang T, Wang P, Legrand X, Soulat D. Influence of the tufting yarns on formability of tufted 3-Dimensional composite reinforcement. Composite: Part A, 2015; 78: 403-411 .

[82] Henao A. Mechanical performance of through-thickness tufted sandwich structures. Composite Strutures, 2010; 92: 2052-2059.

[83] Sickinder C. Structural Stitching as a Method to design High-Performance Composites in Future. TechTextil Conference, 2001.

[84] Pérès P. Composite behavior of assemblies with AEROTISS® 03S technology. 16th international conference on composite materials, 2007.

[85] Cartié DDR, Dell'Anno G, Poulin E, Partridge IK. 3D reinforcement of stiffener -to-skin T-joints by Z-pinning and tufting. Journal of Engineering Fracture Mechanics, 2006; 73: 2532–2540.

[86] Dell'Anno. G, Cartié DDR, Allegri G, Partridge IK, Rezai A. Exploring mechanical property balance in tufted carbon fabric/epoxy composites. Journal of Composite, Part A, 2007; 38: 2366–2373.

[87] Colin de Verdiere M, Pickett AK, Skordos AA, Witzel V. Effect of tufting on the response of non crimp fabric Composites. ECCOMAS Thematic conference on mechanical response of composites. Porto, Portugal, 12-14 September 2007.

2 TUFTING PROCEDURE: A METHOD TO MANUFACTURE OR ASSEMBLE THROUGH-THICKNESS REINFORCEMENTS

2.1 Introduction

Developed from conventional stitching technology, tufting technology is a method used to link together dry reinforcements or strengthen composite by inserting thread through the thickness of the preform. It involves the novel aspect that it uses a single needle to introduce a thread into the structure without tension. In traditional stitching technology or other technology such as braiding and knitting technology, threads are bound by forming a knot or interlocks in the preform. Because of the shear force between the threads, the performance of the reinforcement is weakened. Comparing with other 3D forming technologies, tufting applies a tension-free tuft which can reduce the sewing effect to interlaminar performance and avoid weakened zone around the tuft.

In order to carry out the tufting process, automated tufting equipment has been designed and developed using a CAD software in this study. This equipment consists of four parts:

the tufting system, the presser foot system, the feeding system and the frame. The tufting system carries a tufting needle which is controlled by a pneumatic cylinder to insert tufting yarn with different tuft lengths. Another pneumatic cylinder is linked with the presser foot and is installed alongside to adjust the pressure. The feeding system carries the tufting thread bobbin and provides tufting thread with a set length and pre-tension. The frame helps to move the tufting head. With this equipment, the important tufting parameters such as tufting density, tuft length, tufting direction and pressure of presser foot can be controlled. The maximum tuft length is determined by the range of pneumatic cylinder controlling the needle. With this self-designed and fabricated equipment, it is possible to produce tufting preforms.

2.1.1 Introduction of stitching process

Traditional stitching composites can be produced on sewing machine by dealing with one or two systems of yarns, which is inserted by a needle from the top side through the thickness and received by a cycloid gear at the bottom side. Different configuration of stitch could be sewed such as lock stitch, modified lock stitch and chain stitch.

The traditional interlock pattern or double lock stitch is usually used in garment industry. As shown in **Figure 2-1**a, two threads cross in the middle of textile to form a loop which becomes a stress concentrated point. Traditional interlock pattern cannot be applied in composite industry because of its fragile thread crossed points. As a result, modified lock stitch appeared which is presented in **Figure 2-1**b. In this kind of pattern, yarns were less curled and fibres were less damaged which can confirm continuous production, improve interlaminar strength and enhance damage tolerance [1].

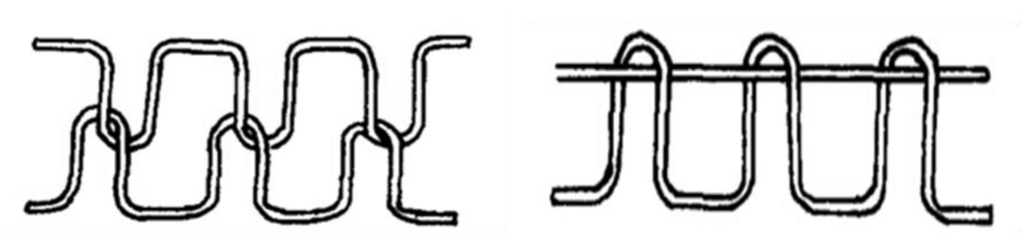

(a) (b)

Figure 2-1 Schema of conventional lock stitch (a) and modified lock stitch (b). [1]

Another stitching method called chain stitch is shown in Figure 2-2. It presents a more complicated seam trajectory which is like knitting process. Compared with lock stitch, chain stitch provides a better producing efficiency because there is no need to change bobbin thread [2].

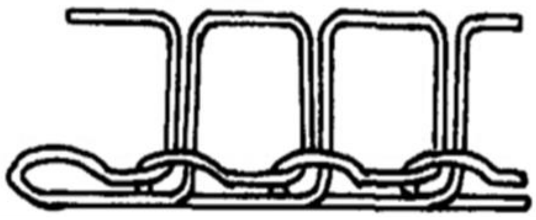

Figure 2-2 Schema of chain stitch. [2]

However, most composite reinforcements which have a 3D structure with simultaneous large spatial expansion are not adapted to process of traditional two-side stitching. For instance the two thread lockstitch requires access to the work piece from both sides. As a result, two kinds of one-side stitch patterns are developed to handle thicker preforms and to meet different industrial needs.

To overcome the existing limits of the well-known stitching techniques, ALTIN Nähtechnik has brought out the OSS® technology which only requires access to the work piece from one side. The stitch formation mechanism of OSS® technology is based on the principle of the simple chain stitch. A stitching thread is manipulated by two stitching tools, a conventional needle and a catcher (see Figure 2-3a). Both stitching tools are driven along a translatory route at the top side of the work piece, and their moving axes form a point of intersection below the stitching material. The inserting angles of the stitching tools can be varied within certain limits. The final position of the stitching thread in the fibre reinforced plastic structure is determined by the inserting angles. The optical angles are determined to be 45° and 90° [3]. The catcher-needle takes over the loop of the stitching thread produced by the needle and pulls it back through the work piece to the top side through the loop of the previously formed stitch which is located on the shaft of the catcher-needle. In this way the interlocking of the stitching thread is formed. The interlocking of the sewing thread take place on the top side which reduce damages and curls to the yarn and improve interlaminar strength and enhance damage tolerance. The stitch pattern is presented in

Figure 2-3b. OSS® technology is suitable to strengthen structures with the form of "L" or "T" [3]. It is not necessary to arrange stitch formation element underneath the work piece, only need to consider the free space for penetration of the needles [4-6].

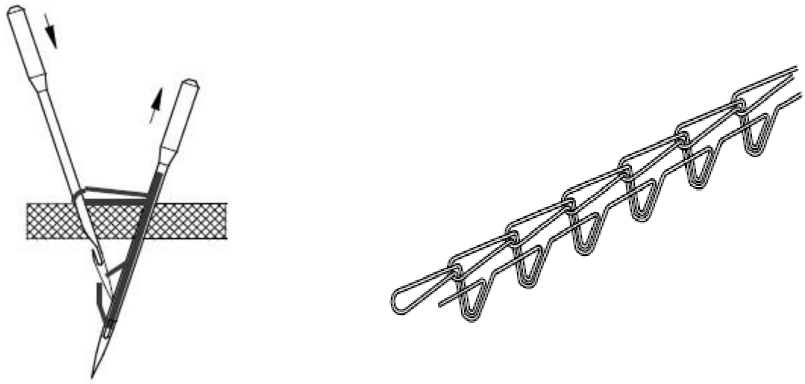

(a) (b)

Figure 2-3 One-side stitching needle (a) and schema of OSS® technology (b). [3]

In above-mentioned stitching process, a dual-threading system makes the seam by forming loops and knots. This kind of seam significantly deteriorates the mechanical performance of the 3D fibre architecture. The tufting technology or Aerotiss® 03S developed by ASTRIUM is based on the conventional stitching process but involves the novel aspect that it uses a single needle to introduce a thread into the structure without tension (see Figure 2-4). The major target of this technology is the insertion of load taking threads in z-direction, which can be executed also under various angles. This results in a reduction of the stitching effect on the in-plane properties and is achieved by not interlocking the stitches of the seam which would require a tightening of each single stitch [3].

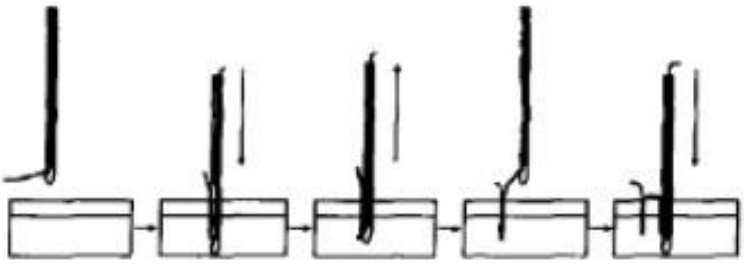

Figure 2-4 Tufting technology: Aerotiss® 03S. [7]

After injection of the resin, the structure is consolidated in one piece with higher properties than one without reinforcement through the thickness. Essentially, tufting is equivalent to Z-pinning, but used to reinforce dry fabrics (prior to resin injection) using Liquid Composite Moulding techniques [8, 9]. Compared to Z-pinning technique, the stitches don't introduce resin cavity. Because of the efficient embedment of the stitching yarns inside the fibre preforms, load transmission is more efficient. The performance of such joint is strongly linked to compromise of the required quantity of stitching yarns and the volume fraction of fibre in the joint area [10, 11].

2.1.2 Introduction of tufting technology

Tufting is a relatively novel technique which is based on the ancient methods of carpet making and recently used for achieving through-the-thickness reinforcement in thermoset polymer matrix composites. It is ideally suited to load-bearing structures intended to be made via dry-fabric/liquid resin infusion processes. The tufting technology involves the insertion of yarns in z-direction (through the thickness) in order to strengthen fibre-reinforced plastics or link two or more fabric preforms together. A threaded needle is inserted into a dry-fabric or bound preform and then removed from the fabric along the same trajectory. The "tuft" of thread relies on friction from the fabric itself and/or hold provided by underlying ancillary material (e.g. foam) to remain in place, and the loop of thread, which appears at the bottom of the work piece or hidden in the fabric preform according to different needs [12], is not locked in place. The tufting process can be used to bind thick structures because of its need for only one side access.

Compared with traditional stitching techniques, where two threads are bound by forming a knot in the preform which weakens the performance of reinforcement, tufting applies a tension-free tuft which can reduce the sewing effect on interlaminar performance and avoid the zone around the tuft being weakened [8, 13, 14]. Free loops can be hidden in fibrous structure or appeared at the bottom of workpiece according to different need.

2.2 Parameters of tufting process

Comparatively to the untufted panels, tufting increases significantly the stiffness and ultimate stress under bending, core shear and flatwise compression [8]. The percentage of gain depends on the structural parameters of the tufted panels. Tufting process can be fully automatized. It is thus possible to change various parameters such as tuft length, tufting thread diameter, space between tufting points and areal tufting density (see Figure 2-5).

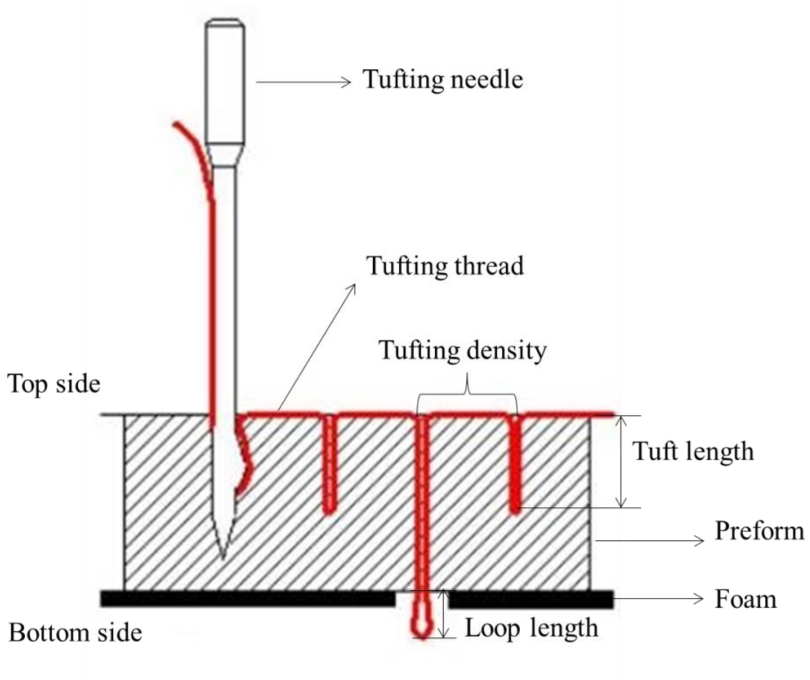

Figure 2-5 Parameters of tufting process.

2.2.1 Tufting density

Tufting density refers to the total number of tufts in a measured area of fabric (units of tufts/cm^2 or tufts/m^2). When the preform is tufted with a permanent tufting density, tufting spacing can be used to describe tufting density. Tufting spacing refers to the distance between two points of tufts. In this study, tufting spacing applied varies from 5mm to 20mm according to different test requirements. Interlaminar shear strength grows with tufting density because of the additional insertion of fibrous structure along thickness. However more points are tufted, overall performances of material are worse because of the damage caused by the needle and misalignment of fibre. Thus, for the high tufting density (step of 12.5 mm) the improvement of the performances can reach 250% for bending rigidity and 1000% for the shear failure stress [6]. It is obvious that the increase of the tufting density improves the mechanical properties considerably. On the other hand this increase leads to an increase of the mass and consequently a loss of specific properties. Mathieu de Verdier et al [16] studied the response of tufted/untufted carbon–epoxy non crimp fabric composites and concluded that 13.3% reduction in tensile strength, 12.6% reduction in tensile modulus, 10.52% reduction in compressive strength and 11.2% reduction in compressive modulus. Consequently, a compromise must be found.

2.2.2 Tuft length

Based on industrial carpet manufacturing process, tufting requires the insertion of additional tows through the layers of a laid-up dry perform. The length of tows inserted into fibrous preform is called tuft length or tufting depth. According to the difference between tuft length and preform thickness, tufting procedures can be divided into two sections: the tows are fully inserted (Figure 2-6a) or applied to a partial depth through the preform thickness (Figure 2-6b). When tufting thread is partially inserted into fibrous structure, tuft length is equal to the length of tows inserted but shorter than preform thickness. When tufting thread is fully inserted, a loop of yarn is formed at the bottom side which is held by foam. In this case tuft length is the sum of preform thickness and loop length. In our case, tuft length can be up to 50mm which is decided by the range of pneumatic cylinder which control the movement of needle. Tuft length can affect mechanical properties of tufting preforms.

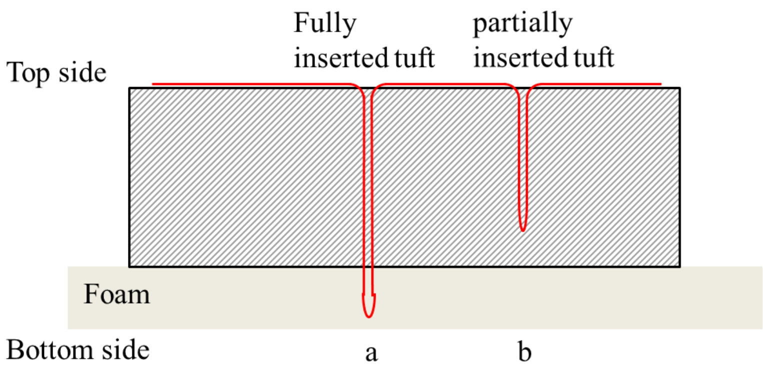

Figure 2-6 Schematic of the thread arrangement in a tufted preform.

2.2.3 Other parameters

Tufting angle is another parameter which influence preforms structure. During the tufting process a thread is introduced into a preform by a needle under varies angles. The mostly used tufting angles are 90 °, 60 ° or 45 °. Concerning the effect of the tufting angle on the mechanical properties, a compromise should be found. The angle of 45 ° offers the best performance on bending and shear behavior, whereas the angle of 60 ° presents the best properties on the compression behavior [17]. The choice of structural parameters will depend on the specification of the structure.

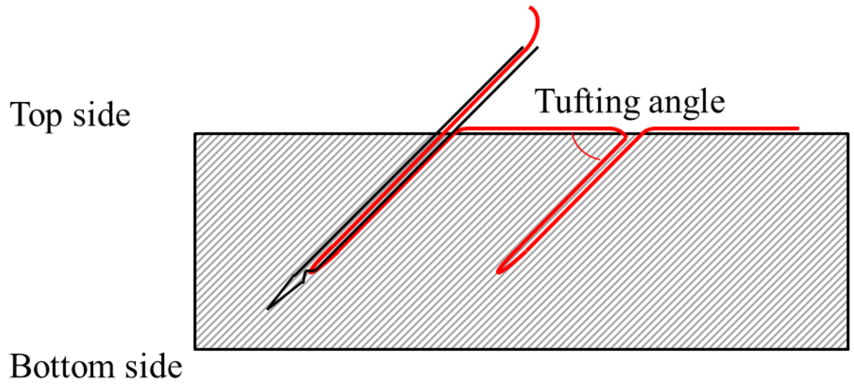

Figure 2-7 Schematic of tufting angle.

The choice of tufting thread can also affect tufting process. Specialized continuous yarns are required in tufting process. The thread must be not only suitable for tufting but also compatible with the liquid resin moulding type processes for composites manufacture and with the subsequent mechanical and durability performance demands on the final composite. An ideal thread would have a high tensile strength, certain extensibility and should be resistant to abrasion. The most used tufting threads are Kevlar, glass fibres, carbon fibres and PET [17]. Among them Kevlar is used mostly because of its high resistance to abrasion and impact as well as its low density. Tufting thread should have also a relatively high twist level, which gives the need of high flexibility in bending to withstand the sharp kink from the needle during insertion. This is particularly important when the filaments adopted are fragile in bending, as in case of carbon fibre[13]. Tan et al.[18] study the effect of stitching parameters on the low-velocity impact damage. They show that thread diameter does not really affect energy absorption but allows better delamination limitation.

The form of tufting needle is also a parameter to effect tufting structure. To enable the insertion of thread loops into the dry preform without interlocking, tufting needles with an inclined hole at the tip of the needle is needed. Needles with different diameters are chosen according to the preforms structure and tufting thread's performances. Most tufting thread such as flex, Kevlar or twisted carbon yarns can be tufted into soft preforms with these needles. However, when tufting a fragile carbon thread into a thicker and harder preform, another hollow needle with a cavity in the middle of the needle is specially designed. Tufting thread is protected by the hollow needle to avoid the additional friction from the preform. The choice of tufting needle is crucial depending on the performances of tufting thread and materials.

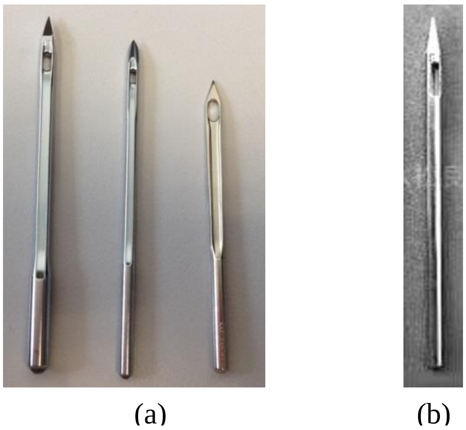

Figure 2-8 Tufting needles with inclined hole (a) and hollow needle (b).

Other parameters such as pressure of presser, tufting pattern can also affect tufting preform performances.

2.3 Tufting machine

In order to carry out tufting process and to deal with tufting parameters, an automated tufting facility is designed to produce the through-thickness reinforced dry fibre preforms. Reinforcement of complicated structures is no longer limited by the design or the size of the tufting machine.

2.3.1 Functions of the machine

This equipment consists of four parts: tufting system, presser foot system, feeding system and the frame. Tufting system carries a needle which is controlled by a pneumatic cylinder to insert tufting yarn with different tuft lengths. Presser foot is linked with another pneumatic cylinder which is installed alongside to adjust pressure and to press the preform to avoid tufting thread being drawn off. Feeding system carries tufting thread bobbin and provide tufting thread with a certain length and pre-tension. The frame carries the preform and all other systems and provides the possibility to measure and control tufting density.

2.3.2 Designing of the machine

After considering of all functions of the machine, a tufting equipment has been designed and developed by using the CAD software “solidworks”. The drawing of tufting device is shown in Figure 2-9(a).

To obtain the functions above, several pieces are designed and manufactured. After a lot of attempts and debugs, the combination of finals pieces is determined, which are shown in Figure 2-9(b) and Figure 2-9(c). All pieces are introduced according to their functions in follow paragraphs.

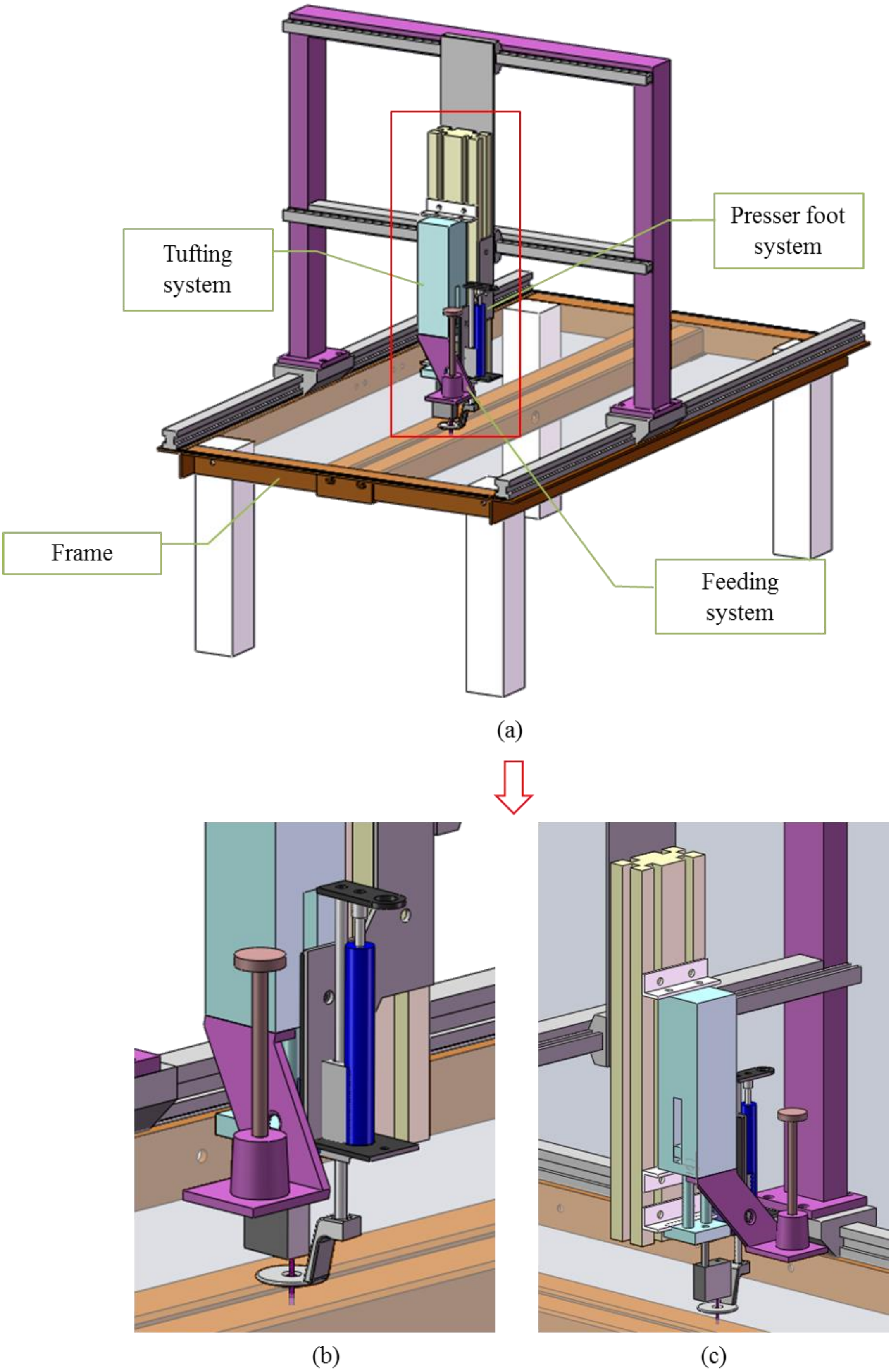

Figure 2-9 Design drawing of tufting equipment in solidworks.

I. Functions of tufting system

i. Tufting fibrous structures

To realize the function of tufting fibrous structures, a needle is positioned above the fibrous part which is fixed to a pneumatic cylinder. The needle is perpendicular to the surface of the fibrous part. Tufting thread is carried by the needle to be inserted into of remove from fabrics. The displacement of the needle is controlled by the pneumatic cylinder which provides a maximum movement distance of 50mm. It means the tuft length can be up to 50mm which is determined by the pneumatic cylinder. A metal joint is installed to link the needle and the pneumatic cylinder. By turning the screw, the joint can be turned or be tightened to change the positon of the needle. To adjust tufting direction, all tufting system can be inclined and fixed to reach different tufting angle. Tufting needles with inclined holes or hollow needles with different diameters can be chosen to meet different needs of tufting yarns and preforms.

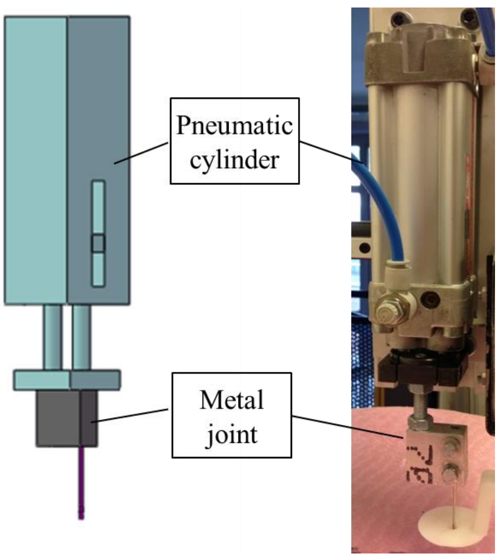

Figure 2-10 Pneumatic cylinder and needle.

ii. Controlling tuft length

To achieve different tuft lengths, a frame piece is added to carry pneumatic cylinder and needle. The height of this frame piece can be adjusted to meet a suitable position. A brake is applied to control the distance of movement of cylinder. When air enters into the cylinder, the needle descends. The tip of the needle pricks fibrous structure and stops in the middle of the preform or exceeds the material that depends on the thickness of the workpiece and the height of the needle. When the air comes out of the cylinder, the needle goes up automatically that tufting thread remains in the fibrous part.

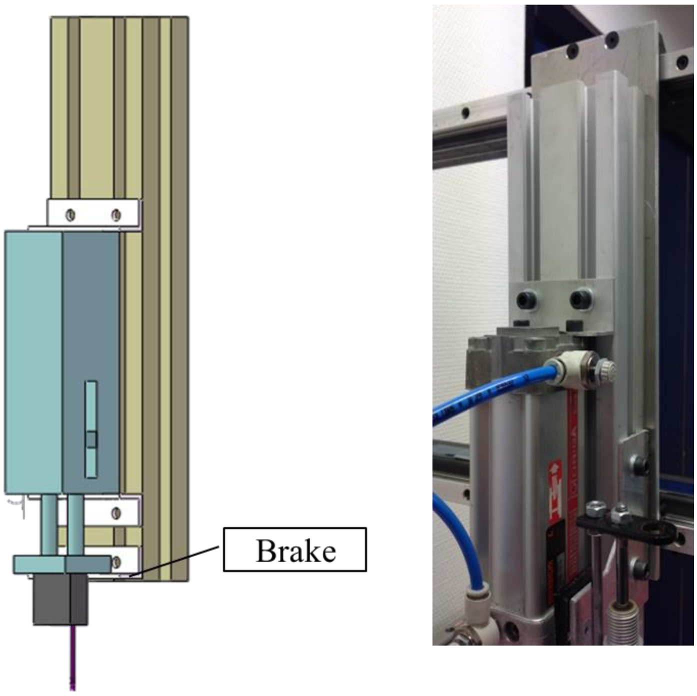

Figure 2-11 Frame piece for changing height and the brake.

Since the heights of the cylinder (H_c), length of the brake (L_b) and length of needle (L_n) are changeable, so before tufting, it is important to estimate the positions of all the pieces. With all these heights, tuft length can be calculated. The heights of different pieces are shown in Figure 2-12.

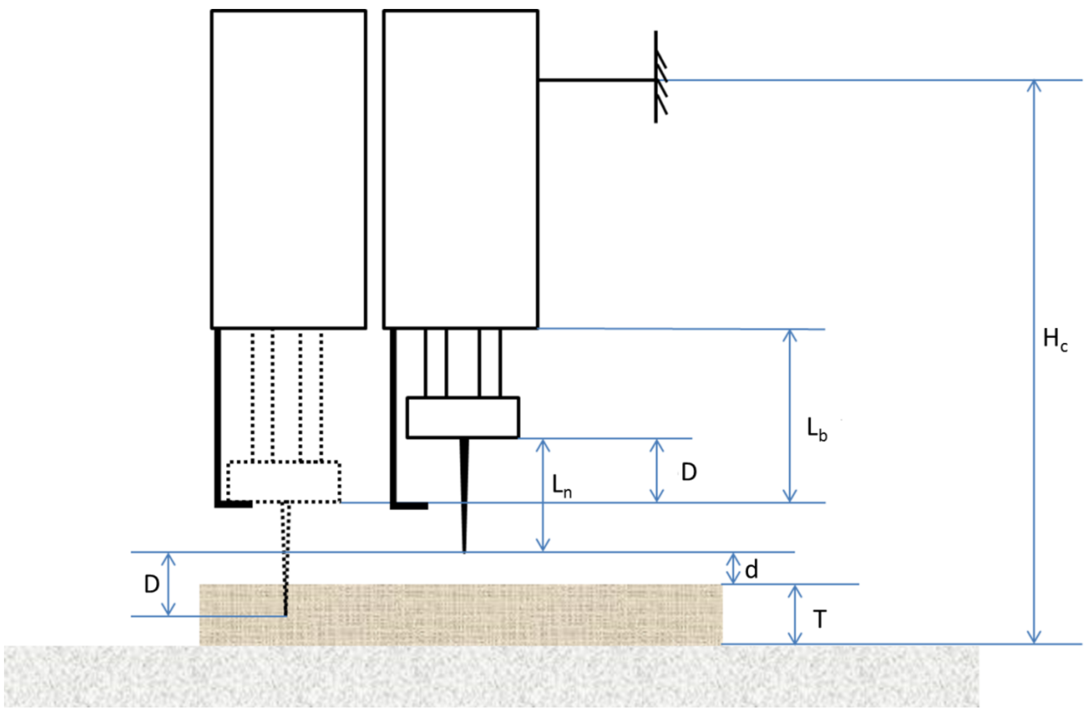

Figure 2-12 Estimating of tuft length.

H_c: Height of the cylinder

T: thickness of the preform

d: distance between the tip of needle and the surface of preform

D: displacement of the needle

L_b: length of the brake

L_n: length of the needle

TL: tuft length

Tuft length can be adjusted by modifying the height of the cylinder, the length of the brake and the length of the needle. Tuft length can be calculated by using the displacement of the needle minus the distance between the tip of needle and the surface of preform:

$$\mathbf{TL = D - d} \qquad \textbf{2-1}$$

When tufting a fibrous structure, tuft length can be greater or shorter than the thickness which depends on the requirement of finished product. When tufting thread is partially inserted into fibrous structure, tuft length is shorter than preform thickness. When tufting thread is fully inserted, a loop of yarn is formed at the bottom side which is held by foam. In this case tuft length is greater than preform thickness.

With this system, it is easy to change the needle when tufting different materials. Tuft length can be used modified by adjusting the position of needle and cylinder. When the presser foot is changed, the needle can be always assured at the middle of the presser foot hole by turning the metal joint. The maximum displacing distance of cylinder is 50mm, which fix the maximum tuft length in this case at 50mm. To tufting thicker pieces, a pneumatic cylinder with a longer distance can be adapted.

II. Functions of feeding system

i. Carrying tufting thread bobbin

Tufting thread is convolved on a bobbin which is to be installed on the frame next to the needle which provides tufting thread with a free tension. A plastic bobbin support is fabricated by using the 3D printer (shown in Figure 2-13). To protect tufting thread, a plastic pipe is involved and placed around the thread.

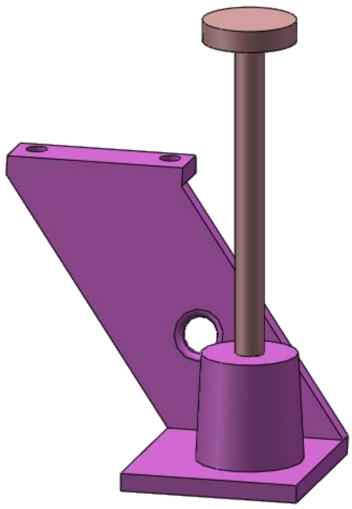

Figure 2-13 Plastic bobbin support.

ii. Carrying tufting thread bobbin

To protect tufting thread from additional tension and prevent undesirable stretching during tufting process, a certain distance of thread should be reserved before each tuft. This reserved distance can be calculated according to Figure 2-14.

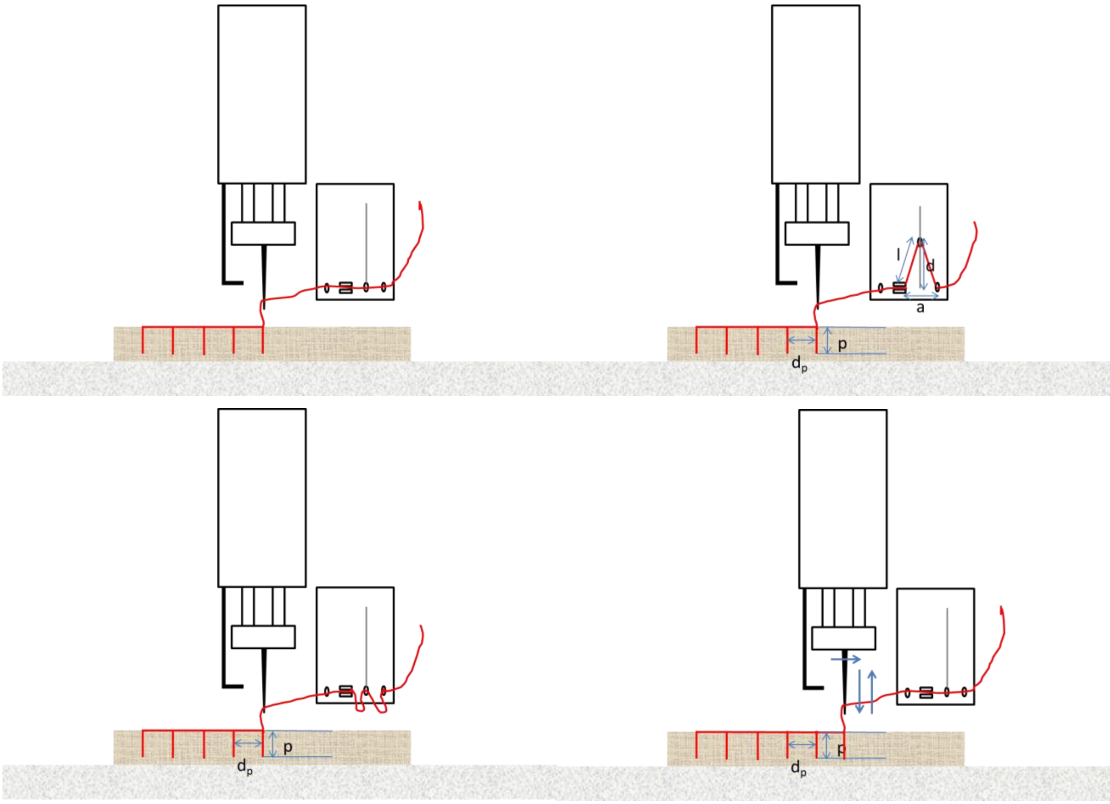

Figure 2-14 Calculation of reserved distance of tufting thread.

d: distance between the hooks

l: length of thread between the clamp and the hook

a: distance between the clamp and guide ring which is constant.

p: tuft length

dp: distance between two tufting points (tufting spacing)

Known:

$$(a/2)^2+d^2=l^2 \quad \text{2-2}$$

$$2l=d_p+2p \quad \text{2-3}$$

So,

$$d=\frac{\sqrt{(d_p+2p)^2-a^2}}{2} \quad \text{2-4}$$

With the Equation 2-4, the distance of reserved tufting thread can be calculated with tuft length and tufting spacing. When a tuft is formed, the thread is clamped to avoid dragging out from former tufting point. After that the hook is raised to reserve a distance which is needed for the latter tuft. Then the clamp releases to continue tufting the next point.

With the aid of the principle and the formula, a feeding system is designed which is shown in Figure 2-15.

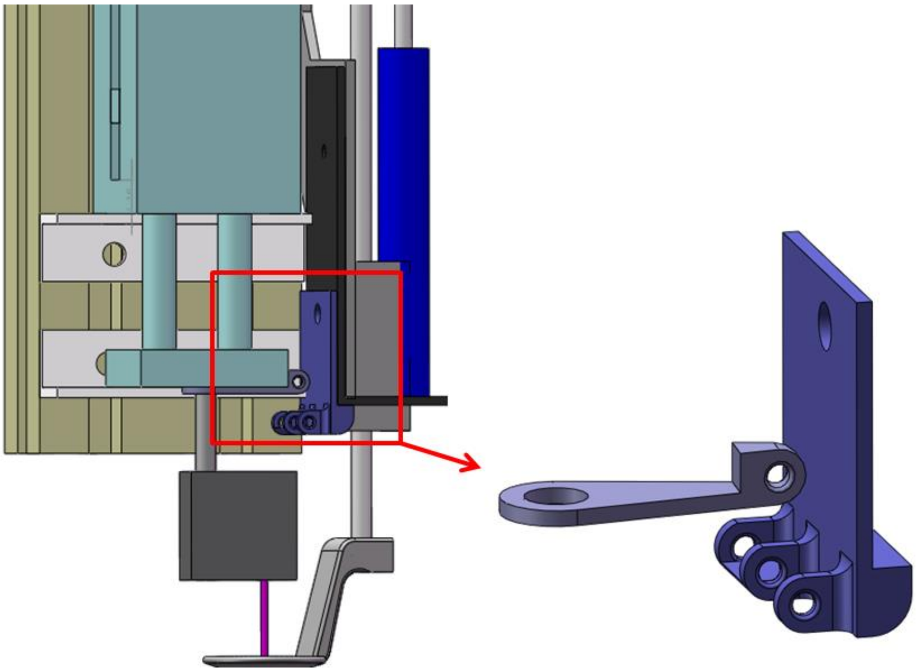

Figure 2-15 Feeding system.

The feeding system is designed to carry tufting thread bobbin and reserve tufting thread with a regular tension. Guide rings are put between needle system and presser foot system to minimize thread journey and to avoid frictions.

For this moment, the simple feeding system is developed to realize tufting process. In future work, another system for reserving thread can be designed which can be controlled by a small pneumatic cylinder. The reserved distance can be calculated more precisely and be adjusted more accurately.

III. Functions of presser foot

i. Pressing preform with different pressure

Traditional sewing machine uses a presser foot for pressing pieces and guide pieces to move along a relative direction. In tufting equipment, presser foot brings pressure on fabrics to avoid any unwanted movement. When several layers of fibrous parts are tufted, the presser foot can also play the role to fix the layers. Presser foot can be easily installed or removed from the frame. The shape of presser foot can be diverse. To control the presser foot, a pneumatic cylinder is installed next to the needle system on the frame. This cylinder is perpendicular to the surface of the presser foot. The maximum distance of this cylinder is 25mm. The pressure of presser foot can be changed by turning valve. A metal plate is fabricated to fix the cylinder and change the height of the presser foot. To prevent rotation of presser foot, a guiding piece is made and inserted between the plate and the cylinder.

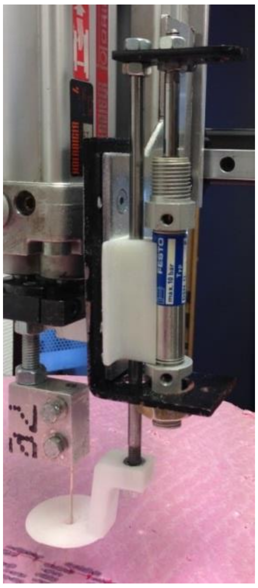

Figure 2-16 Presser foot system..

ii. Avoiding tufting thread being dragged out of fibrous preform

A plastic presser foot is printed with 3D printer and is installed to press the preform. Thanks to its pressure and friction, tufting thread is tightened by surrounding fabric instead of being dragged out of fibrous preform. Two practical presser foots are shown in Figure 2-17. In the middle of the presser foot, a hole is made to allow the needle goes through. The round presser foot shown in Figure 2-17(a) which has a circle shape can ensure that the pressure is balanced around the tufting point. By using this round presser foot, tufting head can be moved to different directions. Another shape with a flat bottom shown in Figure 2-17(b) can ensure that the presser foot is stable when it presses the preform. With this tufting head, the tufting direction could not be modified.

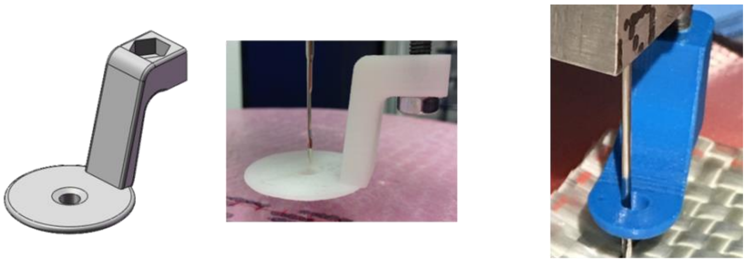

(a) (b)

Figure 2-17 Round presser foot (a); uni-directional presser foot (b).

During tufting process, the presser foot system plays an important role which provides a pressure to fibrous preform. Then during feeding process, it tightens fabric to provide a friction to hold tufting thread. The presser foot can be changeable to meet different needs. The cylinder which control the presser foot has a moving distance of 25mm which is enough for the most of situation. The pressure of presser foot can be adjusted by regulating the energy of pneumatic system.

IV. Functions of the frame

i. Supporting fibrous preform and other systems

The frame of this equipment is made of metal, which is shown in Figure 2-18a. To support the fibrous structure, a plexiglass is added to the frame. As sometimes the needle has to penetrate through the fabric and leave a loop at the bottom, a piece of foam is put under the preform to protect the needle. The chosen foam should has a proper density and softness in order to reduce the abrasion to tufting thread and also to have a enough grip force to hold the loop. The foam can also provide a friction to prevent relative movements between the textile and the plexiglass. To measure tuft length and tufting spacing, rulers are pasted on the frame.

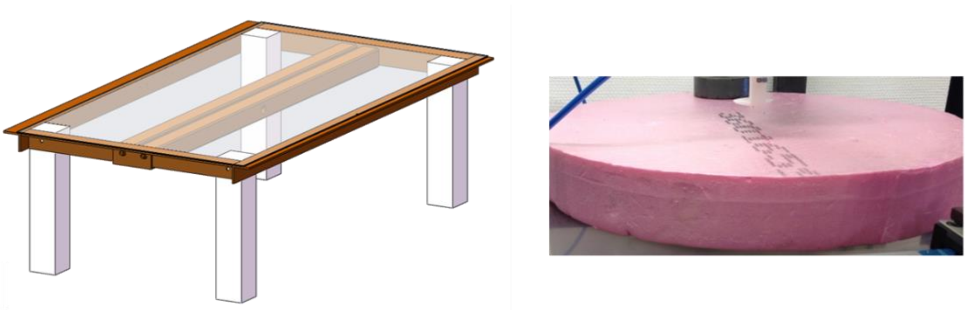

(a) (b)

Figure 2-18 The frame (a) and the foam (b).

ii. Displacing tufting head, measuring and changing tufting density

To realize numerous tufting points at different position, several rails are paved all around the frame (see Figure 2-19). Tufting head can be guided to move along all directions. An automatic control device is linked to this equipment which allows an optimization of efficiency.

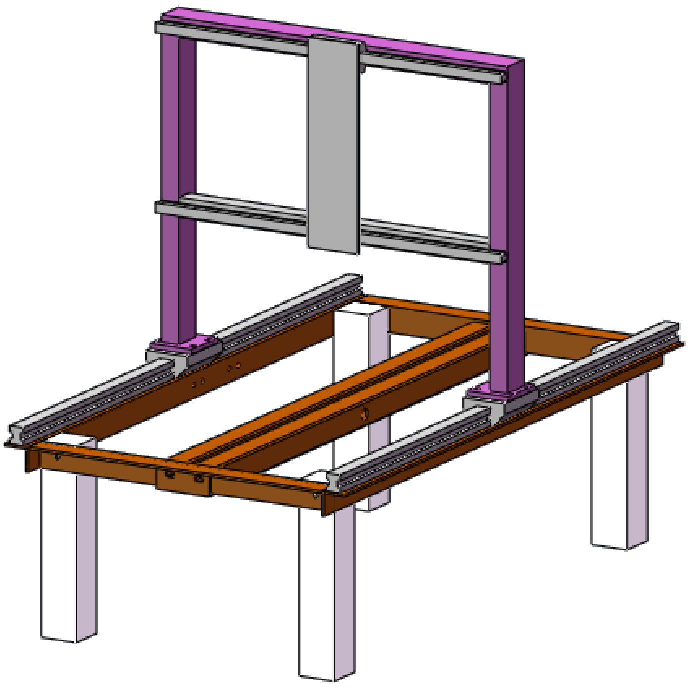

Figure 2-19 The frame with guiding rails.

To automatically control tufting equipment, a software is created. With this software, initial and terminate position of tufting head, tufting spacing and distance between lines should be input. These parameters should be set up before each tufting line. It has also a security system to prevent reversal order movements of needle and presser foot.

2.3.3 Assemblage of the machine

Once all the components are fabricated, they are assembled on the frame. Figure 2-20a shows the front view of tufting machine without feeding system and Figure 2-20b shows the side view of tufting machine with feeding system.

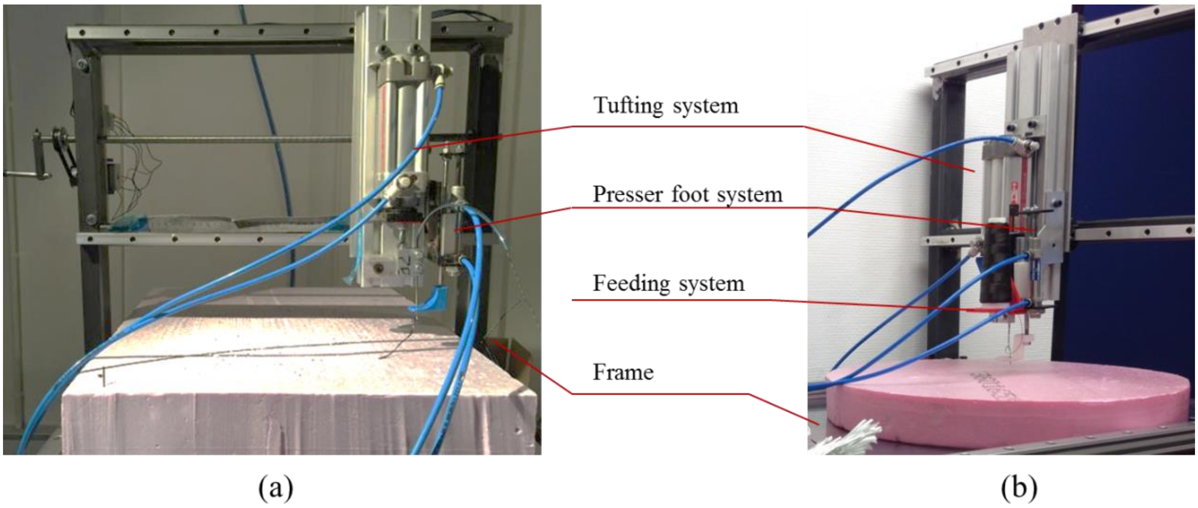

Figure 2-20 Assemblage of tufting machine.

2.3.4 Operating instructions of the machine

With this equipment, several tufting parameters such as tufting density, tuft length, tufting direction and pressure of presser foot can be controlled. The maximum tuft length is determined by the range of the pneumatic cylinder controlling the needle. The main parameters of the tufting equipment are shown in Table 2-1. The choice of tufting needle is crucial depending on the performances of tufting thread and materials.

Table 2-1 Main parameters of tufting equipment.

Parameters	**Values**
Size of tuft machine	700×400 mm^2
Needle inserting speed (after optimisation)	60 mm/s
Needle retreating speed (after optimisation)	60 mm/s
Needle diameter	2 mm
Maximum needle stroke	50 mm

The tufting machine can be manually or automatically operated. Two pneumatic cylinders are applied to control the movements of tufting needle and presser foot. Before programming the machine, a manual operating console with two twist switches were used to control cylinders (shown in Figure 2-21). Pressure of presser foot and needle moving speed can be adjusted by twisting pneumatic valve. A barometer is installed under the valve to monitor pneumatic pressure. After several tests, the optimum pressure for our experiments is 3 bars. Switch A at the left side is used to control the presser foot, and the other switch B at the right side is used to control tufting needle. The presser foot or the tufting needle can be raised by turning the corresponding switch on the right and be descended by turning the switch on the left.

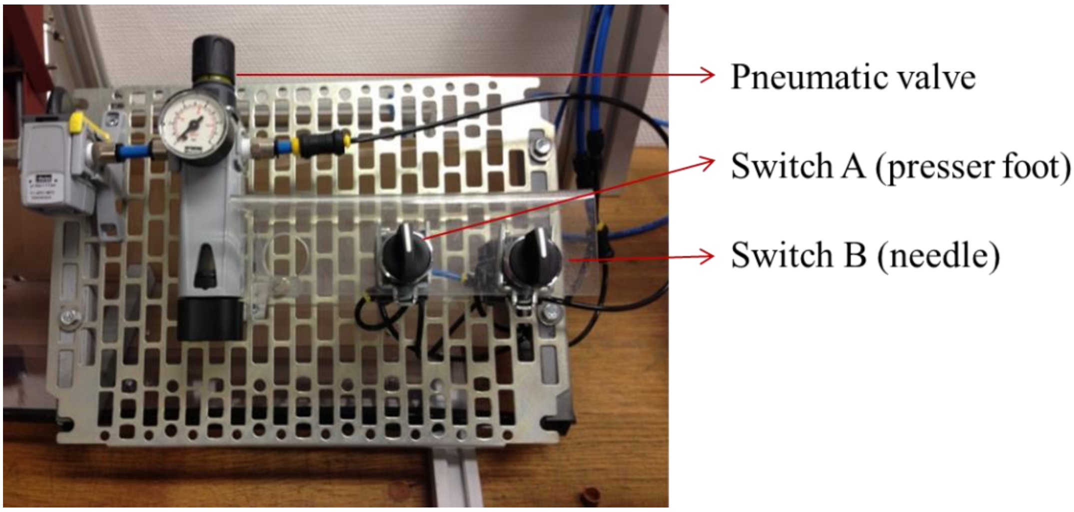

Figure 2-21 Manual operating console of tufting machine.

Before using tufting machine, tufting thread and dry fabrics should be chosen and prepared. Suitable presser foot and tufting needle should be installed. According to following experiments, the number of layers and the thickness of fabrics should be estimated. The maximum thickness of the preform is 50mm.

The tufting process is as follows:

Preparation:

1. Installation of tufting yarn bobbin, threading tufting yarn along the path indicated in Figure 2-22;

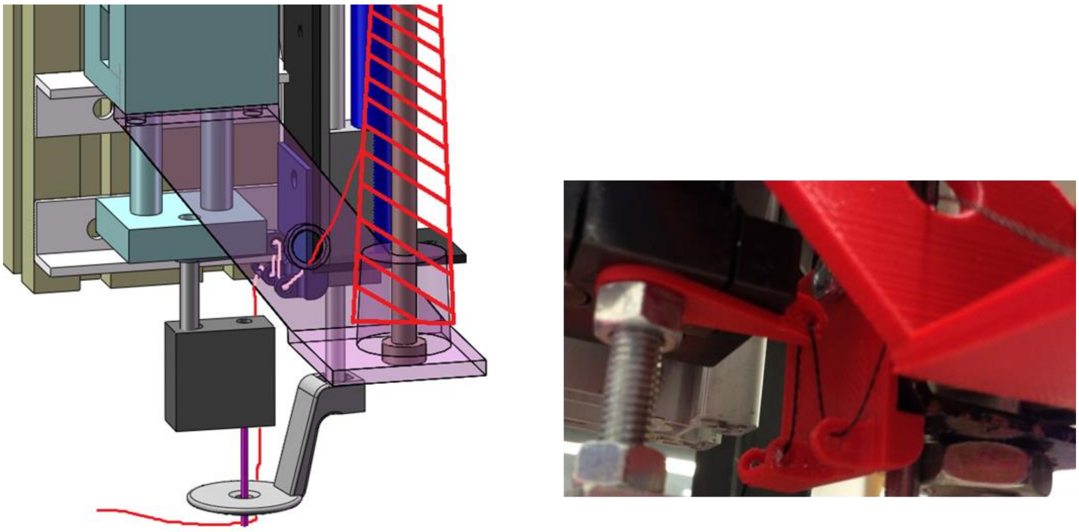

(a) (b)

Figure 2-22 Path of threading tufting yarn.

2. Switching on the system of pneumatic energy, turning two switches on the left to raise tufting needle and the presser foot, adjusting the positions of the cylinders and the brake according to tuft length, placing the machine in the initial state (Figure 2-23a);
3. Placing fabric preform on the foam, pinning the fabric with weight.

Tufting process:

4. Descending presser foot by turning switch A on the right to press fabrics and to prevent unwanted displacement between fabric and the foam (Figure 2-23b);
5. Turning switch B on the right to descend the needle to tuft the fabric (Figure 2-23c);
6. Turning switch B on the left to raise the needle, tufting thread remains in the fabric, the first tuft is formed (Figure 2-23d). At the same time, tufting thread on the bobbin passes from the hooks and is booked for the next tuft point;
7. Turing switch A on the left to raise the presser foot (Figure 2-23e);
8. According to tufting density, remove tufting system to the right position of the next tufting point;
9. Repeating the process 4 to process 9, realizing several tufting points to make sure that the tufting process can be carried on continuously.

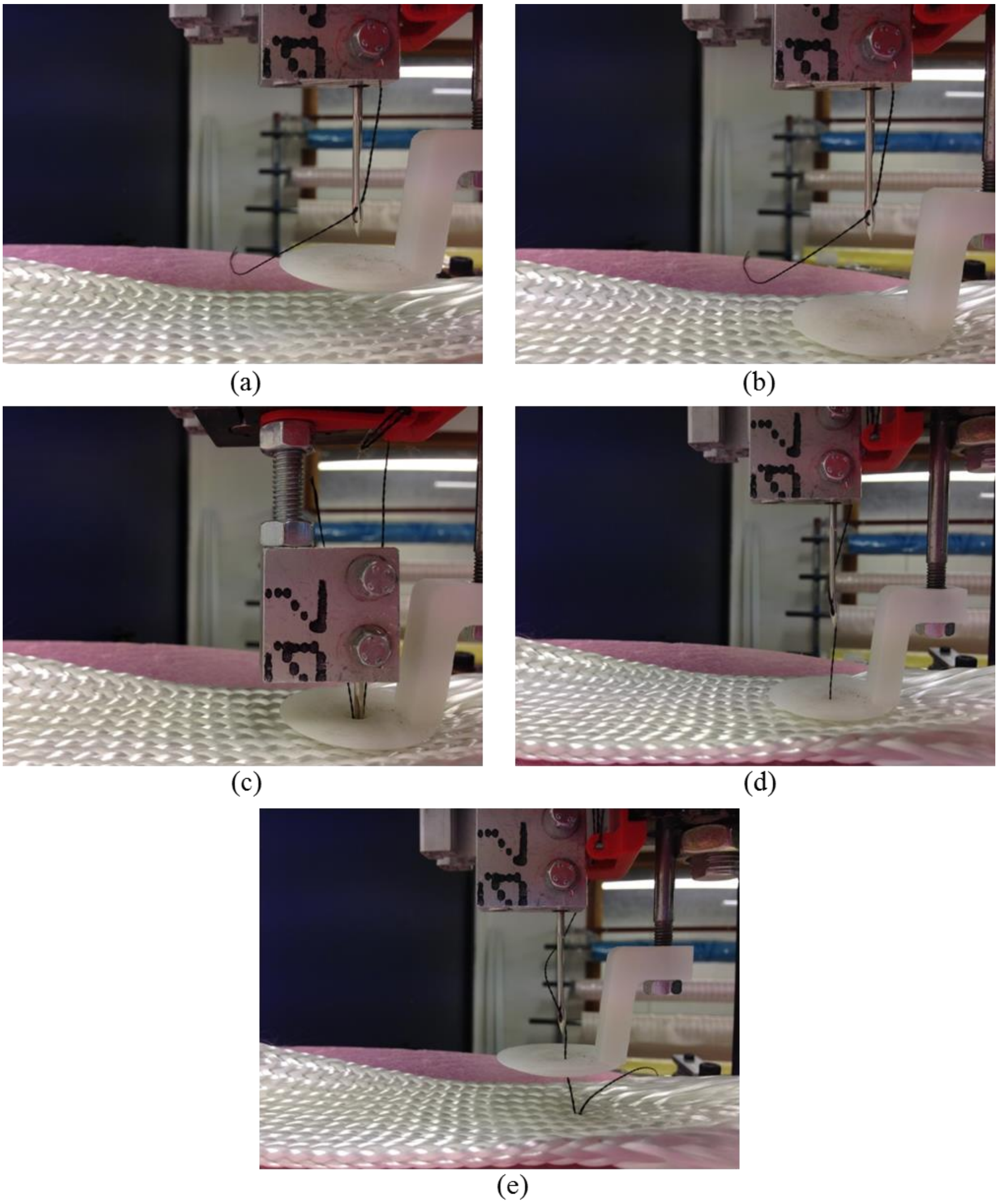

Figure 2-23 Tufting process.

During tufting several points one by one with manual mode, tufting parameters are adjusted to make sure that the machine is adapted to selected tufting thread and fabric. After all parameters are fixed, the machine can be switched to automatic mode.

The method of application is as follows:

1. First of all, check that the power strip is turned off and the entrance of pneumatic air is closed. Once verified, connect the PCDuino power by plugging the plug on the sector;
2. Then PCDuino is turned on and the home screen is shown in Figure 2-24. Once reaching home screen, launch the application "Geany";

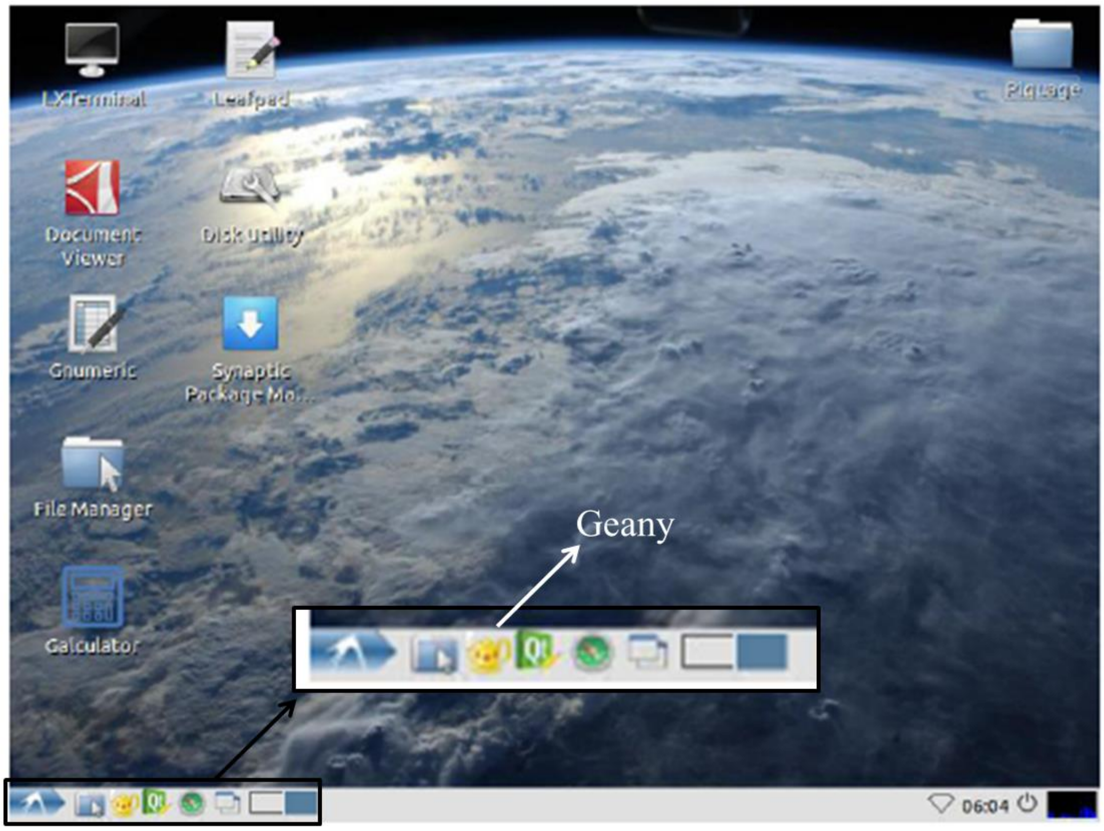

Figure 2-24 Home screen of the PCDuino.

3. By opening "Geany" programming code lines with the title of the file "autoMain.py" appear. Turning on the power strip and opening the air supply. Compiling "autoMain.py" to start the program (See Figure 2-25).

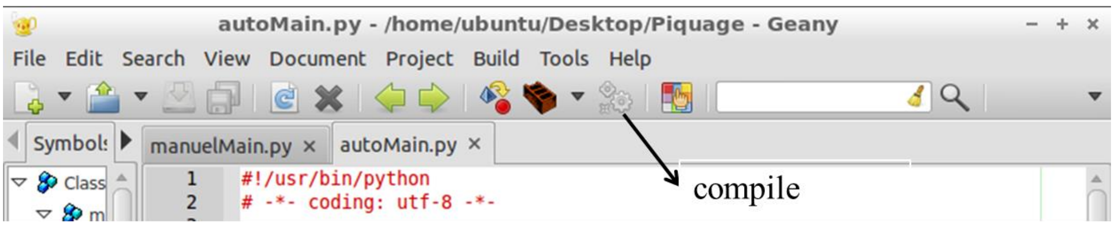

Figure 2-25 Launch the interface.

4. After compiling the program, a terminal will then open for entering the coordinates of the initial position of tufting system. These coordinates cannot be less than 0 and cannot exceed the limit of the axis (400 for X and 700 for Y). Once les coordinates are receipted, the needle and presser foot will then be put in the up position. Once these actions are completed the machine's control panel will then appear (see Figure 2-26).

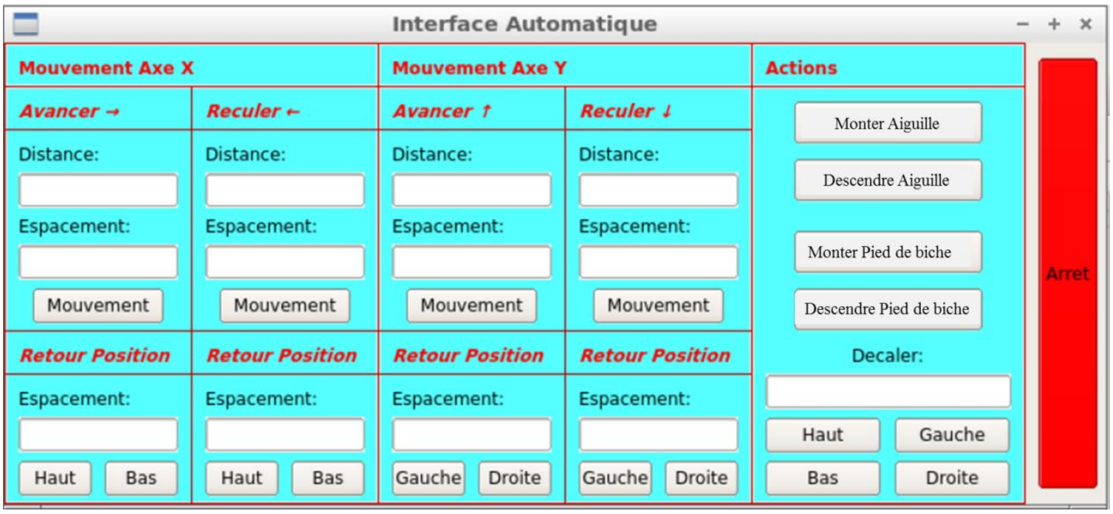

Figure 2-26 The interface of automatically controlling system.

This window has three parts, two parts for controlling of two motors and another part for manual mode.

5. Actions on motors:

Taking the part of "Mouvement Axe X" as an example to show the usage of the interface, the same principle is applied to the motor for Y axis. The automatic mode requires the user to enter the tufting distance (as "Distance" in the interface) and tufting density (as "Espacement" in the interface). The tufting distance represents the distance of tufting line which is generally shorter than the length of tufting sample. Tufting density represents the distance between two adjacent tufting points. Take an example, to tuft a line of 8cm with the density of 5mm, inputting informations on the interface as shown in Figure 2-27:

Figure 2-27 Interface for controlling motor of X axis.

After inserting the values, simply click the button "mouvement" to run the machine.

Once one line is finished, it is possible to return the tufting system to the previous position with a displacement to upper or down position. The displacement can be input in "Espacement" under "Retour Position" and then press the up ("Haut") or down ("bas") button.

6. During the automatic tufting process, if a defect appears, it is possible to stop the movement in progress by click the red stop button on the right of the interface. Then shift to manual mode (as shown in Figure 2-28) to detect the problem or adjust tufting parameters. With the manual mode, the movement of tufting needle and presser foot can be controlled by pressing the buttons. The button "Monter Aiguille" is for raising the tufting needle, "Descendre Aiguille" to descend the needle, "Monter Pied de biche" to rise the presser foot, and "Descendre Pied de biche" to descend the presser foot. And tufting density or tufting spacing can be indicated in "Decaler" and then press on of the button at the bottom to move tufting system to a direction.
7. After finish tufting process, turn off the PCDuino and close the air supply.

Repeating attempts are carried out to optimize tufting process when changing materials. A number of tufting needles and presser foots can be chosen to reach needed tufting product.

2.4 Characterization of tufting yarn

The tufting yarns used in the study are two different carbon threads, TORAYCA® FT300 and TENAX® carbon thread.

TORAYCA® FT300 is produced by the treatment of an acrylic fibre precursor, with pyrolysis, surface treatment and sizing processes. The properties of the thread are shown in Table 2-2.

Table 2-2 Properties of TORAYCA® FT300

Thread reference	Yield	Number of filaments	Elongation	Tensile strength
TORAYCA carbon fibre FT300 3000-59A	198g/1000m	3000	1.5%	3530MPa

The calculated breaking strength of resinified thread is 193.6N. This thread is tested to tuft several layers of glass woven fabric with the hollow needle and the needle with inclined hole. It is observed that when tufting thin and lightweight glass fabric, the thread can work well with both of the two needles and the tufting thread is lightly abraded which can be accepted during tufting process. When tufting thick and high weight glass fabric, tufting thread is damaged seriously because the filaments adopted are fragile in bending. In this case, tufting thread breaks within three tufting points that tufting process cannot be continued. To solve this problem, twisted thread is proposed to give the need of high flexibility in bending to withstand the sharp kink from the needle during insertion.

According to previous research, carbon threads made with two or three highly twisted yarns (up to 300 turns per meter) in which each single yarn is twisted in the opposite direction over 250 times per meter are flexible enough to be successfully tufted or stitched[19]. With the limitation of needle's diameter, carbon thread is twisted with a twist of 194±18 tours per meter. The twisted thread is shown in Figure 2-28.

Figure 2-28 TORAYCA® FT300 carbon fibre and twisted thread.

Then tensile test of these two carbon threads are conducted. The tests are carried out on MTS tensile testing machine. Initial length of each specimen between clamps was approximately 250mm. Samples were conducted at constant speed of 250mm/min until rupture. The breaking strength of two threads are measured, 79.6±12.4N for untwisted thread, and 87.0±8.0N for twisted thread. Compared with untwisted thread, the twisted thread is more suitable for tufting process for thick fabric. When tufting thick and high weight woven fabric, the hollow needle is required to protect the twisted thread.

A 67×2tex TENAX® carbon multi-filament sewing thread is also used in this study. This thread is specially designed to stitching process with special reverse twist and a slight PU coating to optimize yarn process ability. Table 2-3 shows the properties of TENAX® carbon thread.

Table 2-3 Properties of 67×2tex TENAX® carbon thread

Thread reference	**Yield**	**Number of filaments**	**Elongation**	**Tensile strength**
67×2tex TENAX® carbon multi-filament sewing thread	140g/1000m	1000×2	1.5%	4100MPa

The calculated breaking strength of TENAX® carbon thread is 99.9N. This thread is specially designed for stitching process as well as tufting process that it is suitable to tuft a large amount of fabrics with the hollow needle and also the needle with inclined hole. Because of the PU coating, the tufted thread is well protected.

2.5 Conclusion of chapter 2

Stitching technology is widely used as a method for strengthening composite in the thickness and also developing 3D preforms. But most composite reinforcement which has a 3D structure with simultaneous large spatial expansion is not adapted to process of traditional two-side stitching. Facing the limitations of conventional stitching process, one-side stitch process is developed. Tufting technology, a kind of one-side stitching technology, is based on the conventional stitching process but involves the novel aspect that it uses a single needle to introduce a thread into the structure without tension. This technology involves the insertion of yarns in z-direction in order to strengthen fibre reinforced plastics or link two or more fabric preforms together. A threaded needle is inserted into a dry-fabric or binded preform and then removed from the fabric along the same trajectory. The "tuft" of thread relies on friction from the fabric itself and/or hold provided by underlying material (e.g. foam) to remain in place. The loop of thread is not locked in place, which appears at the bottom of work piece or hidden in fabric preform according to different needs. Tufting process can be used to bind thick structures because of its need for only one side access. Thanks to tufting technology, delamination effect can be reduced and the impact resistance and damage tolerance can be increased.

To better apply tufting process to reinforce components, the influence of numerous associated parameters on the mechanical performance must be conducted. The parameters such as tuft length, tufting thread properties, tufting density, type of needle, tufting direction, etc. are studied. An equipment for realizing tufting process with the functions of controlling these parameters is designed and developed.

The CAD software "Solidworks" is applied to design this equipment. The tufting equipment consists of four parts: tufting system, presser foot system, feeding system and the frame. Tufting system carries a needle which is controlled by a pneumatic cylinder to insert tufting yarn with different tuft lengths. Presser foot is linked with another pneumatic cylinder which is installed alongside to adjust pressure and to press the preform to avoid tufting thread being drawn off. Feeding system carries tufting thread bobbin and provide tufting thread with a certain length and pre-tension. The frame carries the preform and all other systems and provides the possibility to measure and control tufting density. After assembled all parts of the machine, an automatic controlling program is linked to the machine for the improvement of the efficiency.

With the developed tufting machine, preforms can be tufted with the maximum tuft length of 50mm and a various tufting density. Tufting needle and presser foot can be chosen and changed according to preforms properties. Several tufting samples are made to test the machine and to improve tufting parameters. Several threads can be chosen as tufting yarns. In this study, two kinds of carbon threads were used to produce tufting samples for further tests. The properties of tufting yarns TORAYCA® FT300 and TENAX® carbon thread are presented.

In next chapters, tufting products are produced by using this tufting machine to carry out mechanical property tests and forming experiments.

Reference of chapter 2

[1] Jiao Y, Li X and Dong F. Investigation on 3D Stitched Composites Behaviour, Journal of Textile Research, 2002;23(2) : 96-99.

[2] Yan L, Chen N and Luo Y. Application and development in stitching technology for composites, Industrial Textile, 2007;2:1-5.

[3] Ing D, Witing J. Recent development in robotic stitching technology for textile structural composites. JTQTM, 2001;2(1): 1-8.

[4] Mitschang P, Ogale A. Tailoring of textile preforms for fibre-reinforced polymer composites. Journal of Industrial Textiles, 2004; 34(2): 77-96.

[5] Wittig J. Robotic Three-Dimensional Stitching Technology, Proc. Int. SAMPE Conference: A material and Processes Odyssey, Long Beach, California, USA, 6-10 May 2001.

[6] Wittig J. Recent development in the robotic stitching technology for textile structural composites. Journal of Textile and Apparel, Technology and Management, 2001; 2(1): 1-8.

[7] Bertrand J, Desmars B. Aerotiss® 03S stitching for heavy loaded structures. JEC-Composites, 2005; 18:34-36.

[8] Henao A, Carrera M, Miravete A, Castejon L. Mechanical performance of through-thickness tufted sandwich structures. Composite Structures, 2010;92:2052-2059.

[9] Sickinger C, Hermann A. Structural stitching as a method to design high-performance composite in future, 2001.

[10] Cartié DDR, Troulis M, Partridge IK. Delamination in Z-pining carbon fibre laminates. Composites Part A: Applied Science and Manufacturing, 2005;35:55-64.

[11] Pérès P, Desmars B, Léard JP. Composite behavior of assemblies with Aerotiss® 03S technology. 16th International Conference on Composite Materials, 2007:1-7.

[12] Dell'Anno G, Cartié DD, Partridge IK, Rezai A. Exploring mechanical property balance in tufted carbon fabric/epoxy composites. Composites: Part A, 2007;38:2366-2373.

[13] C. Sickinder et al. Structural Stitching as a Method to design High-Performance Composites in Future. TechTextil Conference, 2001.

[14] P. Pérès, et al., Composite behavior of assemblies with AEROTISS® 03S technology. 16th international conference on composite materials, 2007.

[15] Technical data of 3M RTM Core. Available from: http://multimedia.3m.com/mws/media/812452O/3mtm-rtm-core.pdf?&fn=3M%20RTM%20Core%20Data%20Page.pdf.

[16] Colin de Verdiere M, Pickett AK, Skordos AA, Witzel V. Effect of tufting on the response of non crimp fabric Composites. ECCOMAS Thematic conference on mechanical response of composites. Porto, Portugal, 12-14 September 2007.

[17] Dell'Anno G, et al. Manufacturing of composite parts reinforced through-thickness by tufting. Robotics and Computer Integrated Manufacturing 2015. Available from: http://dx.doi.org/10.1016/j.rcim.2015.04.004

[18] Tan KT, Yoshimura N, et al. Effect of stitch density and stitch thread thickness on damage progression and failure characteristics of stitched composites under out-of-plane loading. Composites Science and Technology 2013; 74: 194-204

[19] G. Dell'Anno, Effect of tufting on the mechanical behaviour of carbon fabric/ epoxy composites, Cranfield University, Cranfield (UK), 2007, Ph.D. dissertation.

3 INFLUENCE OF TUFT LENGTH THROUGH THE THICKNESS ON MECHANICAL PROPERTIES OF TUFTED COMPOSITES

3.1 Introduction

In aerospace, transport and energy industry, the laminated composites are widely used to manufacture thicker and more complex composite parts. Then 3D fabrics have been developed to replace the multilayered reinforcements in some applications to increase the performance in the thickness [1-4]. Recently, stitching technology is developed to bind dry reinforcements together or to strengthen composites on their through-thickness performance by inserting structural yarns. Tufting process represents the simplest one-sided stitching technology and it is specifically designed for the dry preform/liquid resin moulding process route [5-9].

This chapter is dedicated to the analysis of the influence of tuft length on mechanical properties of tufted preforms and composites. Tufting has emerged as a popular method of localised Through-Thickness Reinforcement (TTR) for dry preforms. The tufting process involves inserting a single threaded needle through a preform, where friction within the preform is responsible for holding the thread in place as the needle is retracted [10]. The threads can be fully inserted or applied to a partial depth through the preform thickness. When the needle penetrates the whole preform thickness, a loop of yarn is formed on the underside of the structure. The loops are not tied or interlocked and the tufting yarns remain in position because of the natural friction between the fabric and the thread. This technology requires access from a single side of the preform, which makes it ideally suitable for local, tailor-made reinforcement of complex, three dimensional shapes. Tufting can be used to reinforce different types of textiles such as woven fabric, braided fabric or non-crimped fabric (NCF) [11]. It requires only one side access of thread and does not require the use of second thread, which makes it simpler and more cost-effective. The influence of reinforcement by tufting during the preforming step has also been highlighted [12]. Recently Hartley et al. [13] have shown, with an experimental study that increasing the number of tufts within a sample significantly increases crash performance by as much as 25 % compared to untufted coupons. Wittig [14] has observed that for the high tufting density (step of 12.5 mm) the improvement of the performances can reach 250% for bending rigidity and 1000% for the shear failure stress. Colin de Verdiere et al. [11] have investigated the effect of tufting on the in-plane and out-of-plane mechanical response of NCF. They have shown that tufting considerably increases delamination resistance in mode I but to a lesser extent in mode II. On the other hand the insertion of tufting yarns leads to an increase of the mass and consequently a loss of specific properties because of the damage caused by the needle and misalignment of fibre. Mathieu de Verdier et al [15] studied the response of tufted/untufted carbon–epoxy non crimp fabric composites and concluded that 13.3% reduction in tensile strength, 12.6% reduction in tensile modulus, 10.52% reduction in compressive strength and 11.2% reduction in compressive modulus.

In this chapter, the manufacturing of tufted composite and tensile characterisation of these tufted samples is outlined. Thick assembled reinforcements are prepared by using tufting equipment described in chapter 2. Microscopic analysis on the cross section of tufted preforms and tensile test results present the influence of tuft length on the mechanical performance. As a result, control of tufting parameters is essential to optimize the process of tufting and mechanical performances of tufted composite.

3.2 Material and method

As the aim of the present study is to investigate the influence of the tuft length on the mechanical properties of tufted composite part, thick tufted specimens need to be prepared.

Thirty-four plies of plain woven E-glass fabrics (HexForce™ 1064) with an area density of 927±10 g/m^2 are stacked. A thin release film with a thickness of 50.75 μm (Cytec E2760, red color) is placed between the 24th and 25th layer to separate the stack into two parts (upper and lower parts) (see **Figure 3-1**). This release film can avoid extra adhesive effect after the vacuum infusion process. Consequently, the tensile test in the thickness direction will be applied only on the inserted tufting threads. The dimensions of the preforms are 250 × 150 × 25 mm^3.

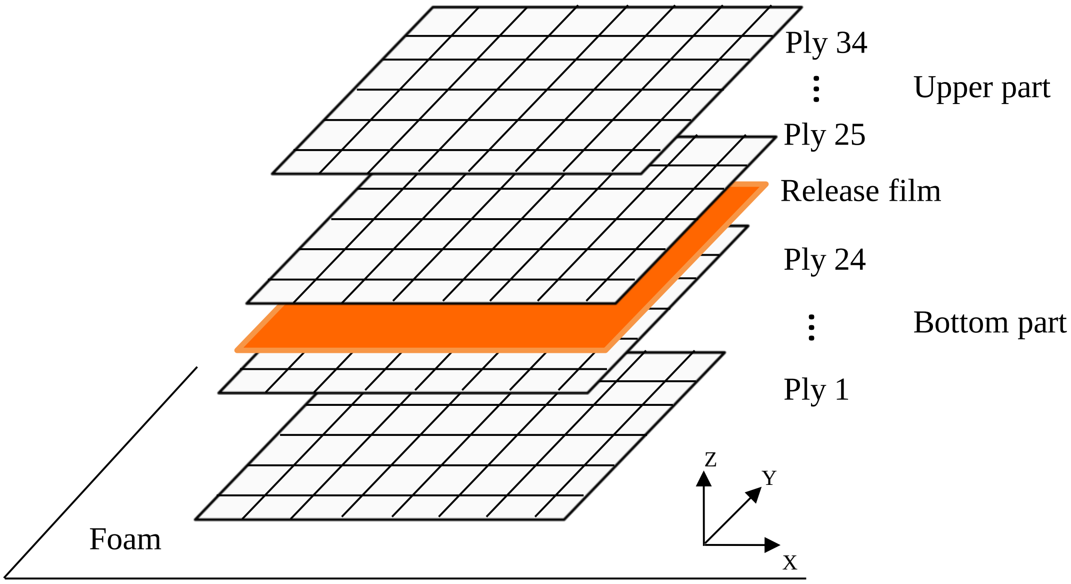

Figure 3-1 The laminate of the preform and the position of release film.

The preform is tufted using a TORAYCA® FT300 3000-59A twisted carbon thread (**Table 3-1 Tufting carbon thread properties.**) with different tuft lengths and a permanent tufting density of 5 mm. The twist of carbon thread is 194±18 T/m. In order to control the tufting quality, it was decided to tuft carbon yarns into a glass-fibre-reinforced fabric. After the liquid resin infusion with an epoxy resin, the glass fabric becomes translucent which makes possible to conduct the observation/micro-observation of the tuft length and tufting yarn loop (carbon yarn loop). These samples are tufted by a hollow needle of 2 mm diameter under the pressure of 2.5 bar.

Table 3-1 Tufting carbon thread properties.

Thread specification	Specific weight	Filament count	Elongation at break
TORAYCA® FT300 3000-59A	198 g/km	3000	1.5 %

Figure 3-2 shows one of the preforms after tufting. In order to study the influence of the tuft length on the mechanical properties of tufted composite part, the Desired Tuft Length (DTL) is changed during the preparation of the tufted reinforcement (from 17.6 to 25.6 mm) for every three lines presented in Figure 3-2. This tufted preform is one of the samples tested. The DTL relating to the stroke of the tufting needle is not the final tuft length observed in the tufted composite piece. The DTL is modified in the tufting and resin infusion processes. Consequently, the tuft length should be controlled well during the tufting stage.

Figure 3-2 Dry tufted preform with a tufting density of 5mm.

3.3 Characterisation of the tufted preform and composite

3.3.1 Preparation of the tufted composite sample

After tufting stage, the tufted 3D preforms are infused with an epoxy resin (SICOMIN SR8200) by liquid resin infusion process [16, 17]. The principal of LRI is shown in Figure 3-3. Several layers of fabrics are stacked in the following order:

- A mould release fabric;
- Tufted preform sample;
- Separating fabric;
- A grid of infusion, which helps in homogeneous distribution of the resin.
-

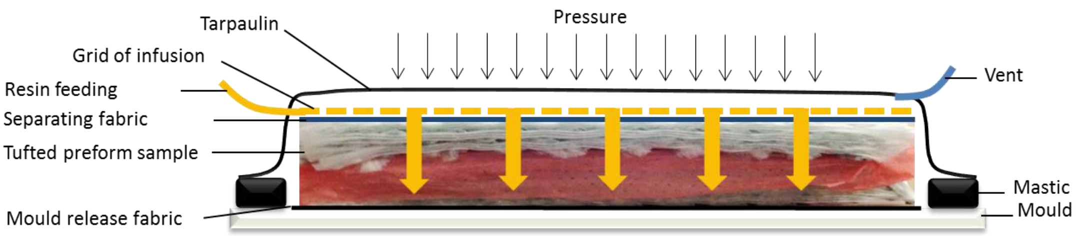

Figure 3-3 The principal of LRI.

To infuse tufted preform, an open mould and a vacuum cover is required. Resin pot is connected with the vacuum cover by a supply channel. Once the vacuum environment is created, the resin is sucked under the cover and percolated into tufted preform. This technique requires low viscosity resin, for this reason the epoxy resin is selected. This process can provide relatively high quality reinforcement with simpler equipment.

Figure 3-4 presents the LRI process. The resin inlet and outlet and the direction of resin flow are noted in Figure 3-4. Once the resin front arrives at the vent (the resin outlet), the pipes are closed and the resin feeding is stopped to maintain the vacuum. The infusion system is left at room temperature for twenty-four hours and then put into an oven at a curing temperature of 60 ℃ for six hours. Finally, the tufted composite part is demoulded after cooling down.

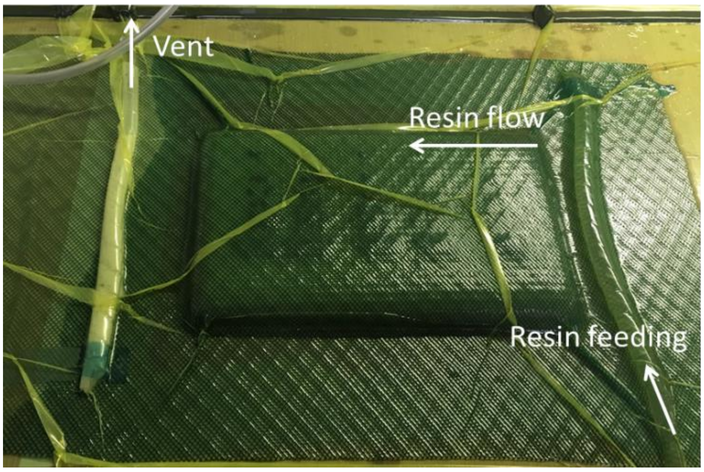

Figure 3-4 The tufted preform sample under vacuum infusion system.

The main properties of the tufted preform and composite are given in Table 3-2. Before tufting, the thirty-four E-glass woven plies were cut and superposed. The initial dimensions of the preform are $250 \times 150 \times 25$ mm^3 and the total initial mass is 587.1 g. As the preform was compressed during the tufting and infusion processes, the thickness of the final composite piece is reduced to 21 mm. Moreover, during the tufting stage, the carbon threads through the thickness present 4.8 g mass and 417 g of resin are infused into the tufted preform. Compared to the initial mass, the mass increases 0.8% and 71.8% respectively during the tufting and infusion stages. The mass increase ratio in the tufting stage depends strongly on the tufting density. The final composite piece presents 41% fibre volume fraction and 0.3% porosity. In order to carry out the next analysis, each tufted composite piece is cut into several cube samples with the dimension of $40 \times 18 \times 21$ mm^3. For each DTL there are five samples; each sample has three tuft lines, and each lines has 7 – 9 tuft points (see Figure 3-5).

Table 3-2 Main properties of the tufted preform and composite

	Before tufting	After tufting	After infusion
Thickness (mm)	25±0.3	23±0.4	21±0.7
Mass of preform/composite (g)	587.1±0.5	591.9±0.5	1008.9±0.3
Mass increase ratio	0	0.8%	71.8%
Fibre volume fraction	–	–	41%

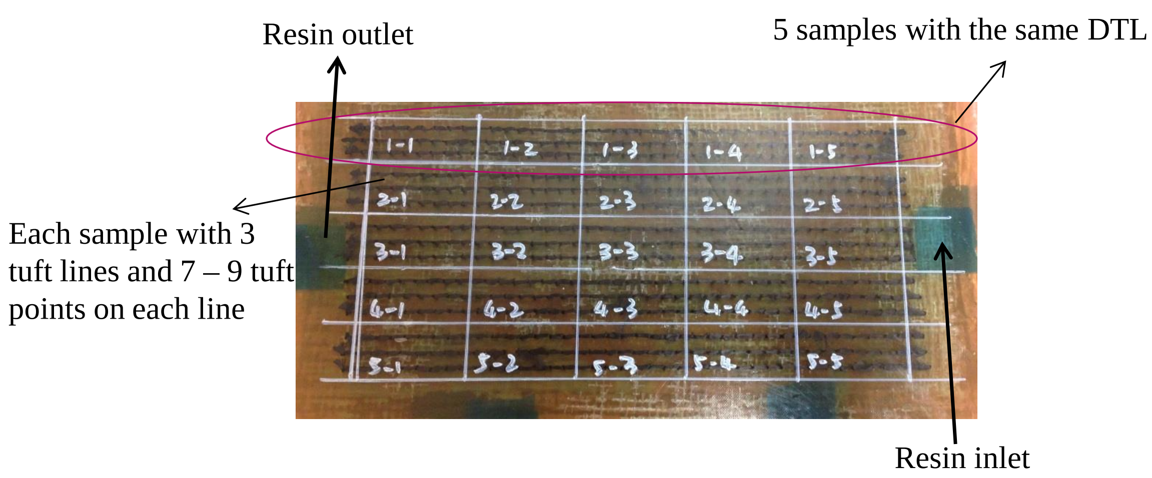

Figure 3-5 The tufted composite samples.

3.3.2 Effective Tuft Length (ETL)

As presented in the "Introduction" section, the aim of this study is to analyse the influence of tuft length on the mechanical properties of tufted composite part. Consequently, the first study should concern how to define the tuft length in the final tufted composite and how to control this length.

The definition of the different tuft lengths is described in Figure 3-6. During the tufting process, the needle is inserted and then removed from the preform on carrying the tufting thread which is held by the preform to remain in place. Therefore, the Desired Tuft Length (DTL) corresponding to the stroke of tufting needle will be modified during tufting due to the drawing-back effect of the tufting needle. The Real Tuft Length (RTL) is the final length measured in the complete composite piece by micro-observation shown in Figure 3-7. If the needle inserts through the whole thickness, the RTL is equal to the thickness of the tufted composite (Figure 3-6). The Effective Tuft Length (ETL) presents that obtained in the lower part, as the tufted preform is divided into two parts (upper and lower parts) by the release film. The thicknesses of the upper and lower parts are 5.6 mm and 15.4 mm respectively. As presented previously, the tuft length presented in the final composite piece is different from the DTL. Figure 3-6 shows the ETL as a schema and Figure 3-7 shows the ETL in a tufted composite sample. It can be noted in Figure 3-7 that the ETL is not quite homogenous in this sample. Consequently, the ETL should be measured and controlled.

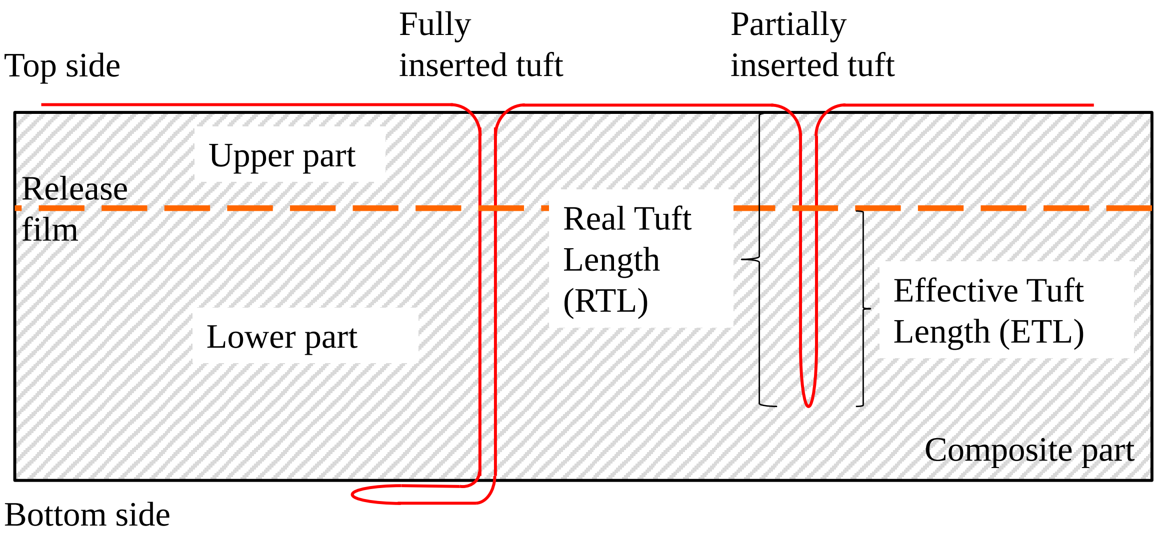

Figure 3-6 Definition of RTL and ETL.

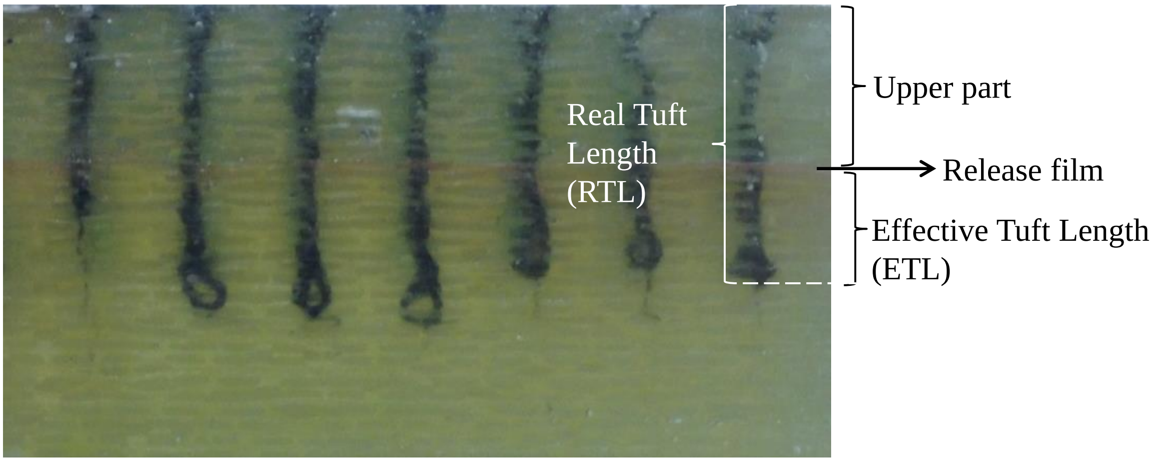

Figure 3-7 RTL and ETL presented on a tufted composite sample.

After optimising the needle insertion and drawing-back speed (59 mm/s), the tuft length can be controlled well. Consequently, the ETL is homogenous in the samples. Figure 3-8 shows the measurement of ETL in a sample with 24.6 mm DTL. It should be recalled here that five tested samples with the same DTL are prepared (cf. 3.3.1). In Figure 3-8, the length of 7.8±0.4 mm presents an average value of seven tuft points in one sample. The five average values for the five samples are calculated, and finally a mean ETL can be obtained.

The RTL in the tufted composite piece corresponds to each DTL shown in Figure 3-2 is listed in Table 3-3. The different lengths due to drawing-back effect of needle can be estimated by the difference between the DTL and the RTL. The drawing-back length corresponding to each DTL is also presented in Table 3-3. It can be seen that there is very little variation in the drawing-back length for different DTL, and it can therefore be considered that the drawing-back effect of the tufting needle is quasi identical even if the desired tuft length is different. Consequently, the real tuft length can be controlled accurately when the tufting process/condition (the tufting needle, tufting thread, tufting speed, preform…) is not changed. In the present tufting condition, the average drawing-back length is 11.5 mm.

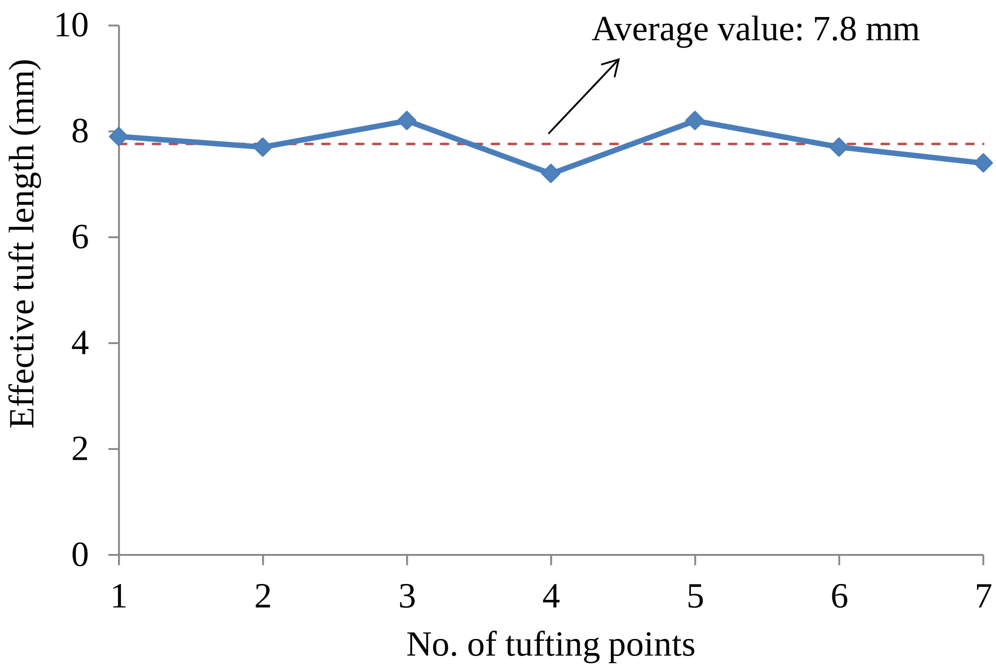

Figure 3-8 Measurement of the ETL (e.g. for a sample with 24.6 mm DTL).

Table 3-3 Measurement of tuft lengths.

DTL (mm)	RTL (mm)	ETL (mm)	Drawing back length (DTL-RTL) (mm)
17.6	6.3	0.7	11.3
19.6	8.1	2.5	11.5
21.6	10.1	4.5	11.5
23.6	12.1	6.5	11.5
24.6	13.3	7.8	11.3
25.6	13.9	8.3	11.7
		Average :	11.5

3.3.3 Micro-observation

Figure 3-9 shows the micro-observation of the cross section of a tufted composite sample. The tufting thread with a free loop and the glass yarns can be observed. The tufted composite is divided into upper and lower parts by the release film. The ETL is shown by the length of the tufting thread inserted into the lower part. There is no concentrated porosity and there are resin-rich zones around the tufting thread. The tufting threads are slightly inclined (inclination < 4°), which is probably caused by the flow of resin during the infusion stage. The tufting thread should be twisted before the tufting process to facilitate insertion and to avoid degradation during tufting. However, a slight degradation of the tufting thread can be observed and the tufting thread has become slightly untwisted during the tufting process.

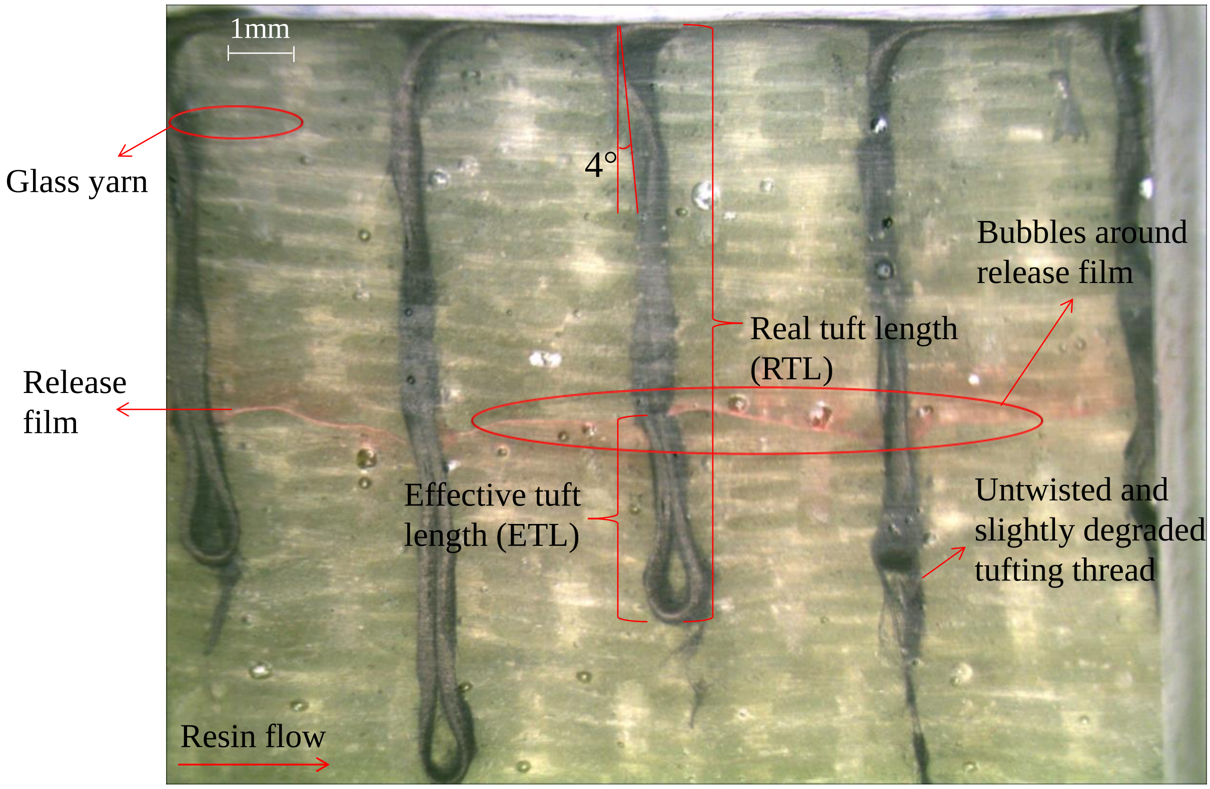

Figure 3-9 Cross section of tufted composite sample under micro-observation.

3.4 Tensile results

The experimental set-up of the tensile tests in the thickness direction of tufted composite is shown in Figure 3-10. The crosshead speed used during the tensile test is 2 mm/min and the dimensions of the sample are 40 × 18 × 21 mm^3 as presented in section 3.3.1. In order to perform the tensile characterisation on the small-size sample, two metal parts with a shape of “T” were applied to adhere top and bottom surfaces of the sample (Figure 3-10). The sample and “T” metal parts are well placed in the axe of the tensile machine to avoid the in-plane shear effects during the tensile test. As the release film is placed between the 24th and 25th layers (see Figure 3-1), there is no adhesive force between the upper and lower parts of composite (see Figure 3-7), which means that only carbon threads (tufting threads) provide tensile force during the tests. As the different tufted composite samples were prepared with different ETL (not only the sample presented in Figure 3-2), the influence of ETL on the tensile properties of tufted composite could be characterised.

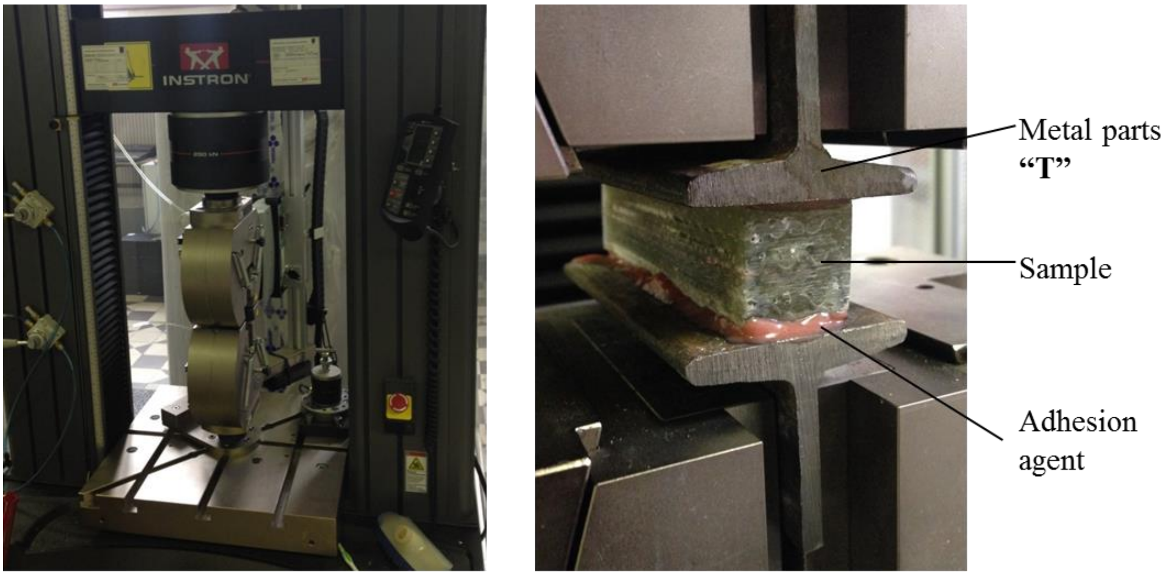

(a) (b)

Figure 3-10 (a) Tensile instrument and (b) tensile test set-up.

The tested samples are broken into two parts at the end of the test due to the presence of release film as shown in Figure 3-11. The tufting threads may be broken clearly at the separation surface. When the ETL is not long enough, the tufting threads may be extracted from the composite sample. Consequently, to characterise completely the tensile properties of tufted composite, the number of tuft points and the broken and extracted tufting threads should be counted besides the breaking load of tufting threads.

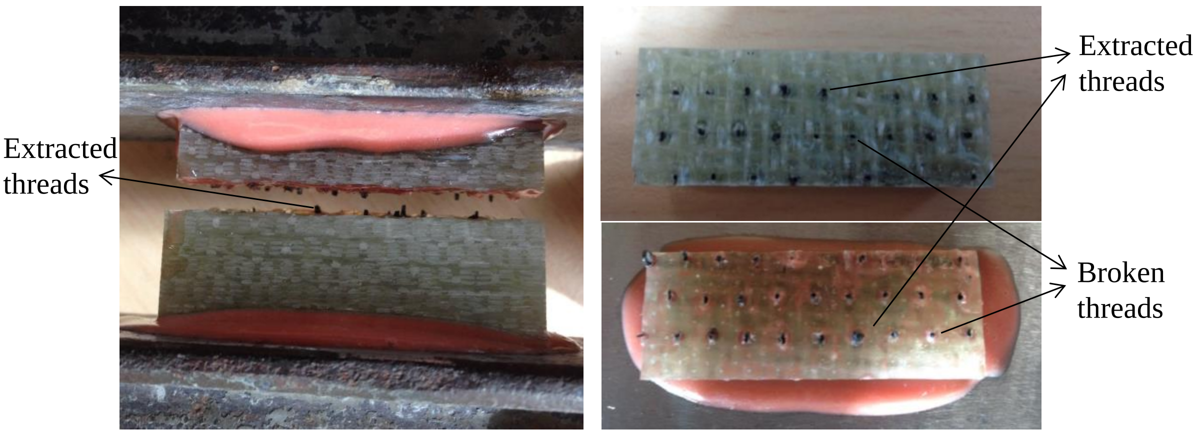

Figure 3-11 Broken surface of tensile test sample.

Table 3-4 shows the numbers of broken and extracted tufting threads corresponding to each ETL. As presented previously, each sample has three tuft lines and each tuft line has 7 – 9 tuft points. Therefore, the number of tuft points in a sample may be different. In addition, there are two tufting threads at each tuft point. It can be noted in Table 3-4 that the smaller ETL, the more tufting threads are extracted from the composite sample. Moreover, all of the tufting threads are broken clearly at the separation surface when the ETL is superior to 7.4 mm.

Table 3-4 Characterisation of tensile samples after break (partially inserted tuft).

Sample Ref.	**ETL (mm)**	**Total tuft points**	**Broken tuft points**	**Slippage tuft points**	**Broken tufting threads**	**Extracted tufting threads**
1	0.6	21	3	18	6	36
2	0.7	21	5	16	10	32
3	2.5	23	12	11	24	22
4	4.6	26	24	2	48	4
5	6.6	21	20	1	40	2
6	7.4	21	21	0	42	0
7	8.9	21	21	0	42	0
8	11.7	21	21	0	42	0
9	13.6	21	21	0	42	0

The maximum tensile load (the breaking load) per tufting thread per ETL is shown in Figure 3-12. Because of the presence of release film in the tufted composite, the tensile load can be considered as being carried 100% by the tufting threads through the thickness. It can be noted in Figure 3-12 that increasing the ETL leads to an increase in maximum tensile load per tufting thread and that this development gradually diminishes. This non-linear evolution can be divided into three parts. At the beginning of the curve (ETL < 3 mm), it can be noted that the maximum load per tuft thread is quasi proportional to the ETL. In the present case (3K carbon tow, epoxy resin), the proportion is about 37 N/ mm, which is a valid law for low ETL (< 3 mm). The predominant phenomenon in the case of low ETL is delamination of the tufting tow, *i.e.* rupture of the resin around the inserted tuft loop. In the second part of the curve (between 3 mm and 8 mm), it is sometimes the rupture of the consolidated tufting thread and sometimes that of the resin around the inserted tuft loop which is predominant, which explains the increase of the standard deviations shown on the curve. The longer the ETL, the more the tufted thread ruptures in comparison with the resin around the inserted tuft loop. Conversely, the shorter the ETL, the more the resin around the inserted tuft loop ruptures in comparison with the tufted thread. Beyond the ETL of 8 mm, the evolution of the tensile load becomes stable and no longer depends on the ETL. In the present case (3K carbon tow, epoxy resin), the maximum tensile force per tufting thread finally converges at 135 N. The predominant phenomenon for ETL > 8mm is the rupture of the consolidated tufting thread, and this is confirmed by the results presented in Table 5: during the tensile test, there is no extracted loop observed in the separation surface of the tufted samples where the ETL > 7.4 mm.

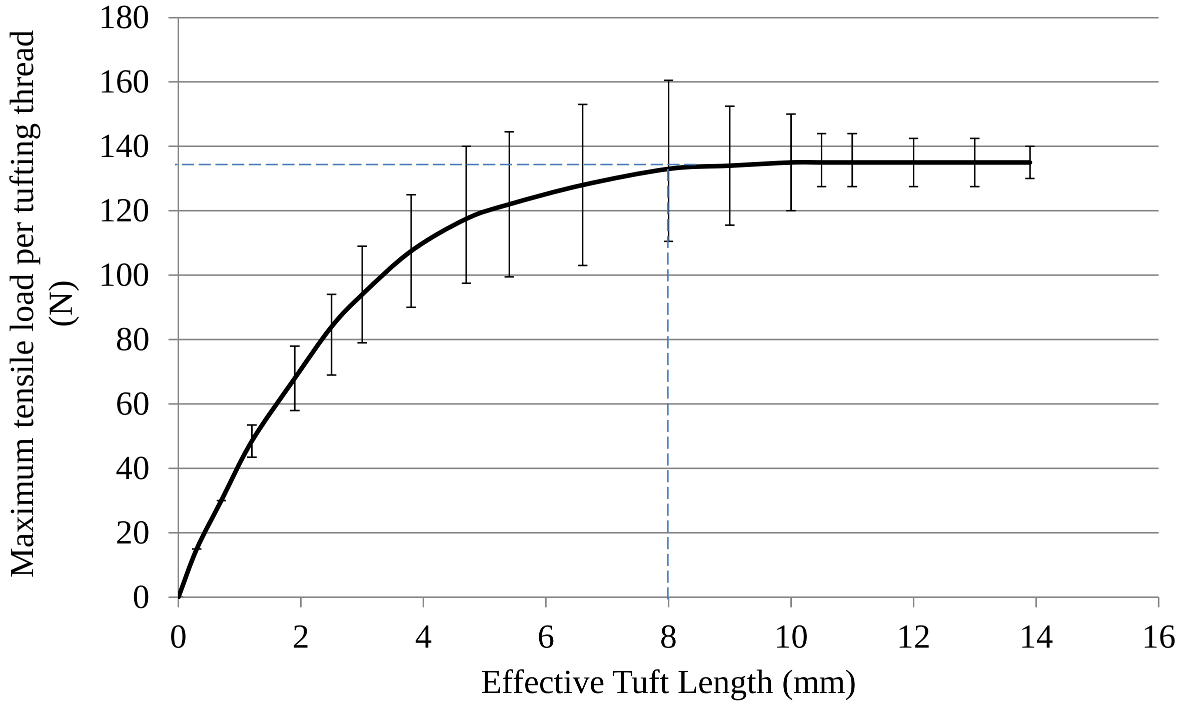

Figure 3-12 Influence of ETL on maximum tensile load per tufting thread for partially inserted tuft case.

Other samples are tufted throughout the thickness (fully inserted tuft), the free loops appear at the bottom side of sample. The tensile characterisation of tufted composite samples obtained by fully inserted tuft is shown in Table 3-5. In order to obtain different thicknesses in the lower part (the ETL in the case of fully inserted tuft), the thickness of the tufted sample (the number of layers) has been changed. In all fully inserted tuft cases, the tufting threads are broken cleanly at each tuft point on the separation surface. The mean value of 84.2 N is obtained for maximum tensile load per tufting thread, which is 37% less than that of partially inserted tuft (135 N in the case of partially inserted tuft). This is probably due to the higher degradation effects presented in the fully inserted tuft case and the more winding threads created under the compression effects during the resin infusion process under vacuum environment.

Table 3-5 Characterisation of tensile samples after break (fully inserted tuft).

Sample Ref.	Total thickness / Thickness in bottom part (mm)	Total tuft points	Broken tuft points	Slippage tuft points	Maximum tensile load per tufting thread (N)
1	13.3 / 10.0	21	21	0	88.9
2	21.0 / 14.6	21	21	0	81.0
3	21.0 / 15.4	21	21	0	79.4
4	21.0 / 15.4	21	21	0	85.5
5	25.0 / 16.4	21	21	0	86.2
				Average:	84.2

3.5 Discussion

The results presented in this section show that the tufting thread may be broken or extracted on the separation surface. In partially inserted tufting, the number of broken and slippage tuft points depends strongly on the ETL. When the ETL is superior to 7.4 mm, no inserted tuft loop is extracted. In this case, the tufting thread is well inserted in the preform and therefore the tufted composite part can be well reinforced through the thickness, which is the aim in using tufting technology in the manufacturing of thick composite pieces. For the tufting thread tested, the tensile strength can be estimated in the final tufted composite part by using the equation below (Equation 3-1):

$$\textbf{Maximum tensile load per tufting thread} = \frac{\textbf{Broken tuft points}}{\textbf{Total tuft points}} \times \mathbf{135\ N} \qquad (\mathbf{3-1})$$

When the broken tuft points are equal to the total tuft points (ETL ≥ 7.4 mm), the maximum tensile load per tufting thread tends to a constant, 135 N. This constant depends on the type of tufting thread and the preform. In partially inserted tufting, the minimum ETL to ensure the effect of through-the-thickness reinforcement of composite (7.4 mm in the present case) does not depend on the thickness of the tufted composite part, but depends on the tufting process (type of needle, tufting speed…), tufting thread and the preform.

During fully inserted tufting, a lower maximum tensile load per tufting thread is obtained compared to partially inserted tufts. This maximum tensile load per tufting thread is quasi constant. The longer stroke of the tufting needle in the preform in fully inserted tufting causes more degradation on the thread (Figure 3-13a). Compared to partially inserted tufting, in fully inserted tufting the tuft loops are inserted more deeply into the foam (outside of the preform), so the tufting threads are probably more degraded due to the greater friction effects present on the interface of the tufting threads/foam than the tufting threads/preform. The degradation in the preform and the foam depends mainly on the structure of the preform and foam: the denser the preform and foam, the more the tufting thread is degraded. On the other hand, the tufting threads throughout the thickness of the preform are well compressed during the resin infusion process. The tufting threads are not straight in the final composite piece, which can be noted in Figure 3-13b: Winding threads can be observed, in particular in the lower part of the composite. By contrast, the inserted threads remain straight in the tufted composite in the case of partially inserted tuft (see Figure 3-9). The winding threads can reduce the quality of the resin infusion due to the greater number of porosities created around them.

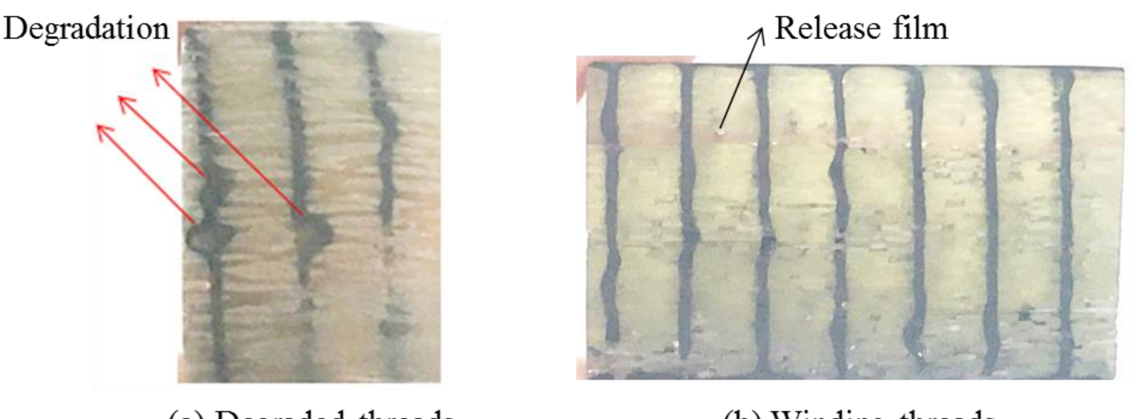

(a) Degraded threads (b) Winding threads

Figure 3-13 Micro-observation of the tufting threads in tufted composite in the case of fully inserted tuft.

3.6 Conclusion of Chapter 3

In this chapter, the manufacturing of tufted composite and tensile characterisation of these tufted samples is outlined. As one of the important process parameters, the influence of tuft length through the thickness on the characterisations of tufted composites have been completely analysed in this study.

In order to better conduct the observation about the tuft length and tufting yarn loop, it has chosen to tuft carbon yarns into a glass fibres reinforced fabric. Thick assembled reinforcements are prepared by using tufting equipment described in chapter 2. Tufted preforms are infused with an epoxy resin by liquid resin infusion process. Microscopic analysis on the cross section of tufted preforms presents the inner structure of tufted composite.

Tensile test results present the influence of tuft length on the mechanical performance. The optimisation of the tufting process has been investigated, and an effective tuft length of 8 mm is the minimum required to guarantee that the multi-layered composite part can be well reinforced through the thickness with the given tufting threads and preform. When the effective tuft length is superior to the optimised one, the tensile strength of the tufting thread in composites tends to constant in the case of partially inserted tuft. To avoid high degradation of the tufting threads, the better method is partially inserted tufting compared to fully inserted tufting.

Degradation during tufting always exists even if twists are added to the tufting threads. Compared to tufting threads with no twists, twisted threads are a better solution for the given tufting threads.

References of Chapter 3

[1] Faggiani A, Falzon BG. Prediciting low-velocity impact damage on a stiffened composite panel. Composites Part A 2010;41:737–49.

[2] Falzon BG, Hawkins SC, Huynh CP, Radjef R, Brown C. An investigation of Mode I and Mode II fracture toughness enhancement using aligned carbon nanotubes forests at the crack interface. Composite Structures 2013;106: 65-73.

[3] Green SD, Long AC, EI Said BSF, Hallett SR. Numerical modelling of 3D woven preform deformations. Composite Structures 2014;108: 747–56.

[4] Mahadik Y, Robson Brown KA, Hallett SR. Characterisation of 3D woven composite internal architecture and effect of compaction. Composites A 2010;41:872–80.

[5] Mouritz AP, Leong KH, Herszberg I. A review of the effect of stitching on the in-plane mechanical properties of fibre-reinforced polymer composites. Composites Part A 1997;28(12) : 979–91.

[6] Mouritz AP, Cox BN. A mechanistic approach to the properties of stitched laminates. Composites Part A 2000;31:1–27.

[7] Dell'Anno G, Cartié DD, Partridge IK, Rezai A. Exploring mechanical property balance in tufted carbon fabric/epoxy composites. Composites Part A 2007;38:2366–73.

[8] Dell'Anno G, Treiber J, Partridge I. Manufacturing of composite parts reinforced through-thickness by tufting. Robot Comput – Integr Manuf 2016;37:262–72.

[9] Henao A, Carrera M, Miravete A, Castejon L. Mechanical performance of through-thickness tufted sandwich structures. Composite Strutures 2010;92:2052-59.

[10] Osmiani C, Mohamed G, Treiber JWG, Allegri G, Partridge IK. Exploring the influence of micro-structure on the mechanical properties and crack bridging mechanisms of fibrous tufts. Composites Part A 2016;91:409–19.

[11] Colin de Verdiere M, Pickette AK, Skordos AA, Witzel V. Evaluation of the mechanical and damage behaviour of tufted non crimped fabric composites using full field measurements. Compos Sci Technol 2009;69:131–38.

[12] Liu L, Zhang T, Wang P, Legrand X, Soulat D. Influence of the tufting yarns on formability of tufted 3-Dimensional composite reinforcement. Composites Part A2015;78:403–11.

[13] Hartley JW, Kratz J, Ward C, Partridge IK, Effect of tufting density and loop length on the crushing behaviour of tufted sandwich specimens, Composites Part B 2017, doi: 10.1016/j.compositesb.2016.12.037.

[14] Wittig J. Recent development in the robotic stitching technology for textile structural composites. Journal of Textile and Apparel, Technology and Management, 2001; 2(1): 1-8.

[15] Colin de Verdiere M, Pickett AK, Skordos AA, Witzel V. Effect of tufting on the response of non crimp fabric Composites. ECCOMAS Thematic conference on mechanical response of composites. Porto, Portugal, 12-14 September 2007.

[16] Wang P, Drapier S, Molimard J, Vautrin A, Minni JC. Characterization of Liquid Resin Infusion (LRI) Filling by Fringe Pattern Projection and in-situ Thermocouples. Composites Part A 2010;41:36-44.

[17] Govignon Q, Bickerton S, Morris J, Kelly PA. Full field monitoring of the resin flow and laminate properties during the resin infusion process. Composites Part A 2008;39:1412–26.

4 INFLUENCE OF THE TUFTING YARNS ON FORMABILITY OF TUFTED 3D COMPOSITE REINFORCEMENT

4.1 Introduction

Resin Transfer Molding (RTM) [1, 2] is the main manufacturing process to produce textile reinforced composite parts in aerospace and defense industries [3, 4]. The first step of RTM process, is carried out to understand the deformability of preform on more and more complex shapes (given by punch and die). During the forming of complex shapes, the textile is subjected to large local and global deformations, which influence the fibre orientation, the fibre volume fraction and the component thickness. These factors along with the occurrence of wrinkles or gaps between the yarns determine the product quality of the final composite product. Fibre misalignments and wrinkles would reduce the mechanical properties of the final composite part. Therefore it is important to control the fibre orientation and fibre placement in order to obtain an optimized load-bearing product.

In recent years, several experimental and numerical studies exist concerning the draping stage of dry reinforcement. B. Zhu et al. [6] observed that the shear distribution in the preform is a combined result of both the mould shape and the initial sample orientation. The evolution of deformation has a non-linear history during a uniform stamping process. The validity of a previously proposed wrinkling criterion was evaluated on the present specimen at room temperature, achieving approximate agreement with the stamping tests.

Detailed and quantitative estimations and optimizations were carried out for the mould shape, blank sheet orientation, blank holder force, forming temperature and stamping speed. S.Allaouim et al. [8] carried out experimental studies which showed that, when working with dry fabric forming, the type and number of defects is a function of the punch geometry, the process parameters, the orientation of the fabric with respect to the punch and the inter-ply friction. Inter-ply friction has a huge effect on the quality of the preform when inter-ply sliding occurs. This inter-ply friction leads to several overhanging yarn shocks that generate high tangential forces, which inhibit the relative sliding of plies. In addition, to reduce the number and amplitude of defects, the layers subjected to severe defects can be placed in the inner position where they are subjected to the compression applied by the upper layers. S.P. Haanappel et al. [9] worked on the formability of two different composite materials used in aerospace industry. The UD/PEEK blanks were very sensitive to wrinkling near doubly curved areas, whereas the 8HS/PPS blanks deformed smoothly without defects in those areas. Both materials showed wrinkling in the curved flanges, however the number of wrinkles, the size, and their distribution depend on the material. P. Harrison et al. [10] did research on the pre-consolidated thermoplastic advanced composite cross-ply sheet comprised of two uniaxial plies orientated at 0/90° which has been thermoformed using tooling based on the double-dome bench-mark geometry. They observed that mitigation of wrinkling was achieved using springs to apply tension to the forming sheet rather than using a friction-based blank-holder. K. Vanclooster et al. [12] carried out forming simulations on woven textile composites by using an explicit finite element method and a kinematic mapping scheme to compare with experimental results that are obtained by determining the fibre orientations of glass/PP woven composites thermoformed on and extended hemispherical shaped mould with different orientations of the blank. As a result they found that the kinematic mapping approach severely fails in predicting the fibre reorientation that occurs during stamp forming for non-symmetrical forming configurations. The FEM-simulation gives a reasonably good prediction of the fibre reorientation and seems the most promising technique in having good draping simulations. M. A. Khan et al. [7] worked on an algorithm which is based on a hypoelastic behavior for the simulation of composite reinforcement forming processes. It is shown that using hypoelastic law with an objective derivative based on the warp and weft fibre rotation tensors can correctly trace the specific behavior of the woven materials. H. Yin et al. [11] used a previously developed simple anisotropic hyper-elastic model to characterize the material behavior of the woven carbon fabric under complex deformation modes and studied the influence of fibre orientation on forming double-curvature parts. P. Boisse et al. [14] analysed the role of tensile, in-plane shear and bending in wrinkling simulations and observed that wrinkling is a global phenomenon depending on all strains and stiffnesses and on boundary conditions, and bending stiffness mainly determines the shape of the wrinkles. N. Hamila et al. [18] proposed a semi-discrete approach for textile composite draping. X. Peng et al. [16, 19] validated the non-orthogonal constitutive model via hemispherical stamping simulation of a square woven composite fabric by a fully continuum mechanics-based approach with finite element method and also has developed a simple hyperelastic constitutive model to characterize the anisotropic and large deformation behavior of textile fabrics. P. Ouagne et al. [20] applied a flax fibre plain-weave fabric to form a complex tetrahedron shape and proposed solutions to prevent the appearance of tow buckling (out of plane bending of tows) on the design of the fabric architecture at the tow or fabric scales. E. Capelle et al. [21] studied the possibility of forming complex shape such as a tetrahedron using two untwisted commercial flax based fabric reinforcements using the sheet forming process and proposed a specially designed non-optimised blank holder set to suppress the defects such as tow buckles or tow sliding. S. Gatouillat et al. [22] proposed a mesoscopic approach for the simulation of woven preforms forming which permits to simulate and to highlight the phenomenon of the loss of cohesion of the woven fibre network. J.Cao et al. [23] conducted trellis-frame (picture-frame) and bias extension tests for both balanced and unbalanced fabrics and compared through collaborative effort to observe the shear deformation which is the dominative deformation mode for woven fabrics in forming. A.G. Colman et al. [24] proposed a novel picture frame shear test design and associated test protocol that aims to provide a practicable solution for the accurate determination of the in-situ shear stiffness of architectural fabrics. J. Launay et al. [26] proposed an experimental device which enables to measure the tensions in the yarns during a picture frame test. They observed that when the forming processes uses tools, especially blank holders, the tensions become significant and play a role in the wrinkle formation by modifying the shear stiffness. B. Liang et al. [27] determined bending rigidity of thermoplastic prepreg at high temperatures by a cantilever test in a thermal environmental chamber and observed that the bending stiffness of the fore-mentioned thermoplastic prepregs are greatly influenced by temperature. P. Boisse et al. [30]

investigated the tensile behavior surface of dry fibre fabric reinforcements with different approaches.

These works shown in [14-19] describe the measurement criteria that can qualify the reinforcement formability behaviours such as intraply shearing, material draw-in, load, fibre orientations, and homogeneity of the fibre density. The formability behaviours also depend on the process parameters such as punch shape, blank-holder pressure, initial orientation of reinforcement, etc. On the other hand, the forming defects such as wrinkling [5-9, 14-17], buckling [20, 21], unweaving or loss of cohesion [5, 22], etc. will be related to the formability behaviours. The forming defects are not acceptable for the deformed preform and consequently for the final composite part. Also, these studies [14-19] indicate that all reinforcements used do not have the same capacities of deformability. The determination of mechanical behaviours of the reinforcements including in-plane shear [23-26], bending [27-29] and tensile [30, 31], is essential and complementary to the preforming tests.

In literature, the preforming of multilayer dry textile reinforcements has been one of the main subjects [7-9, 18, 31-33]. In the considered forming parameters cited previously, the number of layers and the orientation of each ply must be taken into account. The inter-ply behaviour is described through numerical and experimental studies concerning inter-ply sliding and the identification of friction laws [34-36]. However, these studies did not measure the quantities in each ply of the multilayer. The criteria of forming are generally the same ones used in the preforming of a single layer and estimated on the top or bottom ply. The work presented in [34-36] show that preforming of multilayer is not yet controlled and demonstrate the influence of the layer orientations on the sliding and therefore on the final shape.

The deformability of NCF (Non Crimp Fabrics), the fabric reinforced through thickness by stitching, during the preforming is well presented in [36, 43-46]. M. Duhovic et al. [43] and A. Margossian et al. [44] worked on the development of finite element models for simulating the deformation of woven fabric and non-crimp fabric preforms to determine the influence of stitching patterns on the forming behaviour. J. Pazmino et al. [45] and V. Carvelli et al. [46] worked on the formability and deformability of a single layer E-glass non-crimp 3D orthogonal woven reinforcement that the former one involves the forming process on two complex moulds: tetrahedron and double-dome and the latter focused on the measurement of the main deformation modes, tension and in plane shear. On the contrary, in these studies the influence of the specific parameters of the binder reinforcement (density of stitching, orientation relatively to the punch, stitching yarns direction, etc...) on measurement criteria during the preforming is less demonstrated. Moreover, the influence of through-thickness fibres on the preforming defects is not described. In the paper [47-49] concerning the 3D reinforcements performed by tufting technology, the analyses of the influence of through-thickness fibres are entirely carried out during the multilayered E-glass plain weave forming.

In order to improve the understanding of formability of the tufted 3D fabric during manufacturing, the present work analyzes the preforming behaviors of tufted 3D reinforcement in the hemispherical stamping process. Also the preforming behaviours are compared with the samples of the multilayered forming. The experimental data demonstrated the influence of tufting yarns on the material draw-in, interply sliding, and wrinkling phenomenon during forming. Furthermore, the orientations of tufting yarn affected the forming results, which leaded to misalignment defect in the zone of strong in-plane shear.

4.2 Material and method

4.2.1 Tufting process and tufted 3D composite reinforcement

The reinforcement fabric selected in current study is E-glass plain weave produced by Aerovac with an area density of 157 ± 5 g/m^2. The tested preforms were firstly laminated with four plies. The sequence of preform $[\pm 45°, 0°/90°]_2$ is shown in Figure 4-1. The dimensions of the tested preforms are $280 \times 280 \times 1.0$ mm^3. Then the preforms are tufted by TENAX® carbon yarn with different tufting densities corresponding to a tufting spacing. The properties of 67×2tex TENAX® carbon thread are described in Table 2-3 in Chapter 2. In this study, a carbon yarn was tufted into a glass fabric. As mentioned in former chapter, after epoxy resin injection, glass fabric becomes translucent. Consequently, it is possible to conduct the observation about the tufting yarn loop (carbon yarn loop).

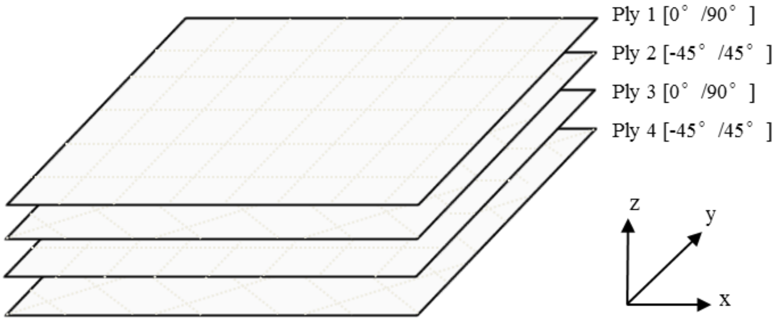

Figure 4-1 The sequence of tested preform.

Figure 4-2 shows the top view of the tufting pattern that the tufting points are arranged according to a square spiral pattern. The tufting spacing represents the distance between two tufting lines which is also demonstrated in Figure 4-2. The tufting density represents the distance between two near tufting points. In this case the tufting spacing and the tufting density are the same.

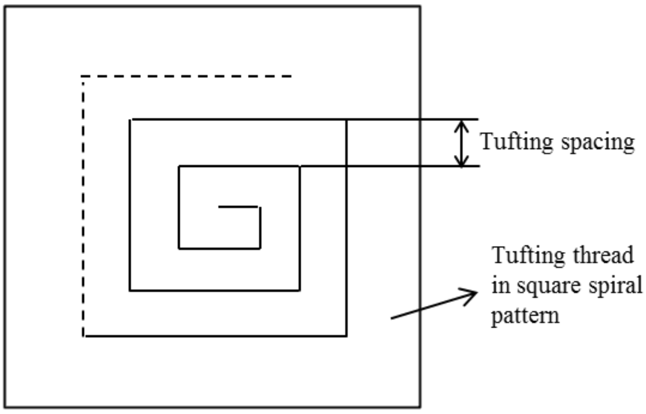

Figure 4-2 The top view of tufting pattern.

The main properties of the tufted 3D fabric specimens are listed in Table 4-1. These samples are tufted by a hollow needle of 2 mm diameter with a tufting length of 10 mm. The tufting densities and spacing used can be changed from 5mm to 20mm.

Table 4-1 Main properties of the tufted 3D fabric specimens.

Ref. of samples	Area density (g/m^2)	Tufting spacing (mm)
Non-tufted	626.3	-
Tufted 2.0	639.0	20
Tufted 1.0	665.8	10
Tufted 0.5	707.9	5

One of the preforms after tufting (Tufted 1.0) is shown in Figure 4-3. As mentioned above, the preform is tufted in a square spiral pattern to assure that the tufting thread is continuous, uninterrupted and inserted in two directions (the warp and weft directions).

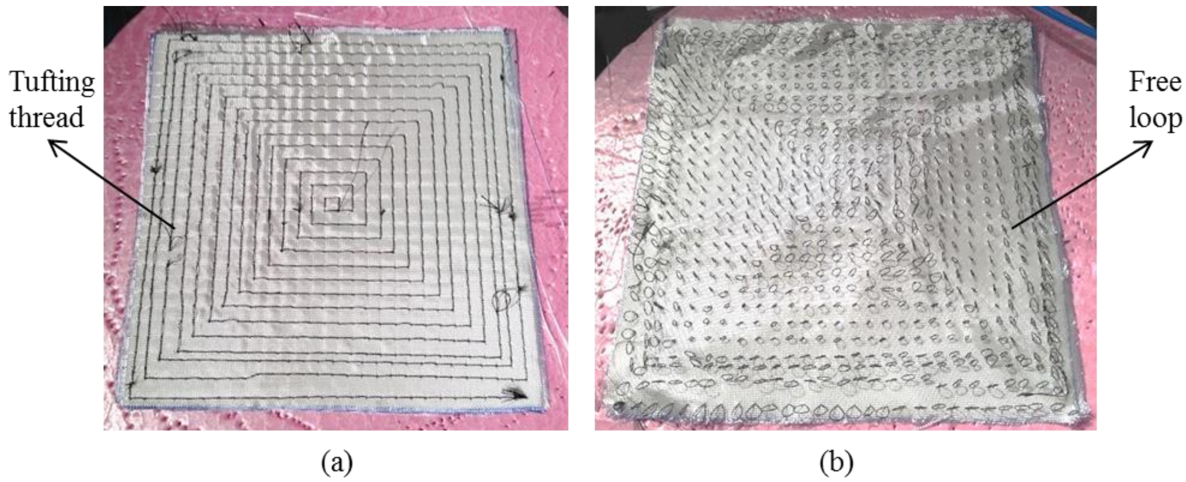

Figure 4-3 Top view (a) and bottom view (b) of tufted sample with a tufting spacing of 10mm.

4.2.2 Hemispherical preforming

In the industry, the most efficient way to form textile composites is through stamping operation, in which a flat sheet is stamped into a particular shape with a pair of punch and die. Stamping is a fast and cost-effective process which can reduce the cycle time by several times in comparison with some other methods of forming complex structural composite products with medium volume.

The hemispherical preforming was performed on a specific forming device shown in Figure 4-4 [39]. This device is used to analyze the double-curved shape forming with a given textile reinforcement under different conditions such as shape and thread of punch, position and pressure of blank-holder, etc. The tufted 3D fabric was placed between the blank-holder and die. Four pneumatic jacks, connecting to the blank-holder, apply an adjustable pressure on the fabric. In order to measure the important forming parameters by optical measurement, such as the material draw-in and inter-layer sliding, the open-die forming was used. An electric jack connected to the punch imposes a movement and a load sensor (500±0.3%) acquires the punch force during the forming. The main parameters of the hemispherical performing are noted in Table 4-2. The main dimensions of forming device are noted in Figure 4-5 [39].

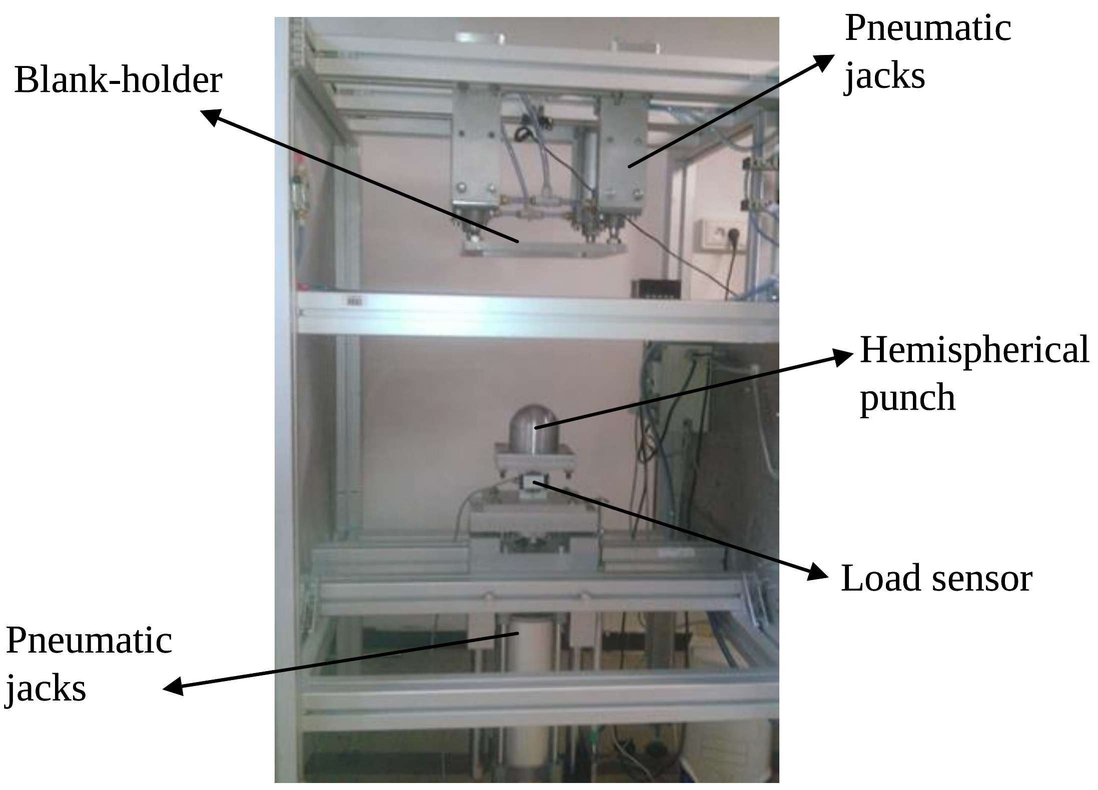

Figure 4-4 The hemispherical preforming device.

Table 4-2 The main parameters of the hemispherical preforming.

Parameter	Value
Stamping speed	45 mm/s
Diameter of hemispherical punch	150 mm
Punch displacement	65 mm
Blank-holder pressure	0.05 MPa

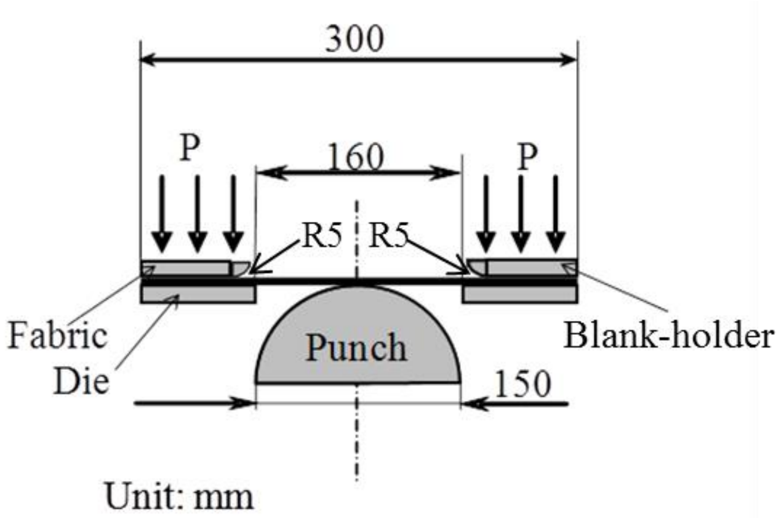

Figure 4-5 The dimensions of the hemispherical preforming device.

4.3 Forming results

Forming experiments were carried out in order to investigate the formability behavior of different preforms. Comparison of the formability between single layer and multilayered reinforcements, 3D tufted preforms with different tufting densities, different sequence and different tufting directions were entirely investigated.

4.3.1 The single layer and multilayered reinforcement forming

Multilayered reinforcement forming is frequently used to manufacture the thick composite parts [32, 52, 53]. Figure 4-6 presents the deformed preform $[0°/90°]_4$ after the hemispherical stamping by using four E-glass plain weave plies. Figure 4-7 shows the deformed preform $[-45°/+45°]_4$ after the hemispherical stamping. These two deformed shapes were symmetric and no wrinkles were observed in the useful zone. As the plies were simply superimposed, the sliding was noted on the interface of plies. The maximum inter-sliding was determined by the difference of material draw-in between the top and the bottom plies.

Figure 4-6 Deformed preform $[0°/90°]_4$ after hemispherical stamping.

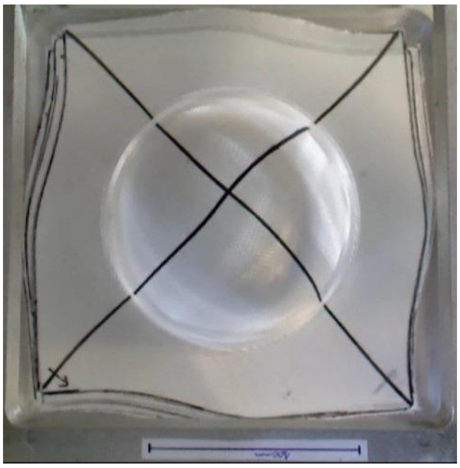

Figure 4-7 Deformed preform: $[-45°/+45°]_4$ after hemispherical stamping.

The maximum force during the two stamping tests was measured and compared with the forming of a single ply. Figure 4-8 shows this comparison of maximum punch force. In multilayered forming, the friction effects on the interface ply/ply are added, therefore the punch force increased during the forming. When the layer orientation was changed from 0°/90° to ±45°, the punch force presented a more significant value in ±45° ply forming due to increased friction surface.

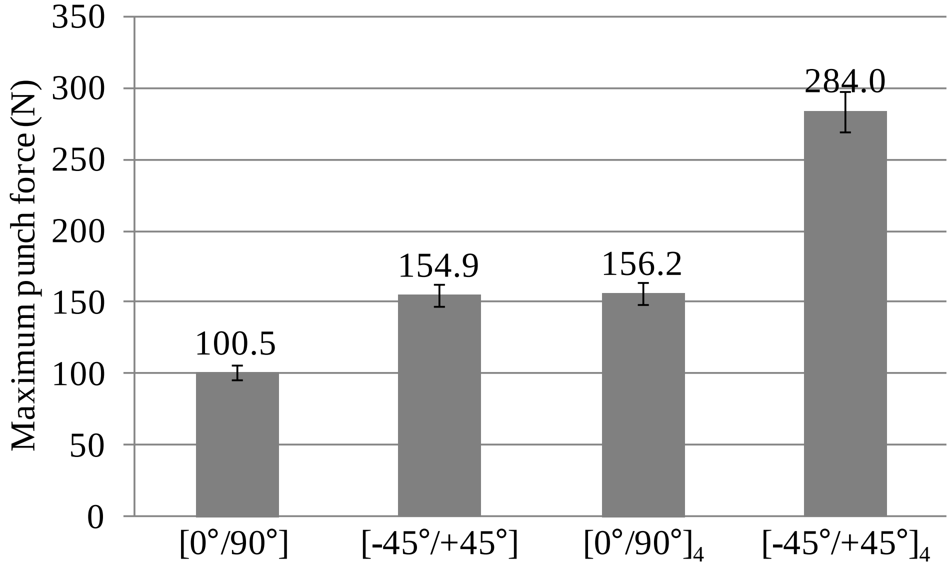

Figure 4-8 The maximum punch force of single and multilayered E-glass plan weaves forming.

The maximum draw-in of a single layer and multilayered E-glass plan weaves forming is presented in Figure 4-9. This maximum draw-in was noted at the central point of four sides of 0°/90° ply and in the four corners of ±45° ply. To the multilayered forming, the maximum draw-in can be always observed on the top ply. Compared to the draw-in between the [0°/90°] and [-45°/+45°] preforms and between the $[0°/90°]_4$ and $[-45°/+45°]_4$ preforms, the draw-in of 0°/90° ply was always bigger than ±45° ply's due to an increasing of friction effects in the ±45° ply between tool/ply and ply/ply. Furthermore, comparing the single-ply and multilayered forming by using the same yarn orientation, the maximum material draw-in was slightly important in the forming of a single ply as the friction coefficient was different on the contact surfaces tool/ply and ply/ply. Normally, the friction coefficient is bigger on the contact surface ply/ply than on the surface tool/ply.

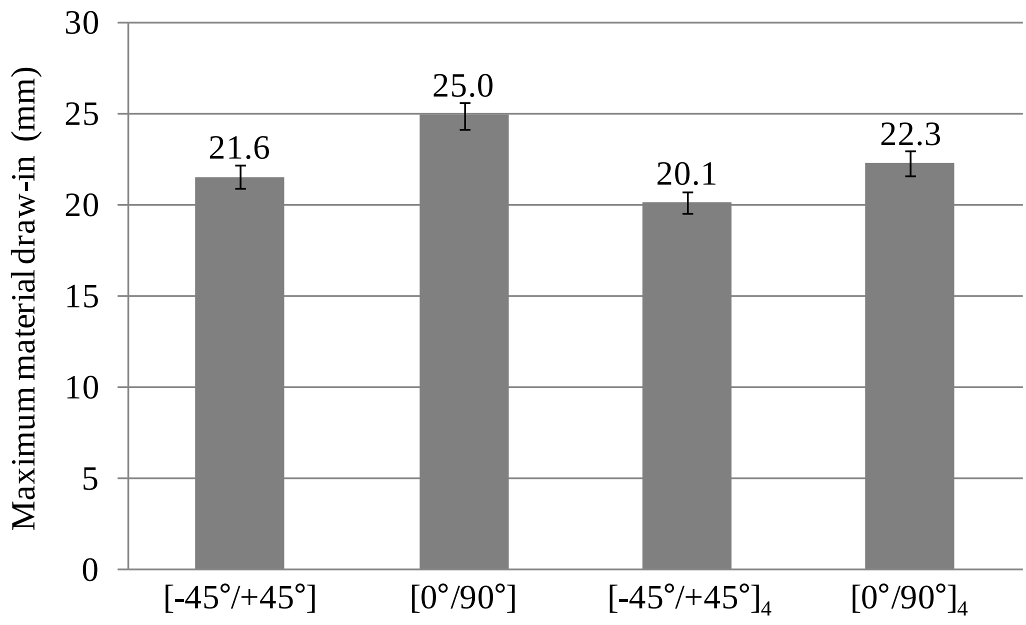

Figure 4-9 The maximum draw-in of single and multilayered E-glass plan weaves forming.

4.3.2 The tufted 3D reinforcement forming

To investigate the influence of tufting spacing or tufting density on the generation of defects during forming process, the preforming of four different tufted 3D fabrics described in Table 4-1 was carried out. The forming conditions are identical to the multilayered forming presented previously in which the punch displacement is 65 mm and blank-holder pressure is 0.05 MPa. The sequence of tested preform, $[\pm 45°, 0°/90°]_2$, was demonstrated in Figure 4-1. The deformed preforms with different tufting spacing are shown in Figure 4-10 to Figure 4-13. Different results corresponding to the influence of tufting spacing can be observed.

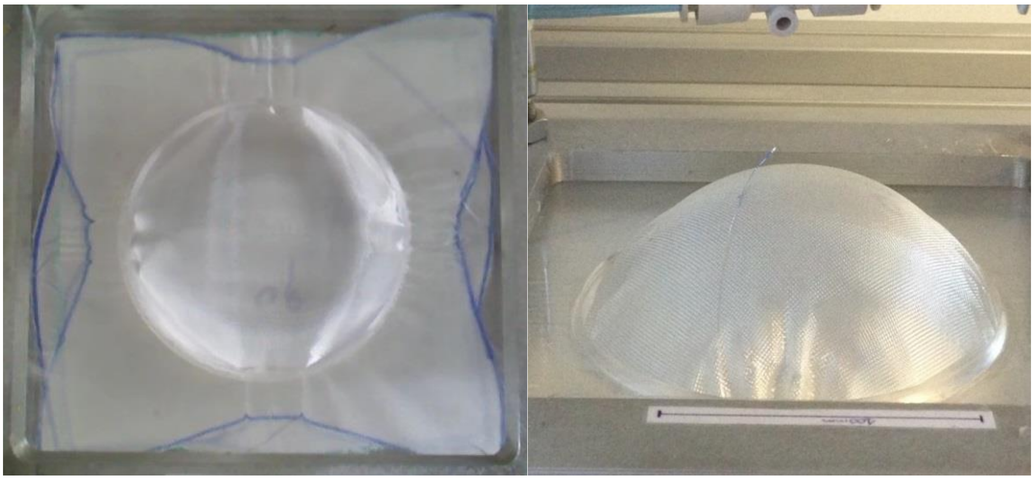

Figure 4-10 Non-tufted preform after performing.

Figure 4-10 shows the deformed non-tufted preform. Wrinkles are observed at the four sides which are distributed irregularly while no wrinkle is observed in the useful zone. The deformed shape is symmetric. A great inter-ply sliding appeared between the 0°/90° ply and ±45° ply.

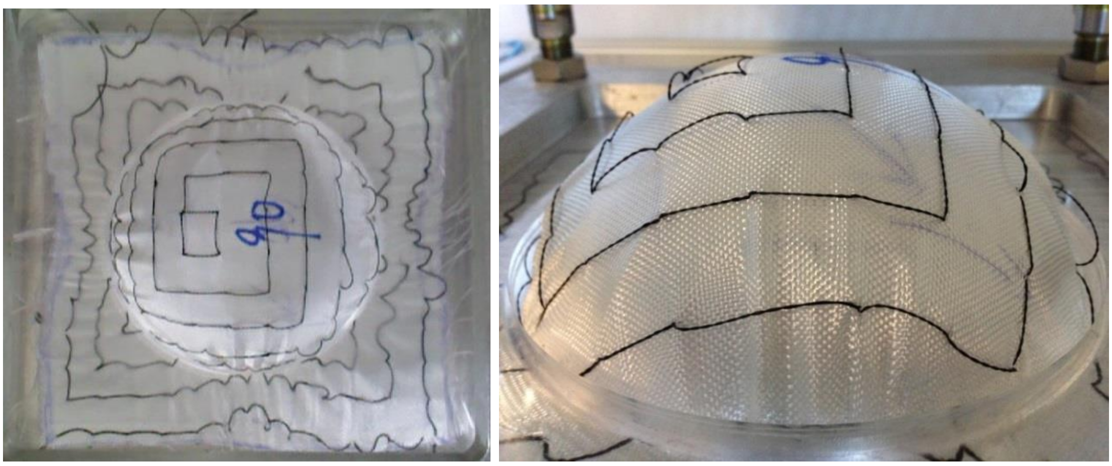

Figure 4-11 3D preform after performing with tufting spacing of 20mm.

Figure 4-11 presents the performing of tufted preform with a tufting spacing of 20mm. The black lines represent carbon fibre tufting thread. With the existence of tufting thread, the effect of inter-ply sliding is reduced but the tufting points are damaged because of this effect. Compared with non-tufted preform, tufted preform with the tufting spacing of 20mm provides wrinkles which are more regular and larger.

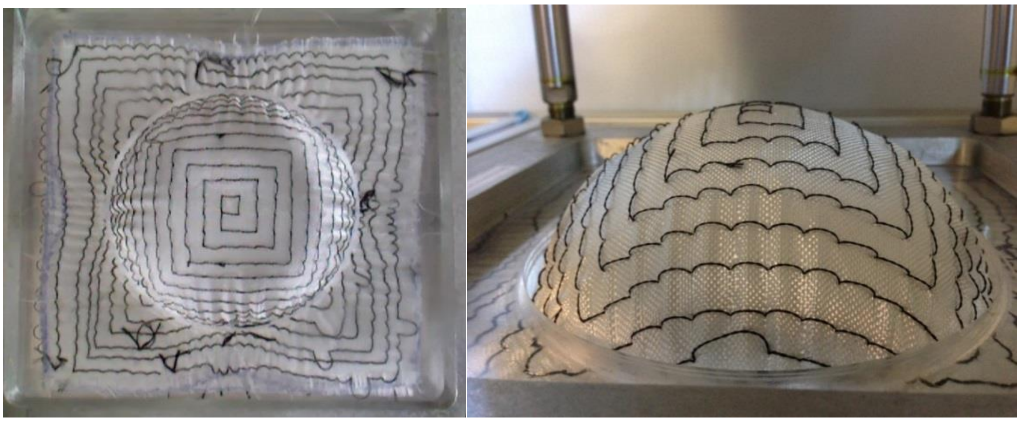

Figure 4-12 3D preform after performing with tufting spacing of 10mm.

The performing of tufted preform with a tufting spacing of 10mm is shown in Figure 4-12. Wrinkles are distributed at the four sides. There is one wrinkle between two near tufting points which is really regular. As the tufting spacing is decreased, the number of tufting points is augmented which provides a slight effect of inter-ply sliding.

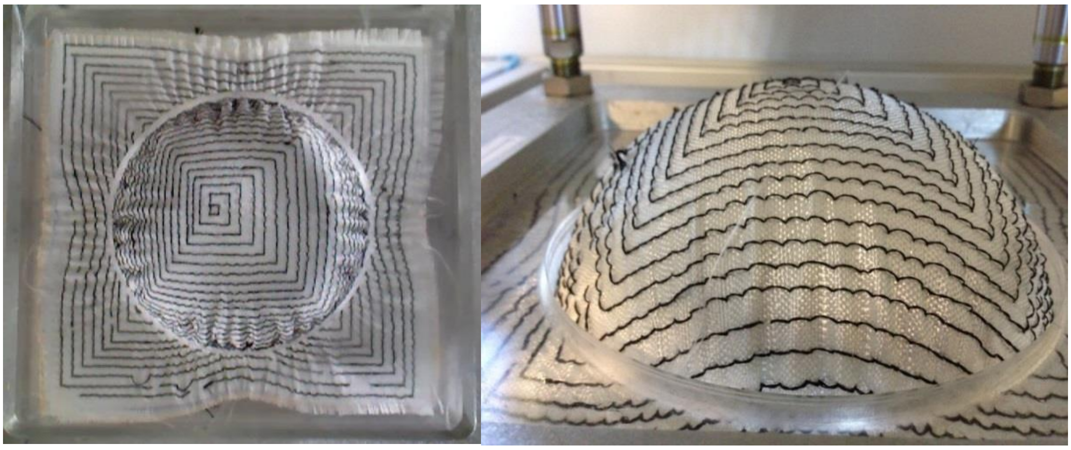

Figure 4-13 3D preform after performing with tufting spacing of 5mm.

Figure 4-13 present the performing of tufted preform with a tufting spacing of 5mm. In this case, irregular wrinkles appear. Because of the high tufting density, the preform is more rigid which needs a larger force to deform. As the tufting spacing is short enough, the appearance of wrinkles doesn't follow tufting points. The effect of inter-ply sliding reduced as while as the draw-in.

Since the tufting yarns can reinforce through the thickness of preform, the inter-ply sliding can be minimized. But, when a weak tufting density was used, the effects of inter-ply sliding can break the tufting yarns (e.g. tufting spacing 10 mm or 20 mm). Consequently, it should adopt a rather high tufting density to reinforce the "Z" direction (e.g. tufting spacing 5 mm). On another hand, a higher tufting density will lead to a heavier and more rigid preform, and hence the preform is more difficulty to be deformed. In order to improve the understanding of tufted 3D reinforcements and of their formability during manufacturing, the investigation of preforming behaviour of each tufted 3D structure will be performed by analysing the in-plane and out-of-plane characterizations.

4.4 Analysis and discussion about the influence of tufting yarns

4.4.1 Influence on the material draw-in

The influence of tufting density on the maximum material draw-in is shown in Figure 4-14. As the deformed preform after forming was quasi-symmetric, the measurement data was the mean value of the four sides. The same preforming test was repeated three times and a good agreement among these tests was obtained.

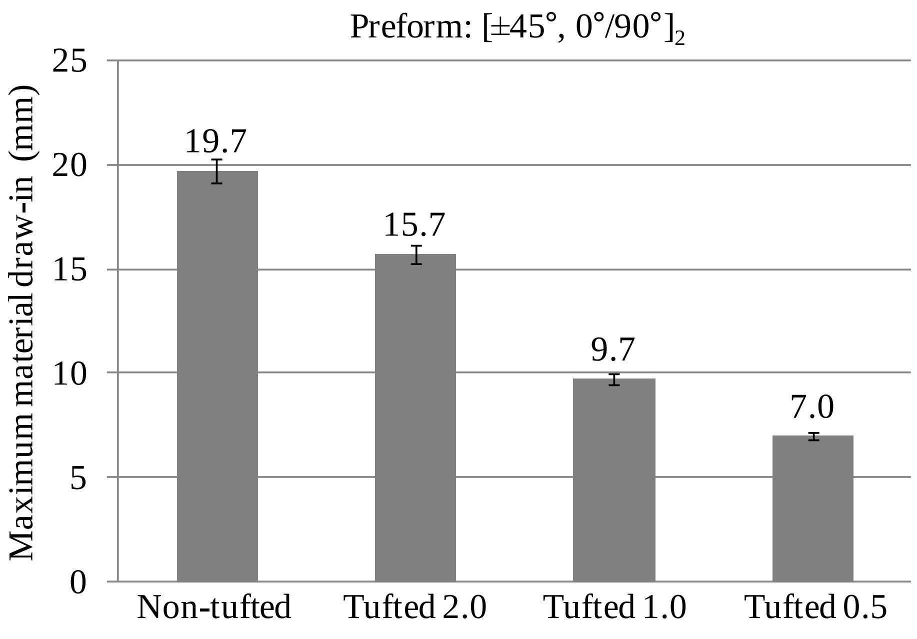

Figure 4-14 Influence of tufting density on the material draw-in.

In the forming of non-tufted preform, a relatively big material draw-in of 19.7 mm was noted at the central point of the four sides of the top ply (see Figure 4-10). Comparing this draw-in to the one in the forming of four plies simply superimposed ([0°/90°]$_4$ and [-

45°/45°]$_4$) (see Figure 4-9), the material draw-in of deformed [±45°, 0°/90°]$_2$ preform was reduced due to the increased friction effects on inter-surfaces. Whereas, it is observed from Figure 4-8 that, the draw-in of non-tufted preform is bigger than the draw-in of other tufted preforms, and with the augmentation of tufting spacing, the draw-in of tufted preform decreases. It is because that the friction coefficient on upper and bottom surfaces of tufted preform was increased due to the presence of tufting yarns. Consequently, it was observed that the material draw-in decreased following an augmentation of tufting density.

4.4.2 Influence on the inter-layer sliding

The sliding on the inter-layer is an important phenomenon during multilayered reinforcement forming. Figure 4-15 shows the inter-layer sliding of six preforms including non-tufted [±45°, 0°/90°]$_2$ preform, tufted [±45°, 0°/90°]$_2$ preform with tufting spacing of 20mm, 10mm, 5mm, simply superimposed [0°/90°]$_4$ and [-45°/45°]$_4$. The influence of tufting density on the inter-layer sliding during the forming can be observed as well as the comparison with the forming of four plies simply superimposed. When the four plies were simply superimposed with the same yarn orientations ([0°/90°]$_4$ and [-45°/45°]$_4$ preforms), a small slippage was observed due to the change of curvature of each layer as the thickness of ply was taken into account. On the contrary, when a quasi-isotropic structure was used (non-tufted [±45°, 0°/90°]$_2$ preform), a big inter-layer sliding was observed as the different deformation of ply was presented after the forming. Consequently, a maximum sliding of 19.7 mm was noted between the ply 1 (0°/90° ply) and the ply 2 (±45° ply). While de introduction of tufting thread through the thickness provides an obviously decreasing inter-layer sliding. Following the increase of tufting density, the inter-layer sliding after forming was reduced significantly. There is almost no inter-sliding which was observed in the forming of the tufted 0.5 sample, the four layers deformed in the same way.

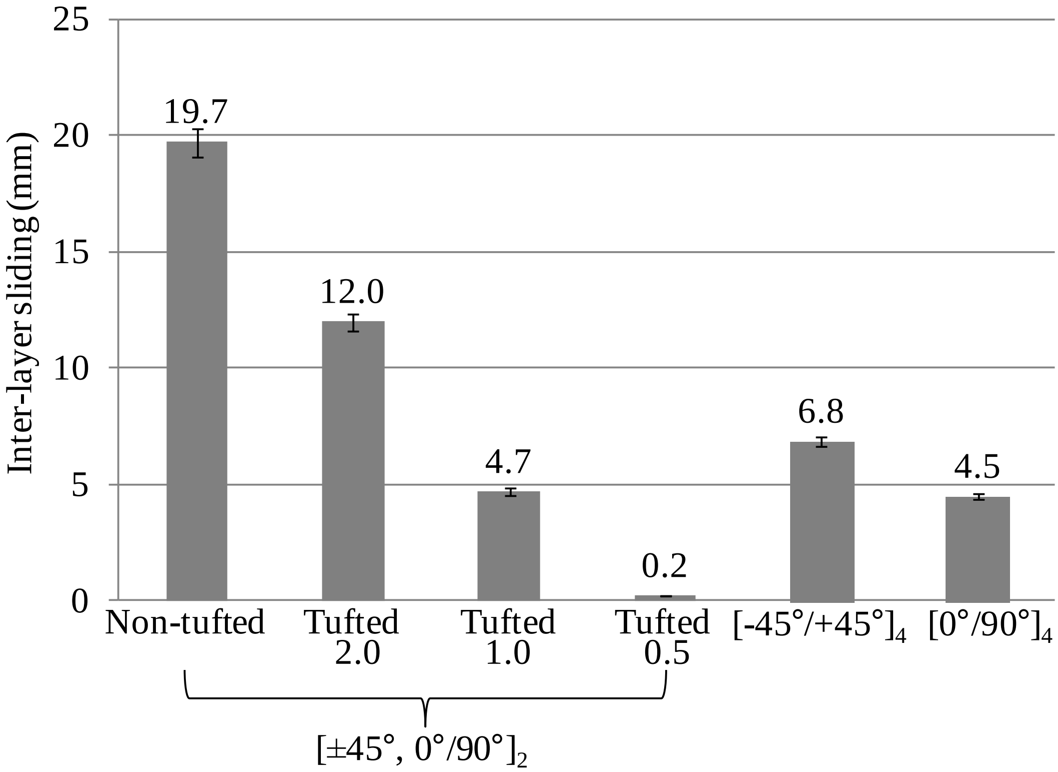

Figure 4-15 Influence of tufting density on the inter-layer sliding.

4.4.3 Influence on the punch force

Punch force describes a constant effort of punch to maintain the final shape of deformed preform. The punch force of non-tufted and tufted preforms with different tufting spacing are noted. The influence of tufting density on the maximum punch force is shown in Figure 4-16. Comparing with non-tufted preform, the tufted preform becomes more rigid with the introduction of tufting thread as presented previously. The punch force increases following the increasing of the tufting density. Comparing the non-tufted with tufted 0.5 preforms, the mass of preform augmented 13 % and the maximum punch force increased 33%. Furthermore, the tufting density increased as the tufted preform was deformed.

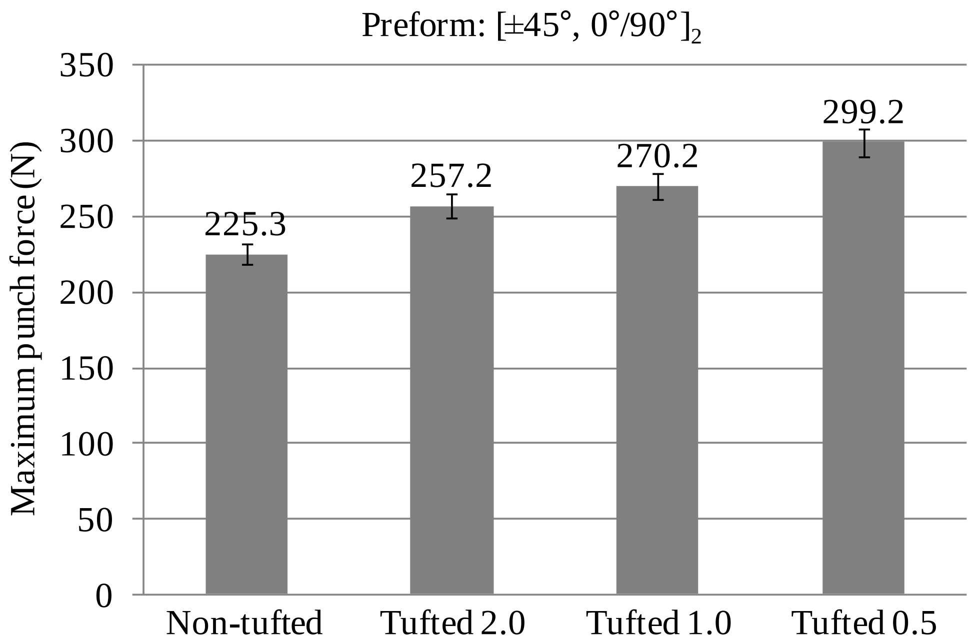

Figure 4-16 Influence of tufting density on the punch force.

4.4.4 Influence on the forming defects

One of the most common defects in tufting is wrinkling. It has been experimentally shown frequently in textile reinforcement forming [14, 21, 27, 32]. The possible relative motion of fibres due to the internal composition of textile reinforcement leads to a weak bending stiffness [54, 55]. Wrinkling is a global phenomenon that depends on strain and force components and boundary conditions of forming [14]. However, the wrinkling phenomenon can be modified by tufting during the forming of tufted preform. Figure 4-17 presents the magnified view of the useful zone. After the forming of non-tufted preform, some big wrinkles with a non-regular shape can be observed in Figure 4-17a. Compared to the deformed non-tufted preform, in the forming of tufted 1.0 and tufted 0.5 preforms the wrinkles were regularly distributed and the size of wrinkle was much reduced. Furthermore, the number and the size of wrinkle were decreased when the tufting density augments. Therefore, it is possible to predicting and control the distribution of wrinkles by inserting tufting thread into the preform.

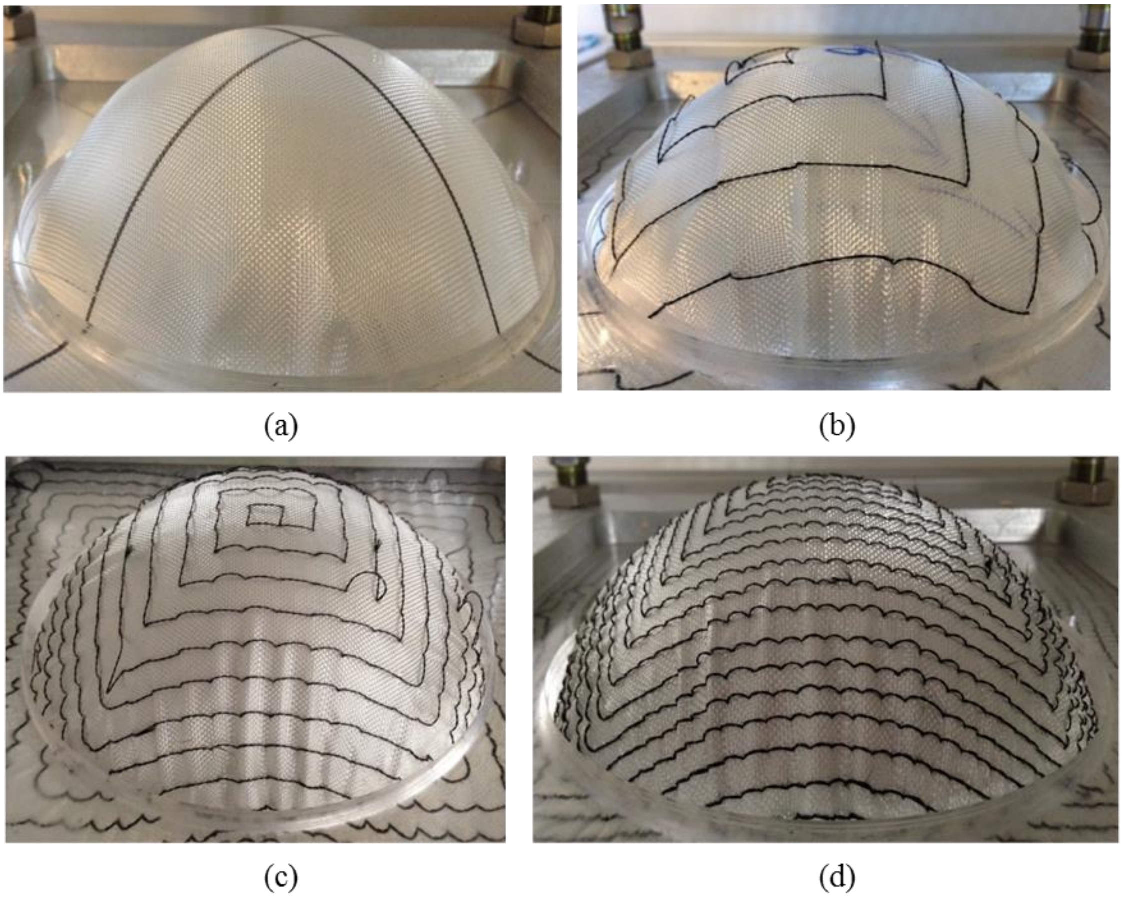

Figure 4-17 Wrinkling phenomena in the forming of (a) non-tufted, (b) tufted 1.0 and (c) tufted 0.5 preforms.

4.4.5 Influence of tufting yarn orientations

To extend research of the influence factor on reinforcement forming, the influence of tufting yarn orientations was proposed to be studied during the forming of tufted fabric. Two plies of E-glass plain weave were superposed and tufted trough-the-thickness, but the tufting yarn orientations was different as shown in Figure 4-18 and Figure 4-19. As the dimensions of ply and the tufting spacing were not changed, mass of preform noted in Table 4-3 was almost the same.

Table 4-3 Influence of tufting yarns orientation in the forming of tufted 3D preforms.

Preforms	**[0°/90°]$_2$ preform tufted in 0°/90°**	**[0°/90°]$_2$ preform tufted in ±45°**	**[-45°/45°]$_2$ preform tufted in 0°/90°**	**[-45°/45°]$_2$ preform tufted in ±45°**
Tufting spacing (mm)	10			
Surface dimensions	280 × 280 mm^2			
Mass (g)	28.9	28.7	29.8	29.6
Maximum punch force (N)	107	113	155	160
Maximum draw-in (mm)	23.1±0.7	23.7±0.7	18.3±0.5	19.2±0.6

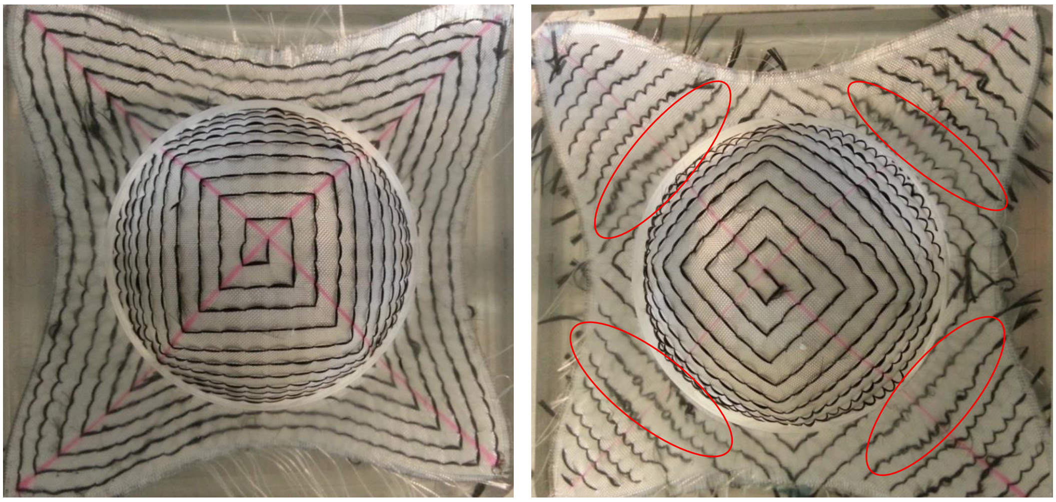

(a) [0°/90°]$_2$ preform tufted in 0°/90° (b) [0°/90°]$_2$ preform tufted in ±45°

Figure 4-18 Hemispherical forming of tufted 3D preforms [0°/90°]$_2$.

Comparing the [0°/90°]$_2$ preforms tufted in 0°/90° and in ±45° directions, the change of tufting yarn orientations did not modify the global deformation of preform (Figure 4-18) and the punch force (Table 4-3). On the contrary, the misalignment of tufting yarns is shown in Figure 4-18b for [0°/90°]$_2$ preform tufted in ±45° because the orientation of layer is not the same of the tufting yarns. As there is a strong in-plane shear effect in diagonal direction for [0°/90°]$_2$ preform (the zones indicated on the figure), each segment of tufting thread between two tufting points was compressed and then the tufting yams in these strong shear zones are misaligned. The same phenomenon was observed in the forming of [-45°/45°]$_2$ preform tufted in 0°/90° and in ±45°. As the strong shear zones are presented in longitudinal and transversal directions in [-45°/45°] ply forming, the misalignment was noted in the deformed $[-45°/45°]_2$ preform tufted in 0°/90° (Figure 4-19a). Table 4-3 presents that in the forming of the $[-45°/45°]_2$ preform tufted in 0°/90° and the $[-45°/45°]_2$ preform tufted in ±45°, they have almost the same maximum punch force and the same draw-in. Consequently, it is to say that different tufting yarn orientations will not influence the maximum punch force and the draw-in but bring out different distribution of wrinkles and also some other defects such as misalignment. The choice of tufting yarn orientation should be taken into consideration according to the orientation of layers in preform and forming need.

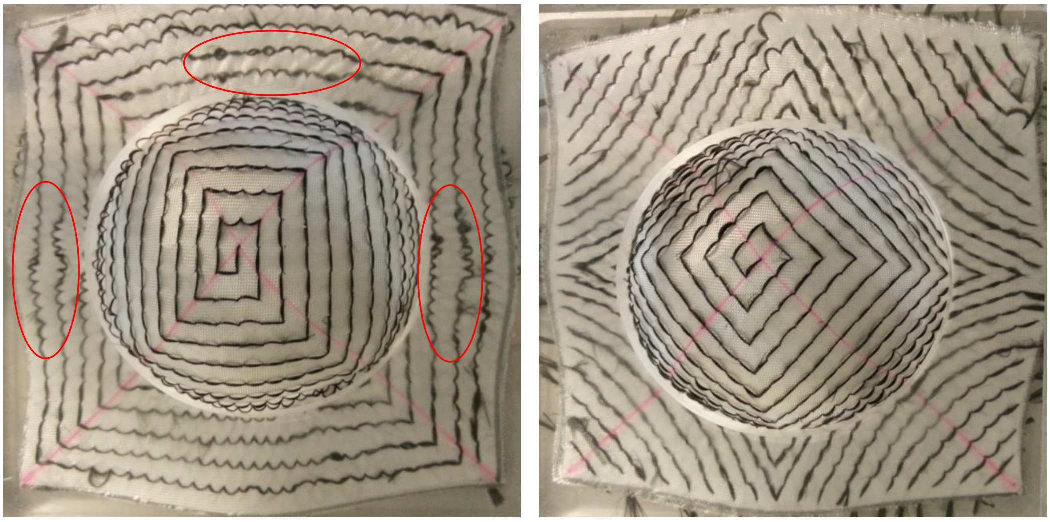

(a) $[-45°/45°]_2$ preform tufted in 0°/90° (b) $[-45°/45°]_2$ preform tufted in ±45°

Figure 4-19 Hemispherical forming of tufted 3D preforms $[-45°/45°]_2$.

4.5 Conclusion of Chapter 4

The influence of tufting yarns during the forming of tufted 3D textile reinforcements has been studied in this chapter. As the tufted preform was reinforced by tufting yarns through-the-thickness, it became more rigid than the non-tufted multilayered preform. Compared to the multilayered reinforcement forming, it requires a bigger punch force in the tufted 3D reinforcement forming. When a quasi-isotropic structure, $[±45°, 0°/90°]_2$, was used in the multilayered forming, a significant inter-ply sliding was observed. After tufting process, the slippage between the plies was reduced following the increasing of tufting density. In the present work, the preform was deformed as a single 3D ply when the tufting spacing decreases to 5 mm.

Wrinkling is one of the forming defects that can be experienced frequently in textile reinforcements forming. The wrinkles were observed in the forming of $[\pm 45°, 0°/90°]_2$ preform but not in the forming of $[0°/90°]_4$ and $[-45°/+45°]_4$ preforms due to an increasing of friction effects on the contact surfaces of plies. The tufting yarns could modify the wrinkling phenomenon, the shape of wrinkles was more regular and the size of wrinkles was strongly reduced in the present forming of the tufted preforms. Therefore, it is possible to control the wrinkling phenomenon in the tufted 3D reinforcement forming by tufting process.

Formability behaviour can be changed during the textile composite forming when the fibre orientations are changed. In tufted 3D reinforcement forming, the tufting yarns orientation did not modify the global deformation of preform. On the contrary, if the reinforced fibres orientation was not same as the tufting yarns orientation, it leaded to the forming defects as misalignment in the strong in-plane shear zones. It is better to place the tufting thread through the reinforced fibres orientation.

Reference of Chapter 4

[1] Long AC. Composites forming technologies. New York, NY: CRC Press, 2007.

[2] Simacek P, Advani SG. Desirable features in mold filling simulations for liquid composite molding processes. Polym Compos 2004; 25(4):355–67.

[3] Christos K. Design and analysis of composite structures: with application to aerospace structures. New York, NY: Wiley, 2010.

[4] Campbell F. Manufacturing technology for aerospace structural materials. Lavoisiers: Elsevier; 2006.

[5] Allaoui S, Hivet G, Soulat D, Wendling A, Ouagne P, Chatel S. Experimental preforming of highly double curved shapes with a case corner using an interlock reinforcement. International Journal of Material Forming 2014;7(2):155-65.

[6] Zhu B, Yu TX, Zhang H, Tao XM. Experimental investigation of formability of commingled woven composite preform in stamping operation. Composites Part B 2011; 42:289–95.

[7] Khan MA, Mabrouke T, Vidal-Sallé E, Boisse P. Numerical and experimental analyses of woven composite renforcement forming using ahypoelastic behaviour.

Application to the double dome benchmark. Journal of materials processing technology 2010;210:378-88.

[8] Allaoui S, Cellard C, Hivet G. Effect of inter-ply sliding on the quality of multilayer interlock dry fabric preforms. Composites: Part A. 2015;68:336–45.

[9] Haanappel SP, ten Thije RHW, Sachs U, Rietman B, Akkerman R. Formability analyses of uni-directional and textile reinforced thermoplastics. Composites Part A 2014;56:80–92.

[10] Harrison P, Gomes R, Curado-Correia N. Press forming a 0/90 cross-ply advanced thermoplastic composite using the double-dome benchmark geometry. Composites Part A 2013;54:56–69.

[11] Yin H, Peng X, Du T, Guo Z. Draping of plain woven carbon fabrics over a double-curvature mold. Composites Science and Technology 2014;92:64–9.

[12] Vanclooster K, Lomov SV, Verpoest I. Experimental validation of forming simulations of fabric reinforced polymers using an unsymmetrical mould configuration. Composites Part A 2009;40(4):530–9.

[13] Gereke Thomas, Döbrich Oliver, Hübner Matthias, Cherif Chokri. Experimental and computational composite textile reinforcement forming: a review. Composites Part A 2013;46:1–10.

[14] Boisse P, Hamila N, Vidal-Sallé E, Dumont F. Simulation of wrinkling during textile composite reinforcement forming. Influence of tensile in-plane shear and bending stiffnesses. Compos Sci Technol 2011;71(5):683–92.

[15] D.Jauffrès,J.A.Sherwood, Discrete mesoscopic modeling for the simulation of woven-fabric reinforcement forming. International Journal of Material forming 2010;3:1205-16.

[16] Peng X, Guo Z, Diu T, Yu WR. A simple anisotropic hyperelastic constitutive model for textile fabrics with application to forming simulation. Composites Part B 2013;52:275–81

[17] Boisse P, Aimène Y, Dogui A, Dridi S, Gatouillat S, Hamila N, Khan MA, Mabrouki T, Morestin F, Vidal-Sallé F. Hypoelastic, hyperelastic, discrete and semi-discrete approaches for textile composite reinforcement forming. International Journal of Material Forming 2010; 3:1229-40.

[18] Hamila N, Boisse P. Simulations of textile composite reinforcement draping using a new semi-discrete three node finite element. Composites Part B 2008; 39:999–1010.

[19] Peng XQ, Ding FF. Validation of a non-orthogonal constitutive model for woven composite fabrics via hemispherical stamping simulation. Composites Part A 2011;4:400-7.

[20] Ouagne P, Soulat D, Moothoo J, Capelle E, Gueret S. Complex shape forming of a flax woven fabric; analysis of the tow buckling and misalignment defect. Composites Part A 2013;51:1–10.

[21] Capelle E, Ouagne P, Soulat D, Duriatti D. Complex shape forming of flax woven fabrics: Design of specific blank-holder shapes to prevent defects. Composites Part B 2014;62:29–36.

[22] Gatouillat S, Bareggi A, Vidal-Sallé E, Boisse P. Meso modelling for composite preform shaping - Simulation of the loss of cohesion of the woven fibre network. Composites Part A 2013;54:135-44.

[23] Cao J, Akkerman R, Boisse P, Chen J, Cheng HS, de Graaf EF, et al. Characterization of mechanical behavior of woven fabrics: experimental methods and benchmark results. Composites Part A 2008;39(6):1037-53.

[24] Colman AG, Bridgens BN, Gosling PD, Jou GT, Hsu XY. Shear behaviour of architectural fabrics subjected to biaxial tensile loads. Composites Part A 2014;66:163-74.

[25] Nosrat-Nezami F, Gereke T, Eberdt C, Cherif C. Characterisation of the shear-tension coupling of carbon-fibre fabric under controlled membrane tensions for precise simulative predictions of industrial preforming processes. Composites Part A 2014; 67:131-9.

[26] Launay J, Hivet G, Duong AV, Boisse P. Experimental analysis of the influence of tensions on in plane shear behaviour of woven composite reinforcements. Compos Sci Technol 2008;68(2):506–15.

[27] Liang B, Hamila N, Peillon M, Boisse P. Analysis of thermoplastic prepreg bending stiffness during manufacturing and of its influence on wrinkling simulations. Composites Part A 2014;67:111-22.

[28] De Bilbao E, Soulat D, Hivet G, Gasser A. Experimental study of bending behaviour of reinforcements. Exp Mech 2010;50(3):333–51.

[29] Syerko E, Comas-Cardona S, Binetruy C. Models of mechanical properties/behavior of dry fibrous materials at various scales in bending and tension: a review. Compos Part A 2012;43(8):1365–88.

[30] Boisse P, Gasser A, Hivet G. Analyses of fabric tensile behaviour: determination of the biaxial tension–strain surfaces and their use in forming simulations. Composites Part A. 2001;32:1395-14

[31] Hivet G, Vidal-Sallé E, Boisse P. Analysis of the stress components in a textile composite reinforcement. Journal of Composite Materials 2013;47:269-85.

[32] Wang P, Hamila N, Boisse P. Thermoforming simulation of multilayer composites with continuous fibres and thermoplastic matrix. Composites Part B 2013;52:127-36.

[33] Li XK, Bai SL. Sheet forming of the multi-layered biaxial weft knitted fabric reinforcement. Part I: On hemispherical surfaces. Composite Part A 2009;40:766-77.

[34] Fetfatsidis KA, Jauffrès D, Sherwood JA, Chen J. Characterization of the tool/fabric and fabric/fabric friction for woven–fabric composites during the thermostamping process. Int J Form 2013;6(2):209–21.

[35] ten Thije RHW, Akkerman R, Ubbink M, L. Van der Meer. A lubrication approach to friction in thermoplastic composites forming processes. Compos Part A 2011;42:950-60.

[36] Bel S, Hamila N, Boisse P, Dumont F. Finite element model for NCF composite reinforcement preforming: Importance of inter-ply sliding. Composites Part A 2012;43:2269-77.

[37] Mouritz AP, Bannister MK, Falzon PJ, Leong KH. Review of applications for advanced three-dimensional fibre textile composites. Composites Part A 1999;30:1445-61.

[38] Mouritz AP, Cox BN. A mechanistic interpretation of the comparative in-plane mechanical properties of 3D woven, stitched and pinned composites. Composites Part A 2010;41:709-28.

[39] Dufour C, Wang P, Boussu F, Soulat D. Experimental Investigation About Stamping Behaviour of 3D Warp Interlock Composite Preforms. Applied Composite Materials 2014;21(5):725-38.

[40] Zhang YF, Sun F, Wang YJ, Chen L, Pan N. Study on intra/inter-ply shear deformation of three dimensional woven performs for composite materials. Mater. Des. 2013;49:151-9.

[41] De Luycker E, Morestin F, Boisse P, Marsal D. Simulation of 3D interlock composite preforming. Compos Struct 2009;88:615–23.

[42] Charmetant A, Orliac JG, Vidal-Sallé E, Boisse P. Hyperelastic model for large deformation analyses of 3D interlock composite preforms. Composites Science and Technology 2012;72:1352-60.

[43] Duhovic M, Mitschang P, Bhattacharyya D. Modelling approach for the prediction of stitch influence during woven fabric draping. Composites Part A 2011;42:968-78.

[44] Margossian A, Bel S, Balvers JM, Leutz D, Freitas R, Hinterhoelzl R. Finite element forming simulation of locally stitched non-crimp fabrics. Composites Part A 2014;61:152-62.

[45] Pazmino J, Carvelli V, Lomov SV. Formability of a non-crimp 3D orthogonal weave E-glass composite reinforcement. Composites Part A 2014;61:76-83.

[46] Carvelli V, Pazmino J, Lomov SV, Verpoest I. Deformability of a non-crimp 3D orthogonal weave E-glass composite reinforcement. Composites Science and Technology 2012;73:9-18.

[47] Dell'Anno G, Cartié DD, Partridge IK, Rezai A. Exploring mechanical property balance in tufted carbon fabric/epoxy composites. Composites Part A 2007;38(11):2366-73.

[48] Cartié DDR, Dell'Anno G, Poulin E, Partridge IK. 3D reinforcement of stiffener to skin T-joints by Z-pinning and tufting. Eng Fract Mech 2006;73(16):2532-40.

[49] Henao A, et al. Mechanical performance of through-thickness tufted sandwich structures. Composite structures 2010;92:2052-59.

[50] Sickinger C, Hermann A. Structural stitching as a method to design high-performance composite in future. Proceedings TechTextil Symposium, 2001.

[51] Pérès P, et al. Composite behavior of assemblies with AEROTISS® 03S technology. In 16th International Conference on Composite Materials. 2007, Kyoto, Japan.

[52] Vanclooster K, Lomov SV, Verpoest I. On the formability of multi-layered fabric composites. In 17th International Conference on Composite Materials. 2009, Edinburgh, UK.

[53] ten Thije RHW, Akkerman R. A multi-layer triangular membrane finite element for the forming simulation of laminated composites. Composites Part A 2009;40:739-53.

[54] Potter K, Khan B, Wisnom M, Bell T, Stevens J. Variability, fibre waviness and misalignment in the determination of the properties of composite materials and structures. Composites Part A 2008;39:1343–54.

[55] Prodromou AG, Chen J. On the relationship between shear angle and wrinkling of textile composite performs. Composites Part A 1997;28A:491-03.

5 GENERAL CONCLUSION

5.1 Conclusion

This thesis is dedicated to improve the understanding of the popular tufting technology which is used to reinforce 3D composite parts. Laminated fibre reinforced composites are used for many decades in many industrial fields. As a directional material, the lack of the through-thickness fibre reinforcement results in a low delamination resistance, poor through the thickness properties and poor toughness. 3D textile reinforced composite materials are developed to replace the multilayered reinforcements in some applications. As an advanced method for strengthening composite in the thickness and also developing 3D preforms, tufting technology is introduced in this thesis. By using the tufting technology, the thick tufted composites are performed, the delamination effect can be reduced and the impact resistance and damage tolerance are increased. Compared to 3D weaving, the main interest of tufting is the possibility to reinforce through the thickness or to perform the linkage between the layers where it is required. Moreover, the tufting pattern can be changed more easily to match our needs (e.g. square spiral tufting, spiral tufting…). Compared to conventional stitching, tufting is much simpler as it does not require that a second thread be used and that the threads be locked. The tufting at one side permits the manufacturing process to be simplified, more efficient and more economical.

In order to apply tufting process to reinforce textile preforms, numerous parameters including tufting length, tufting thread properties, tufting density, type of needle, tufting direction, etc. are studied. Self-designed tufting equipment with the functions of controlling these parameters is developed. The four parts (tufting system, presser foot system, feeding system and the frame) to form the tufting equipment and their functions are introduced. Tufting system is designed to carry a threaded needle to insert into textile preforms with different tuft lengths. Presser foot is used to press the preform with adjusted pressure to avoid tufting thread being drawn off. Feeding system carries tufting thread bobbin and provide tufting thread with a certain length and pre-tension. The frame carries the preform and all other systems and provides the possibility to measure and control tufting density. This tufting machine can be used automatically to reinforce or assemble different kinds of textile structures with adjustable tufting parameters. Different tufting threads and textile preforms are tufted with this equipment to improve tufting process.

With this tufting equipment, several tufting samples are fabricated and tested to observe the influence of tufting parameters on the forming behaviours and mechanical properties of tufted preforms and composites. In order to better conduct the observation about the tuft length and tufting yarn loop, carbon yarns are chosen to be tufted into a glass fibre reinforced fabric.

Firstly, the effect of tuft length through the thickness on the characterisations of tufted composites is completely analysed. Thick assembled reinforcements are prepared by using the above mentioned tufting equipment. Tufted preforms are infused with an epoxy resin by liquid resin infusion process. Microscopic analysis on the cross section of tufted preforms presents the inner structure of tufted composite. Tensile test results present the influence of tuft length on the mechanical performance. The optimization of the tufting process is investigated and an effective tuft length of 8 mm is the minimum required to guarantee that the multi-layered composite part can be well reinforced through the thickness with the given tufting threads and preform. When the effective tuft length is superior to the optimised one, the tensile strength of the tufting thread in composites tends to constant in the case of partially inserted tuft. To avoid high degradation of the tufting threads, the better method is partially inserted tufting compared to fully inserted tufting.

Then the impact of tufting yarns during the forming of tufted 3D textile reinforcements is studied. Comparing with non-tufted multilayered preform, the tufted preform reinforced by tufting yarns through-the-thickness becomes more rigid. For this reason, it requires a bigger punch force in the tufted 3D reinforcement forming. When a quasi-isotropic structure, $[\pm 45°, 0°/90°]_2$, is used in the multilayered forming, a significant inter-ply sliding is observed. After tufting process, the slippage between the plies is reduced following the increasing of tufting density. Wrinkling is one of the forming defects that can be experienced frequently in textile reinforcements forming. The wrinkles are observed in the forming of [±45°, 0°/90°]$_2$ preform but not in the forming of [0°/90°]$_4$ and [-45°/+45°]$_4$ preforms due to an increasing of friction effects on the contact surfaces of plies. The tufting yarns could modify the wrinkling phenomenon, the shape of wrinkles is more regular and the size of wrinkles is strongly reduced in the present forming of the tufted preforms. Therefore, it is possible to control the wrinkling phenomenon in the tufted 3D reinforcement forming by tufting process. Formability behaviour can be changed during the textile composite forming when the fibre orientations are changed. In tufted 3D reinforcement forming, the tufting yarns orientation does not modify the global deformation of preform. On the contrary, if the reinforced fibres orientation was not same as the tufting yarns orientation, it leads to the forming defects as misalignment in the strong in-plane shear zones. It is better to place the tufting thread through the reinforced fibres orientation.

5.2 Perspective

Our home-made tufting device is an academic device. Even if this device is automated, it presents several limitations including productivity speed, precision of feeding system, tufting length and orientation of tufting point. In the future work, these obstacles could be resolved enabling more detailed study of the manufacturing and tufting effect. With a large amount of attempts, the tufting equipment can be improved little by little to meet the industrial need.

With the optimised tufting machine, it is important to investigate other types of tufting reinforcement using other threads to observe the influence of different tufting parameters on the tensile characterization. On the other side, it is also possible and necessary to study de influence of tufting on the properties of composites materials such as resistance to inter-laminar shearing, bending and impact resistance, etc.

Forming stage as the first and very important manufacturing step of RTM process, is to be deeply studied. In the future work, the studies about the forming behaviour by using other tufting form and other classical punches (tetrahedral, square box…) are quite necessary. In order to predict the feasible forming conditions, the aspect of numerical modeling and simulation of tufted 3D reinforcements forming need to be developed.

The process of through-the-thickness tufting leads to the formation of loops at the bottom side of the preform. It would be interesting to study the importance of these loops including how to limit them and how to take advantage of them to improve the performances of the preforms.

Finally, tufting process is not only a means to reinforce preforms, but also a process to be used to assemble multiple preforms. Therefore, more researches can be conducted to study the structural assembly ability of tufting process.

Résumé

Titre : Contribution à l'étude du piquage pour renforcement des composites

Dans plusieurs industries, les composites 3D sont largement utilisés pour fabriquer les pièces composites épaisses et complexes. La technologie de piquage permet de lier des renforts secs ensemble ou de renforcer les composites dans l'épaisseur grâce à des fils structuraux. Cette thèse est consacrée au développement de cette technologie et à l'analyse de l'influence des paramètres de piquage sur les comportements de préformage et les propriétés mécaniques de la préforme et du composite piqués.
Le procédé de piquage est décrit dans la thèse. La configuration d'équipement est conçue pour réaliser ce procédé. Les paramètres de piquage peuvent être contrôlés par l'utilisateur.
L'influence de la profondeur de piquage sur les propriétés mécaniques des 3D préformes renforcées par le piquage est analysé. Des 3D échantillons composites sont piqués avec des profondeurs de piquage variées. Les résultats d'essais mécaniques en traction et l'analyse microscopique sur la section transverse de l'éprouvette montrent que la profondeur influence fortement les performances mécaniques des composites. Le contrôle de ces paramètres est indispensable pour optimiser l'utilisation du piquage et améliorer les propriétés des renforts assemblés.
Les comportements de préformage du renforcement piqué dans le procédé d'emboutissage hémisphérique sont aussi analysés. L'influence des fils de piquage sur l'avalement des plis, le glissement entre les couches et le phénomène de plissement lors de la formation est démontrée. De plus, les orientations du fil de piquage ont affecté les résultats de formage, qui ont conduit à un défaut de désalignement dans la zone où le cisaillement dans le plan est fort.
Mots clés : Tissus/textiles, Renforcement tridimensionnel, Composite 3D, Piquage, Performances mécaniques, Emboutissage.

Abstract

Title: Development and optimization of the tufting process for textile composite reinforcement

Three-dimensional fabrics are widely used in several industries to manufacture thicker and more complex composite parts. Tufting technology is employed to bond dry reinforcements together or to reinforce the composites in the thickness by structural yarns. The thesis is dedicated to the development of tufting technology and the analysis of the influence of tufting parameters on preforming behaviours and mechanical properties of tufted preform and composite.
The tufting process and the self-designed equipment configuration are described in detail in the thesis. The tufting parameters can be completely controlled by user.
Influence of tufting length through the thickness on mechanical properties of 3D tufted preform and composite is analysed in this study. 3D composite samples are prepared with varied tufting length. Tensile tests are carried out to determine the influence of the tuft length on the mechanical performance of tufted samples. The tensile results and microscopic analysis on the cross section of 3D specimen show that the tuft length strongly influences on the mechanical properties of composite. Therefore, the control of these parameters is necessary to optimize the tufting process and thus improve the mechanical performance of assembled thick reinforcements.
The preforming behaviours of tufted 3D reinforcement in the hemispherical stamping process are also analysed. The experimental data demonstrates the influence of tufting yarns on the material draw-in, interply sliding, and winkling phenomenon during forming. Furthermore, the orientations of tufting yarn affected the forming results, which leaded to misalignment defect in the zone of strong in-plane shear.
Key words: Fabrics/textiles, 3-Dimensional reinforcement, 3D composite, Tufting, Mechanical performance, Stamping.